NSWC TR 85–24

AD-A157 068

ALTERNATE ALTITUDE TESTING OF SOLID CLOTH PARACHUTE SYSTEMS

BY WILLIAM P. LUDTKE

UNDERWATER SYSTEMS DEPARTMENT

1 MAY 1985

NAVAL SURFACE WEAPONS CENTER

Dahlgren, Virginia 22448 • Silver Spring, Maryland 20910

UNCLASSIFIED

SECURITY CLASSIFICATION OF THIS PAGE (When Data Entered)

REPORT DOCUMENTATION PAGE	READ INSTRUCTIONS BEFORE COMPLETING FORM
1. REPORT NUMBER: NSWC TR 85-24	2. GOVT ACCESSION NO.: AD-A157068
	3. RECIPIENT'S CATALOG NUMBER:
4. TITLE (and Subtitle): ALTERNATE ALTITUDE TESTING OF SOLID CLOTH PARACHUTE SYSTEMS	5. TYPE OF REPORT & PERIOD COVERED: Final; Fiscal Year 1985
	6. PERFORMING ORG. REPORT NUMBER:
7. AUTHOR(s): William P. Ludtke	8. CONTRACT OR GRANT NUMBER(s):
9. PERFORMING ORGANIZATION NAME AND ADDRESS: Naval Surface Weapons Center (U13), 10901 New Hampshire Ave., Silver Spring, MD 20903-5000	10. PROGRAM ELEMENT, PROJECT, TASK AREA & WORK UNIT NUMBERS: 5U15MA OM and N
11. CONTROLLING OFFICE NAME AND ADDRESS:	12. REPORT DATE: 1 May 1985
	13. NUMBER OF PAGES: 85
14. MONITORING AGENCY NAME & ADDRESS(if different from Controlling Office):	15. SECURITY CLASS. (of this report): UNCLASSIFIED
	15a. DECLASSIFICATION/DOWNGRADING SCHEDULE:

16. DISTRIBUTION STATEMENT (of this Report)

Approved for public release; distribution unlimited.

17. DISTRIBUTION STATEMENT (of the abstract entered in Block 20, if different from Report)

DTIC ELECTE JUL 3 1 1985 A

18. SUPPLEMENTARY NOTES

19. KEY WORDS (Continue on reverse side if necessary and identify by block number)

Solid Cloth Parachutes
Parachute Technology
Scale Effects
Altitude Effects
Opening Shock
Parachute Stress

20. ABSTRACT (Continue on reverse side if necessary and identify by block number)

Retardation systems used for very high altitude at low dynamic pressures or for low altitude cargo delivery often require exceptional test equipment and/or facilities. As tests become more complex, higher developmental costs are incurred. This report describes a technique which theoretically permits parachute systems to be tested under more convenient conditions of altitude, velocity, and system mass resulting in the same conditions of opening shock force and parachute stress distribution.

DD FORM 1 JAN 73 1473 EDITION OF 1 NOV 65 IS OBSOLETE

S/N 0102-LF-014-6601

UNCLASSIFIED

SECURITY CLASSIFICATION OF THIS PAGE (When Data Entered)

FOREWORD

Retardation systems used for very high altitude at low dynamic pressures or for low altitude cargo delivery often require exceptional test equipment and/or facilities. As tests become more complex, higher developmental costs are incurred. This report describes a technique which theoretically permits parachute systems to be tested under more convenient conditions of altitude, velocity, and system mass resulting in the same conditions of opening shock force and parachute stress distribution.

Several unique properties of solid cloth parachutes are developed along with the criteria for alternate altitude testing. Methods of calculation are provided and test techniques proposed.

Approved by:

G. P. KALAF, Head
Underwater Weapons Division

CONTENTS

ILLUSTRATIONS

TABLES

INTRODUCTION

The flight testing of solid cloth parachutes sometimes calls for unique test conditions such as very high altitudes for extremely low dynamic pressures, or heavy payloads, such as cargo, tested at low altitudes. Each of these conditions may require exceptional test equipment and/or facilities such as balloon-borne and rocket-assisted high-altitude vehicles or large cargo aircraft for low-altitude heavy payloads.

These requirements can add significantly to the overall test program cost and complexity. In order to reduce development test costs and complexity, a theoretical study has been conducted to determine the possibility of altering the test conditions in a manner which would permit the use of lower cost test assets and still obtain the same parachute opening shock forces and stress distributions. The results of this study show that if the system mass and test velocity are varied, as shown in the accompanying method for a constant Ballistic Mass Ratio (BMR) scale parameter, the opening shock force and stress distributions are constant for all altitudes. ——— > 1473

The examples in the study indicate that high-altitude testing may be accomplished at low altitudes by reducing the test velocity and increasing the payload mass, and low-altitude cargo parachute systems may be tested by reducing the payload weight and increasing the test velocity and altitude.

In the case of the modified high altitude testing, a test method is proposed which improves test observation and control. Modified cargo testing permits several test vehicles to be mounted on the wing racks, of an A7 type aircraft for example, with properly weighted existing test vehicles for the same total weight of one conventional test from a C-130 aircraft. Eventually full systems tests may be desired; however, parachute development time and costs can be reduced by alternate altitude testing.

As the study progressed, several unique effects of altitude on solid cloth parachute performance were developed. These effects are:

a. The Ballistic Mass Ratio as a scale parameter.

b. Variation of opening shock force at variable and constant Ballistic Mass Ratios.

c. Parachute stress distributions.

d. Average steady-state pressure coefficients and the variation as a function of the inflation time ratio, t/t_o.

e. Parachute inflation distance and inflation reference time.

f. System impulse as a function of Ballistic Mass Ratio.

g. Parachute performance as related to the inflation time ratio, t/t_o, for a constant Ballistic Mass Ratio.

Although the study was specifically for solid cloth parachutes, the results may be considered as guideposts for trends in the testing of other types of parachutes.

APPROACH

The study is based upon two conditions: (a) the premise that the Ballistic Mass Ratio satisfies stated criteria required for a genuine scale parameter, and (b) an opening shock force analysis which was presented at the fourth AIAA Aerodynamic Decelerator and Balloon Technology Symposium in 1973. Since this paper is to be used extensively, it is included as Appendix A of this report for the convenience of the reader. Appendix B provides a worksheet for use as a guide on how to most effectively use Appendix A. The development of the subject matter is to be a combination of theoretical development combined with examples to demonstrate the results.* It is suggested that for best understanding of this report the reader should review Appendix A first. Essential formulae from Appendix A are reviewed below as a basis for development.

THE BALLISTIC MASS RATIO AS A SCALE FACTOR

A method of scaling parachute inflation and steady-state performance has been a long-sought element of parachute-system analysis. In the search for a scaling parameter, a most important requirement must be kept in mind. That is, that for any quantity to be a valid scaling parameter, it must relate to the variables which affect performance.

In model testing of airplanes, missiles, ships, etc., in wind tunnels and towing basins, Reynolds number, Froude number, and Mach number are acccepted scale factors. These parameters, together with ballistic coefficient (W/C_DS_o) and surface loading (W/S_o), have not provided a general correlation of parachute test data. A viable scaling parameter for general use in deployable decelerator testing has not been developed, although some

*Where formulae from Appendix A are cited, the parenthesis in the right hand margin of the page denotes the appendix page and formula number, respectively. Hence, (A7-13) reads as page A7 formula 13. Formulae marked with a single number in parenthesis pertain to the presented development.

experimenters have successfully modeled particular cases. A look at the methods of testing gives us a clue as to why the aforementioned scale factors do not apply to parachute deployment. In the testing of airplanes, missiles, ships, etc., a rigid model is constructed and mounted in the test facility where data is recorded at one or more constant velocities. Thus, three parameters which are important to parachute testing are eliminated. First, the geometry of a deploying parachute undergoes dramatic changes as compared to the constant geometry of a rigid model. Second, the deploying parachute geometry is a function of deployment time. Third, the velocity profile obtained during a parachute deployment is dependent upon the mass of the assembly being retarded. Transient geometry, time, and weight are not factors in the aforementioned scale parameters. This leads to some very important conclusions:

a. Reynolds number, Froude number, and Mach number are valid scale factors for airplanes, missiles, ships, etc., because they contain the variables which affect performance.

b. These established scale parameters are unsuitable for parachute deployments because they do not contain important variables which affect parachute performance.

c. For any quantity to be valid scale parameter in any process, it must contain those variables which affect system performance.

A fundamental example of a "mass ratio" scale factor can be developed by means of a theoretical horizontal point mass trajectory. For simplicity, only the steady state (constant drag area, C_DS_o) will be considered; however, the developed mass ratio is also applicable for parachute deployments.

Example 1: Determine the velocity profile of an automobile which is being retarded on a norizontal road by a fully deployed parachute. Assume negligible automobile aerodynamic drag and road friction forces.

With reference to Figure 1.

$$-F = ma$$

$$F = \frac{1}{2}\rho V^2 C_D S_o$$

$$-\frac{1}{2}\rho V^2 C_D S_o = \frac{W}{g}\frac{dV}{dt}$$

$$\frac{\rho g C_D S_o}{2W}\int_o^t dt = \int_{V_s}^{V} \frac{-dV}{V^2}$$

Integrating and solving for the velocity ratio

$$\frac{V}{V_s} = \frac{1}{1 + \frac{\rho g V_s t C_D S_o}{2W}} \qquad (1)$$

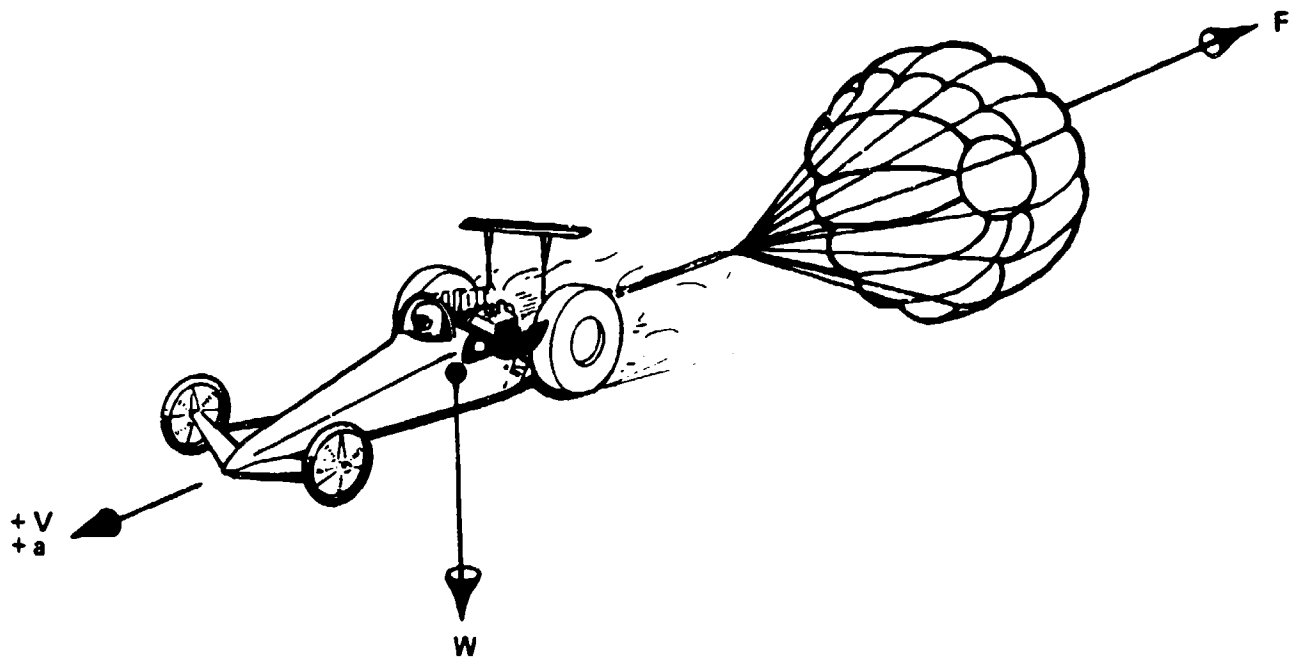

FIGURE 1. RETARDED AUTOMOBILE OF EXAMPLE 1

The quantity $2W/\rho g V_s t C_D S_o$ is in effect a ratio of masses. It can be visualized as in Figure 2 to be the ratio of the mass of the system, W/g, to the mass of air contained in a right circular cylinder of face area $C_D S_o$, length $V_s t$, and mass density ρ. If this quantity is denoted by M, then Equation (1) becomes

$$\frac{V}{V_s} = \frac{1}{1 + \frac{1}{M}} \qquad (2)$$

and it is seen that the velocity profile is only a function of the mass ratio. Figure 3 illustrates the concept of how the air mass is affected as the automobile moves along the retarded trajectory. As time increases, additional air mass is affected, and at each instant, a definite velocity ratio and mass ratio exist, as shown in Equation (2). The mass ratio contains the basic variables (altitude, ρ; parachute aerodynamic size, $C_D S_o$; system mass, W/g; velocity, V_s; and time) necessary to define a scale factor for deployable decelerator application. Apparent mass is another effect which should probably be included, but is not presently sufficiently understood or defined as to permit inclusion in the analysis. For the inflating parachute the methods for obtaining the dynamic drag area ratio signature include the effects of apparent mass.

Note that the length $V_s t$ in Figure 3 is not a true trajectory distance because of the use of the constant initial velocity V_s. The true distance (TD) is:

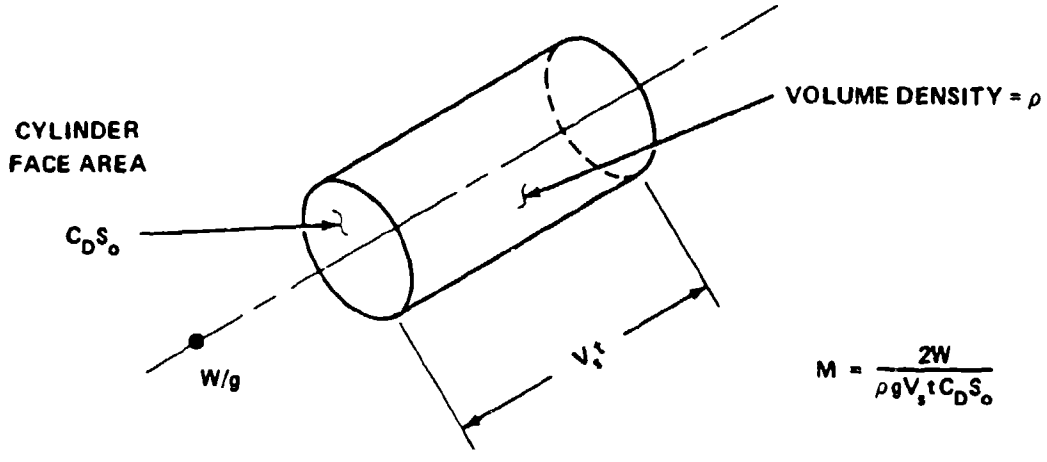

FIGURE 2. VISUALIZATION OF THE MASS RATIO CONCEPT

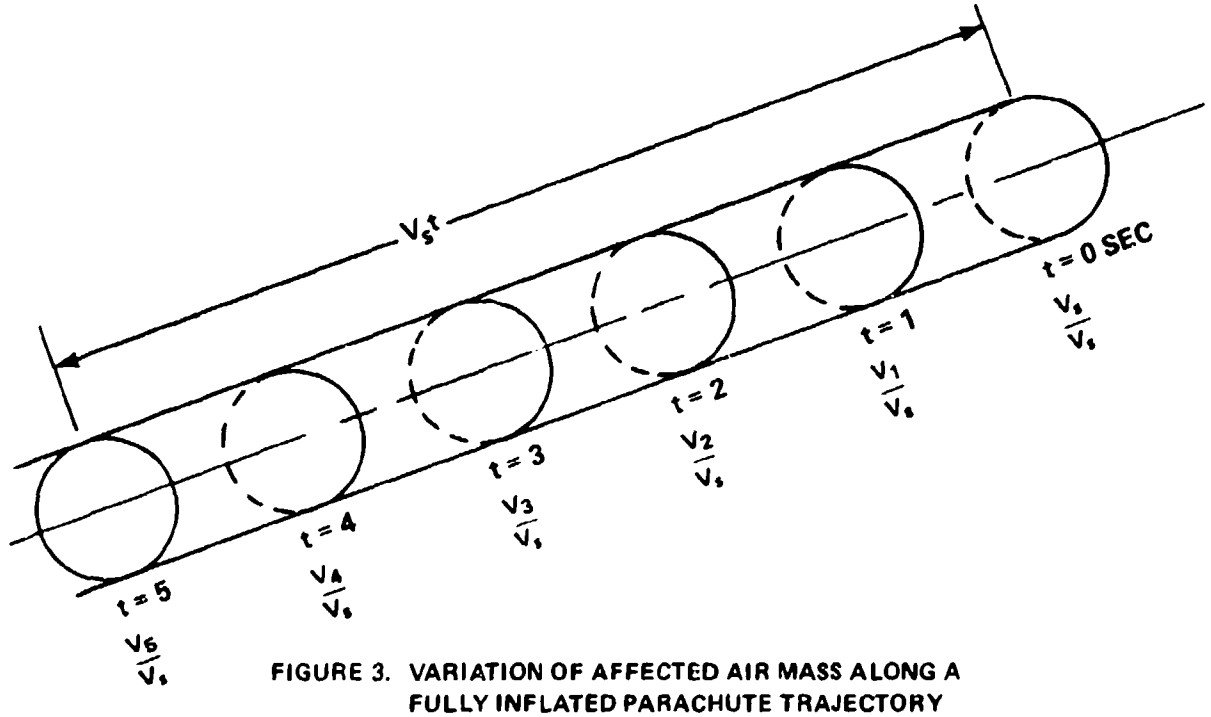

FIGURE 3. VARIATION OF AFFECTED AIR MASS ALONG A FULLY INFLATED PARACHUTE TRAJECTORY

$$TD = \int_o^t V dt$$

$$= \int_o^t \frac{V_s dt}{1 + \frac{\rho g V_s C_D S_o t}{2W}}$$

Let $$C = \frac{\rho g V_s C_D S_o}{2W}$$

$$TD = \frac{V_s}{C} \int_o^t \frac{C dt}{1 + Ct}$$

$$TD = \frac{V_s}{C} \ln (1 + Ct) \qquad (3)$$

Appendix A describes a method of calculating the opening shock forces of several types of solid cloth parachutes which utilizes the developed mass ratio as applied to the inflation stage of operation. Equations (13) and (14) on page A-7 of Appendix A relate the parachute geometry, air flow properties of the canopy cloth, drag area signature, and deployment conditions to the inflation reference time t_o. The dependency of the mass ratio on the system parameters is illustrated in the flow chart of Figure 4. Therefore, the mass ratio fulfills the scaling requirement that it relates to the variables which affect performance and is a valid scale factor. Since the mass ratio determines the ballistic performance of the retarded trajectory the name "Ballistic Mass Ratio" (BMR) is appropriate.

Although the present discussion is limited to solid cloth parachutes the Ballistic Mass Ratio approach is valid for all types of parachutes. Testing at a constant BMR at all altitudes requires a modification in system weight to offset changes in air density and inflation distance ($V_s t_o$). For other types of parachutes, the definition of the variation of inflation distance with altitude is the key to alternate altitude testing. The basic idea is not complex. Since it is required that tests are to be conducted at a constant dynamic pressure, the inflation distance associated with the required density and velocity is defined. This causes a change in the BMR. The system mass is then adjusted accordingly to return the BMR to the original value.

When a given solid cloth parachute system is tested at constant dynamic pressure over a wide range of increasing altitudes, a decrease in inflation time and an increase in opening shock force occurs. An explanation of this phenomena is as follows. The opening shock force may be expressed as

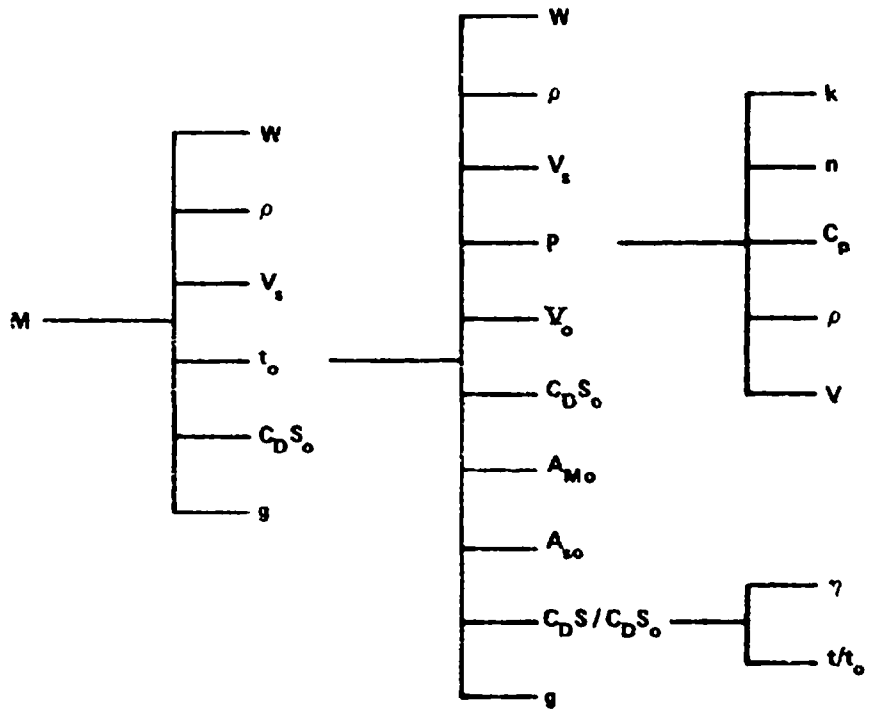

W = SYSTEM WEIGHT, LB

ρ = DENSITY AT DEPLOYMENT ALTITUDE, SLUGS/FT^3

V_s = SYSTEM VELOCITY AT SUSPENSION LINE STRETCH, FPS

t_o = REFERENCE TIME OF UNFOLDING PHASE OF CANOPY INFLATION, SEC

C_DS_o = SYSTEM STEADY STATE DRAG AREA, FT^2

g = GRAVITY, FT/SEC^2

P = CANOPY CLOTH PERMEABILITY, $FT^3/FT^2/SEC$

V_o = STEADY STATE CANOPY VOLUME, FT^3

A_{Mo} = STEADY STATE MOUTH AREA, FT^2

A_{so} = CANOPY SURFACE AREA, FT^2

$\frac{C_DS}{C_DS_o}$ = DRAG AREA SIGNATURE

η = INITIAL AREA

t/t_o = DEPLOYMENT TIME RATIO

k & n = CLOTH AIR FLOW CONSTANTS

C_p = CANOPY PRESSURE COEFFICIENT

V = INSTANTANEOUS TRAJECTORY VELOCITY, FPS

FIGURE 4. DEPENDENCE OF MASS RATIO AND INFLATION REFERENCE TIME ON PARACHUTE GEOMETRY, AIR FLOW PROPERTIES, DRAG-AREA SIGNATURE, AND DEPLOYMENT CONDITIONS FOR SOLID CLOTH PARACHUTES

$$F_{max} = F_s \, x_{imax}$$

$$F_s = q \, C_D S_o$$

where x_{imax} shall be shown to be a function of the drag area ratio at line stretch, $\eta = C_D S_i / C_D S_o$, and the BMR. The shock factor determines the percentage of the steady-state drag force that will be realized as opening shock force. For altitudes above sea level there is a decrease in air density and inflation reference time. Both of these effects increase the BMR and the maximum shock force. Testing at a constant BMR results in the same opening shock force at all altitudes.

The decrease in inflation reference time is due to the decrease in air density. For constant dynamic pressure as altitude increases the test velocity must be varied

$$V_s = V_{SL}\sqrt{\frac{\rho_{SL}}{\rho}}$$

From Equation (14) of page A-7 of Appendix A

$$t_o = \frac{14W}{\rho g V_s C_D S_o}\left[\varepsilon^{K_1} - 1\right]$$

or

$$t_o = \frac{14W}{g C_D S_o V_{SL}\sqrt{\rho_o \rho_{SL}}}\left[\varepsilon^{\frac{g\rho V_o}{2W}\left[\frac{C_D S_o}{A_{Mo} - kA_{so}\left(\frac{C_p\rho}{2}\right)^{1/2}}\right]_{-1}}\right]$$

At all altitudes the V_{SL} remains constant, and the primary variable is density. Other possible variations may be due to drag coefficient rise caused by a decrease in canopy cloth air-flow properties, and possible changes in geometry caused by the rise in drag coefficient. Otherwise, the reference time is only a function of system constants and altitude.

DISCUSSION OF APPLICABLE APPENDIX A FORMULAE

During the inflation of a parachute canopy the instantaneous force can be described as the steady state drag force, F_s, times some instantaneous shock factor, x_i.

$$F = F_s x_i$$

where x_i at any instant is a function of the instantaneous drag area signature, C_DS/C_DS_o, and the instantaneous velocity ratio $(V/V_s)^2$.

The drag-area signature is indicative of the type of parachute being used and is dependent on the deployment time ratio, t/t_o, and the method of deploying the parachute described by the initial drag-area ratio, $\eta = C_DS_i/C_DS_o$.

For the types of solid cloth parachutes of Appendix A the general case drag-area signature was determined to be

$$\frac{C_DS}{C_DS_o} = \left[(1-\eta)\left(\frac{t}{t_o}\right)^3 + \eta\right]^2 \qquad \text{(A4-4)}$$

The parachute drag-area signature may be presently obtained by two methods:

a) Infinite mass wind-tunnel tests where the methods described on pages A-3 and A-4 are used.

b) Free flight tests where event times have been established and simultaneous measurements of parachute force and dynamic pressure have been recorded during deployment.

Then:

$$C_DS_T = \frac{F_T}{q_T}$$

and the drag area signature at any instant

$$\frac{C_DS_T}{C_DS_o} = \frac{F_T}{q_TC_DS_o} = \frac{C_DS}{C_DS_o}$$

This writer prefers the wind tunnel method as it offers better control of test conditions and events, but the second method may offer a better utilization of existing field test data over a range of altitudes, velocities, and various types of parachutes.

The importance of the discovery that the dynamic drag-area signature and geometry, as a function of the time ratio, t/t_o, are independent of altitude, velocity, and system mass has not yet been fully realized. This independence separates the geometry of deployment from the forces generated during inflation, and also the stress distributions in the canopy.

For simplicity in demonstrating the principles of this analysis η is to be considered as zero.

Hence,

$$\frac{C_D S}{C_D S_o} = \left(\frac{t}{t_o}\right)^6$$

Utilizing Newton's third law of motion in the horizontal test attitude* results in:

$$\frac{1}{t_o}\int_0^t \frac{C_D S}{C_D S_o}\,dt = \frac{2W}{\rho g V_s t_o C_D S_o} V_s \int_{V_s}^{V} \frac{-dV}{V^2} \qquad \text{(A2-2)}$$

which leads to the velocity ratio equation:

$$\frac{V}{V_s} = \frac{1}{1 + \frac{1}{7M}\left(\frac{t}{t_o}\right)^7} \qquad \text{(A4-7)}$$

and the shock factor:

$$x_i = \frac{\left(\frac{t}{t_o}\right)^6}{\left[1 + \frac{1}{7M}\left(\frac{t}{t_o}\right)^7\right]^2} \qquad \text{(A5-8)}$$

Equation (A2-2) also utilized what has come to be known as a Ballistic Mass Ratio (BMR).

$$M = \frac{2W}{\rho g C_D S_o V_s t_o} \qquad \text{(A4-6)}$$

*Parachutes tested in vertical fall exhibit an opening shock force of 1g greater than horizontally deployed canopies. This is a limitation on the development.

One of the variables in the BMR is the inflation distance, $V_s t_o$, which is the product of the system velocity at line stretch, V_s, and the reference opening time, t_o.

$$V_s t_o = \frac{14W}{\rho g C_D S_o} \left[\varepsilon^{\left[\frac{g\rho V_o}{2W} \left[\frac{C_D S_o}{A_{Mo} - A_{so}\, k \left(\frac{C_p \rho}{2} \right)^{1/2}} \right] \right]} - 1 \right] \qquad \text{(A7-14)}$$

Note that when:

$$0 = A_{Mo} - A_{so}\, k \left(\frac{C_p \rho}{2} \right)^{1/2} \qquad (4)$$

a critical inflation condition exists, and at any test velocity the t_o time is infinite. As altitude increases, the density ρ approaches zero and equation (4) becomes positive and the parachute will inflate. For imporous canopies k=0 and the parachute always inflates. These boundary conditions agree with general field test experience.

The inflation distance is not dependent on the test velocity V_s. Rather it is a function of system weight, w, and density altitude, ρ; the steady-state geometric characteristics of the particular type of parachute, and drag area, $C_D S_o$; volume, $\underline{V}_o$; mouth area, A_{Mo}; Surface area, $A_{so}=S_o$; cloth airflow properties, k and n; and average pressure coefficient, C_{pav}.

The average pressure coefficient for the steady-state parachute was determined as follows:

The steady-state drag force, in a wind tunnel for example, may be written

$$F = qC_D S_o$$

but it may also be written

$$F = \Delta P_{av} S_p$$

where S_p is the projected area of the inflated canopy and ΔP is the average pressure differential acting on S_p.

$$\Delta P_{av} S_p = F = qC_D S_o$$

$$C_{P_{av}} = \frac{\Delta P_{av}}{q} = \frac{C_D S_o}{S_p}$$

$$S_o = \frac{\pi}{4} D_o^2 \text{ and } S_p = \frac{\pi}{4} D_p^2$$

$$\frac{S_o}{S_p} = \left(\frac{D_o}{D_p}\right)^2 = \frac{1}{\left(\frac{D_p}{D_o}\right)^2}$$

$$C_{p_{av}} = \frac{C_D}{\left(\frac{D_p}{D_o}\right)^2} \tag{5}$$

Ratios of D_p/D_o from Reference 2 are presented in Table 1 for several types of parachutes.

TABLE 1. RANGE OF AVERAGE STEADY STATE CANOPY PRESSURE COEFFICIENTS

PARACHUTE TYPE	C_D RANGE	D_p/D_o RANGE	$C_{p_{av}}$ RANGE
FLAT CIRCULAR	0.75 0.80	0.70 0.67	1.531 1.782
EXTENDED SKIRT	0.78 0.87	0.70 0.66	1.592 1.997
CROSS	0.60 0.78	0.72 0.66	1.157 1.791

For a flat circular parachute with a C_D=0.75 and D_p/D_o=0.67

$$C_{P_{av}} = \frac{0.75}{(0.67)^2}$$

$$C_{P_{av}} = 1.671$$

It may be concluded that the average steady-state canopy pressure coefficient is the canopy drag coefficient based on the projected area. The inflation geometry as a function of t/t_o is constant with altitude. It can be deduced from this that if the inflating geometry is independent of altitude, the forces which cause the geometry to develop must also be independent of altitude. These forces come from the pressure distribution along the gore panel. Therefore, at any given t/t_o a definite, repeatable pressure distribution exists which varies with t/t_o, but is constant for all altitudes and the C_{pav} is constant with altitude.

The Air Force Flight Dynamics Laboratory conducted field tests of a 28-foot (D_o) Solid Flat Circular Parachute (SFCP) system at altitudes of 6,000, 13,000, and 21,000 feet. A result of these tests was the demonstration of the repeatability of the canopy projected area to surface area ratio at all test altitudes. With the data of Figure 5 the average steady-state pressure coefficients for the 28-foot SFCP can be estimated.

$$C_{P_{av}} = \frac{C_D S}{S_p}$$

$$C_D S = C_D S_o \left[(1-\eta)\left(\frac{t}{t_o}\right)^3 + \eta\right]^2$$

$$C_{P_{av}} = \frac{C_D}{S_p/S_o}\left[(1-\eta)\left(\frac{t}{t_o}\right)^3 + \eta\right]^2 \qquad (6)$$

for $0 \leq t/t_o \leq 0.3$

$$C_{P_{av}} = \frac{C_D\left[(1-\eta)\left(\frac{t}{t_o}\right)^3 + \eta\right]^2}{0.0024 + 0.07843\left(\frac{t}{t_o}\right)} \qquad (6a)$$

for $0.3 \leq t/t_o \leq 1.0$

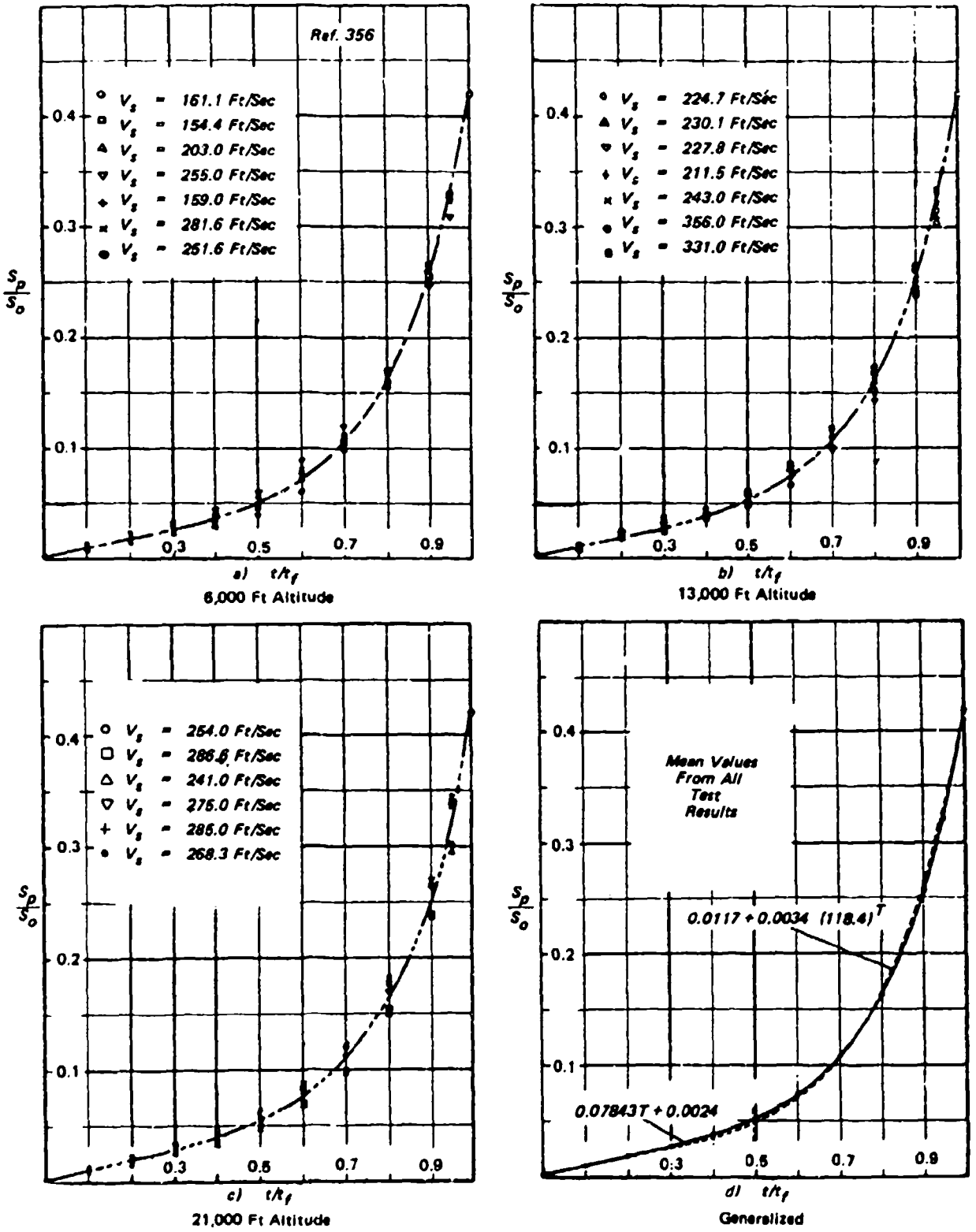

Reproduced from reference 2, page 245

FIGURE 5. NORMALIZED CANOPY AREA GROWTH DURING INFLATION OF 28 FT (D_o) SOLID FLAT CIRCULAR PARACHUTE

$$C_{P_{av}} = \frac{C_D \left[(1-\eta) \left(\frac{t}{t_o} \right)^3 + \eta \right]^2}{0.0117 + 0.0034\ (118.4)^{t/t_o}} \qquad (6b)$$

Figure 6 shows the estimated C_{pav} for the following conditions: $C_D = 0.75$; $\eta = 0.0024$; $t_o = t_f$; and the two variations of S_p/S_o as a function of t/t_f in Figure 5. Cloth air flow properties "k" and "n" may be evaluated by the methods of formulae (A13-29) and (A13-30). Another method is to adapt a least squares fit through the data points. A true average value of k and n in any given parachute requires a large number of permeameter rate of air flow tests due to the variation of the woven cloth air flow rates. Their values may also vary for different parachutes in the same lot. This is most likely one of the causes of performance variations for similar test conditions.

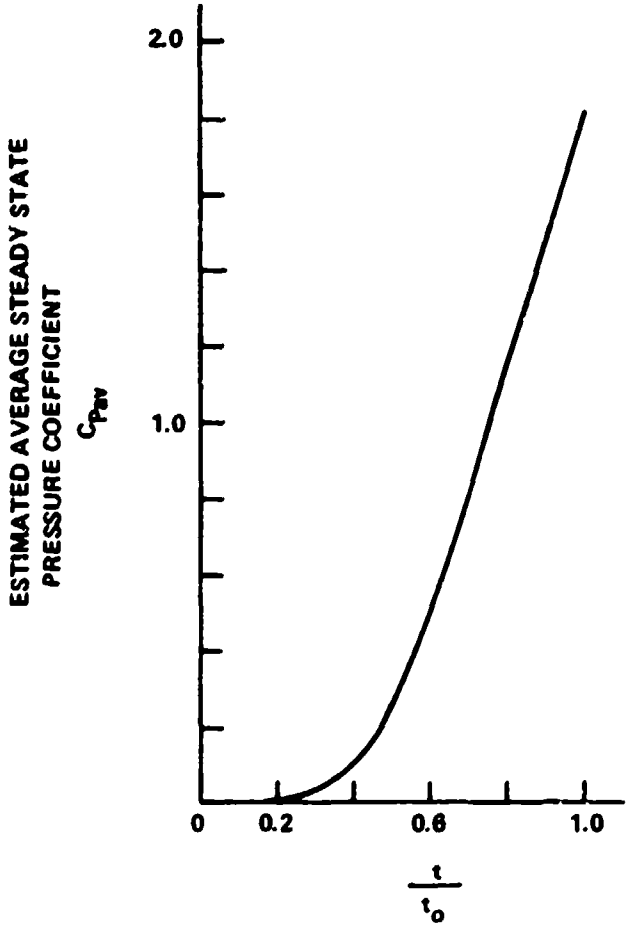

FIGURE 6. ESTIMATED STEADY STATE AVERAGE PRESSURE COEFFICIENT FOR THE INFLATING 28 FT (Do) SOLID FLAT CIRCULAR PARACHUTE OF FIGURE 5

The inflation time and distance may also be calculated by equation (A7-13). In this equation the actual value of "n" for cloth airflow properties is used rather than the assumed value of "n"=1/2. At low altitudes (A7-13) yields a better value of inflation distance than (A7-14).

DEVELOPMENT OF ALTERNATE ALTITUDE TESTING

The drag-area signature is independent of altitude, velocity, and system mass, Reference 1, while the velocity ratio is dependent on the BMR,M. Since the shock factor is a function of the velocity ratio, it is also a function of the BMR,M. For alternative altitude testing, the forces generated may be duplicated at other density altitudes by testing at a constant BMR. The requirements for generating a constant BMR are to adjust the system weight for the particular density altitude desired. Note that density altitude is stressed as this may vary from geometric altitude or pressure altitude used for some altimeters.

Replacement of the inflation distance in the BMR equation (A4-6) by its equivalent (A7-14) results in:

$$\text{Let} \qquad K1 = \frac{g\rho V_o}{2W}\left[\frac{C_D S_o}{A_{Mo} - A_{so}\, k\left(\frac{C_p\rho}{2}\right)^{1/2}}\right]$$

$$M = \frac{2W}{\rho g C_D S_o \times \frac{14W}{\rho g C_D S_o}\left[\varepsilon^{K1}-1\right]} = \frac{1}{7\left[\varepsilon^{K1}-1\right]}$$

$$\varepsilon^{K1} = 1 + \frac{1}{7M}$$

$$K1 = \ln\left(1 + \frac{1}{7M}\right) \tag{7}$$

Solving for the required weight as a function of density altitude.

$$W = \frac{g\rho V_o}{2 \ln\left[1 + \frac{1}{7M}\right]}\left[\frac{C_D S_o}{A_{Mo} - A_{So}\, k\left(\frac{C_p\rho}{2}\right)^{1/2}}\right] \tag{8}$$

The inflation distance at any alternate density altitude is determined by equation (A7-14) and the required weight.

$$V_s t_o = \frac{14W}{\rho g C_D S_o} \left[\epsilon^{\ln\left(1 + \frac{1}{7M}\right)_{-1}} \right] \tag{9}$$

DETERMINATION OF REQUIRED TEST VELOCITY

Since the steady-state drag force is a function of altitude, the steady-state force will remain constant if the tests are conducted at constant dynamic pressure. The dynamic pressure at the original density altitude must be equal to the test altitude.

$$\text{original } q_s = \text{test } q_{ST}$$

$$V_{ST} = V_s \sqrt{\frac{\rho/\rho_{SL}}{\rho_T/\rho_{SL}}} \tag{10}$$

ρ/ρ_{SL} = density ratio at original requirement altitude

ρ_T/ρ_{SL} = density ratio at alternate altitude

INFLATION REFERENCE TIME

The inflation reference time, t_o, at each altitude is calculated for the conditions at that altitude.

$$t_o = \frac{V_{ST}\ t_o}{V_{ST}} \tag{11}$$

Example 2: In order to illustrate the theory developed, a sample problem shall be used.

Problem: A T-10 type parachute is to be tested horizontally at a density altitude of 80,000 feet at 300 feet per second test velocity. The system weight is 250 lb.

Determine: Alternate test altitudes to obtain the same maximum opening shock force.

Solution: For a T-10 type parachute the diameter is D_o=35 ft and the drag area is 721 ft^2

Determine the steady-state parachute geometry, C_{pav}, and cloth air-flow constants k and n.

From Table 2, page (A14) for a 10 percent Extended Skirt parachute of 30 gores

$$\frac{2\bar{a}}{D_o} = 0.650 \; ; \; \frac{N}{\bar{a}} = 0.825 \; ; \; \frac{b}{\bar{a}} = 0.6255 \; ; \; \frac{b'}{\bar{a}} = 0.7962$$

$$\bar{a} = \frac{0.650\ D_o}{2} = \frac{0.650 \times 35}{2} = 11.375 \text{ ft.}$$

The steady-state mouth area, A_{Mo}.

$$A_{Mo} = \pi \bar{a}^2 \left[1 - \left(\frac{N/\bar{a} - b/\bar{a}}{b'/\bar{a}}\right)^2\right] \tag{12}$$

$$A_{Mo} = \pi(11.375)^2 \left[1 - \left(\frac{0.825 - 0.6255}{0.7962}\right)^2\right]$$

$$A_{Mo} = 381 \text{ ft}^2$$

The steady-state canopy volume, $\underline{V}_o$

$$\underline{V}_o = \frac{2}{3} \pi \bar{a}^3 \left[\frac{b}{\bar{a}} + \frac{b'}{\bar{a}}\right] \tag{A14-31}$$

$$\underline{V}_o = \frac{2}{3} \pi(11.375)^3 \, [0.6255 + 0.7962]$$

$$\underline{V}_o = 4382 \text{ ft}^3$$

The cloth air-flow constants, k and n, were determined for the Mil-C-7020, type III Cloth, using the methods on page A-13.

$$k = \frac{87.6255}{60} = 1.46$$

$$n = 0.63246$$

The term, k, as determined for the nominal permeability has units of ft/min. However, calculations are based on ft/sec., hence the division by 60. The average pressure coefficient was taken as C_{pav}=1.7.

Determine the BMR at 80,000 feet

a. Use equation (A7-14) to determine inflation distance

$$V_s t_o = \frac{14W}{\rho g C_D S_o} \left[\varepsilon \frac{g\rho \underline{V}_o}{2W} \left[\frac{C_D S_o}{A_{Mo} - A_{so}\, k \left(\frac{C_p \rho}{2} \right)^{1/2}} \right] - 1 \right]$$

b. Calculate the BMR from equation (A4-6)

$$M = \frac{2W}{\rho g C_D S_o V_s t_o}$$

This value is to be kept constant at all density altitudes.

Calculate the required weight and inflation distance at other density altitudes

a. Required weight from equation (8)

$$W = \frac{g\rho \underline{V}_o}{2 \ln \left[1 + \frac{1}{7M} \right]} \left[\frac{C_D S_o}{A_{Mo} - A_{So}\, k \left(\frac{C_p \rho}{2} \right)^{1/2}} \right]$$

b. Inflation distance from equation (9)

$$V_s t_o = \frac{14W}{\rho g C_D S_o} \left[\varepsilon \ln \left[1 + \frac{1}{7M} \right] - 1 \right] \qquad (9)$$

Determine test velocity at density altitude and inflation reference time t_o.

a. Test velocity from equation (10)

$$V_{ST} = V_s \sqrt{\frac{\rho / \rho_{SL}}{\rho_T / \rho_{SL}}} \qquad (10)$$

b. Inflation reference time at the particular density altitude from equation (11)

$$t_o = \frac{V_{ST}\, t_o}{V_{ST}} \qquad (11)$$

The results of these calculations are summarized in Table 2 and graphically illustrated in Figure 7.

The solution of example 2 using eq. (A7-13) requires the use of a computer due to the value of "n".

$$\underline{V}_o = A_{Mo} V_s t_{oM} \ln\left[1 + \frac{1}{7M}\right] - A_{so}\, k \left(\frac{C_{P_{av}}\, \rho}{2}\right)^n V_s^{2n} \int_o^t \frac{\left(\frac{t}{t_o}\right)^6 dt}{\left[1 + \frac{1}{7M}\left(\frac{t}{t_o}\right)^7\right]^{2n}} \quad \text{(A7-13)}$$

A method of calculation is as follows:

a) For the given density altitude determine the test velocity, V_{ST}, eq (10).
b) Let $dt = t_o/10{,}000$
c) Assume a value of t_o and compute $\underline{V}_o$ for the system parameters listed in the heading of Table 2.
d) Compare the computed canopy volume with the previously calculated canopy volume of 4382 ft^3.
e) If the computed canopy volume does not agree with the 4382 ft^3 within a specified limit of $\pm$ 5 ft^3 then correct t_o and iterate again.
f) Let

$$to = \frac{4382\ t_o}{\underline{V}_{o\ \text{computed}}}$$

g) Calculate the inflation distance.

$$V_s t_o = V_s \times t_o$$

h) Determine the weight required for M = 2.950

$$W = \frac{\rho g C_D S_o V_s t_o M}{2}$$

The integral of equation (A7-13) has an interesting property in that if the integrated function for any altitude is divided by the t_o time for that altitude a constant value at all altitudes is obtained, as shown in Table 3.

TABLE 2. SUMMARY OF CALCULATIONS FOR THE ALTERNATE ALTITUDES OF EXAMPLE 2.

TEST CONDITIONS @ 60,000 FEET				
WEIGHT = 250 LB	A_{MO} = 381 FT^2	k = 1.46	M = 2.950
D_O = 35 FT	$C_D S_O$ = 721 FT^2	n = 0.63246	V_S = 300 FPS
$A_{SO} = S_O$ = 962 FT^2	$\forall_O$ = 4382 FT^3	C_{Pav} = 1.7	F_S = 2782 LB

			Eq (A6 – 14); n = 1/2			Eq (A6 – 13); n = 0.63246		
DENSITY ALTITUDE KILOFEET	ρ/ρ_O	V_{ST} FPS	W LB	$V_S t_O$ FT	t_O SEC	W LB	$V_S t_O$ FT	t_O SEC
80	0.03606	300.0	250.0	85.12	0.284	252.9	86.14	0.287
70	0.05856	235.4	409.7	85.89	0.365	415.9	87.21	0.370
60	0.09492	184.9	671.6	86.88	0.470	684.9	88.61	0.479
50	0.15311	145.6	1099.4	88.16	0.606	1127.6	90.44	0.621
40	0.24708	114.6	1808.0	89.84	0.784	1868.6	92.87	0.810
30	0.37473	93.1	2800.3	91.75	0.986	2916.5	95.67	1.028
20	0.53316	78.0	4072.9	93.79	1.202	4286.5	98.73	1.266
10	0.73859	66.3	5783.1	96.14	1.450	6153.4	102.31	1.543
0	1.00000	57.0	8048.6	98.82	1.735	8673.4	106.51	1.869

TABLE 3. RATIO OF THE INTEGRAL OF EQUATION (A6-13) TO THE INFLATION REFERENCE TIME FOR EXAMPLE 2

$$B = \int_0^{t_o} \frac{\left(\frac{t}{t_o}\right)^6 dt}{\left[1 + \frac{1}{7M}\left(\frac{t}{t_o}\right)^7\right]^{2n}}$$

M = 2.950
n = 0.63246

ALTITUDE THOUSANDS OF FEET	t_O SEC	B SEC	$\frac{B}{t_O}$
80	0.28713	0.04256	0.14823
70	0.37048	0.05492	0.14823
60	0.47924	0.07104	0.14823
50	0.62114	0.09207	0.14823
40	0.81041	0.12013	0.14823
30	1.02758	0.15232	0.14823
20	1.26578	0.18762	0.14823
10	1.54312	0.22874	0.14823
0	1.86861	0.27698	0.14823

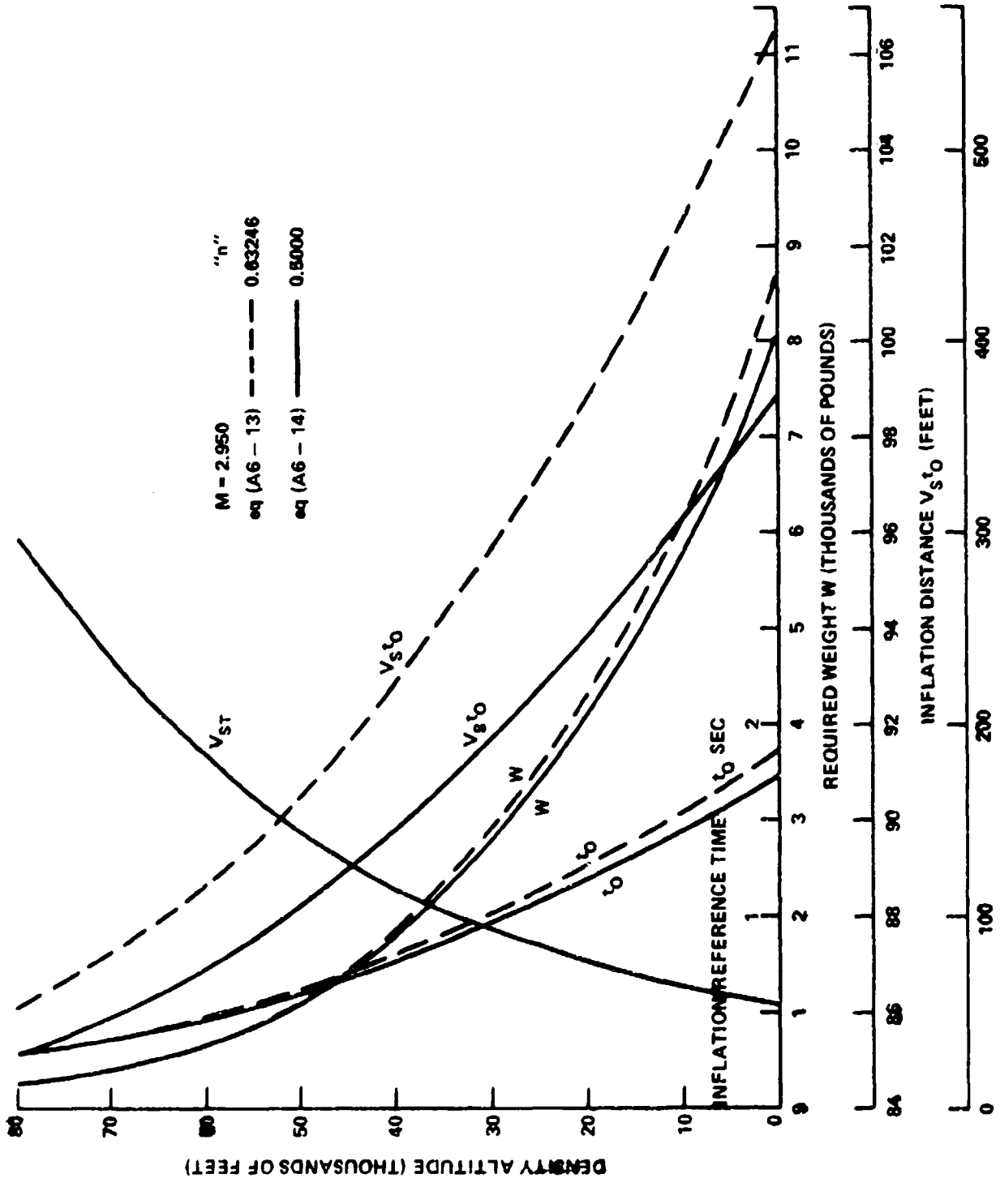

FIGURE 7. EFFECT OF CLOTH AIR FLOW PARAMETER "n" ON THE REQUIRED SYSTEM WEIGHT, INFLATION DISTANCE, AND INFLATION REFERENCE TIME FOR ALTERNATE DENSITY ALTITUDES AT CONSTANT BALLISTIC MASS RATIO FOR EXAMPLE 2

Let $$B = \int_0^{t_o} \frac{\left(\frac{t}{t_o}\right)^6 dt}{\left[1 + \frac{1}{7M}\left(\frac{t}{t_o}\right)^7\right]^{2n}}$$

The integral of "B" is illustrated in Table 4 for various values of BMR and n. With these data the t_o time of eq (A7-13) may be calculated.

$$\underline{V}_o = t_o \left[A_{Mo}\, V_s\, M \ln\left[1 + \frac{1}{7M}\right] - A_{so}\, k\left(\frac{C_{Pav}\,\rho}{2}\right)^n V_s^{2n} \left(\frac{B}{t_o}\right)\right] \qquad (13)$$

For an imporous solid cloth parachute canopy, k = 0 and

$$t_o = \frac{\underline{V}_o}{A_{Mo}\, V_s\, M \ln\left[1 + \frac{1}{7M}\right]} \qquad (13a)$$

Assume a value of t_o and calculate the BMR. For the known values of "BMR" and "n" interpolate "B/t_o" from Table 4 and calculate t_o using eq (13). Figure 8 illustrates a method for limiting the number of required calculations by plotting the assumed and calculated t_o values. The desired t_o is the particular value at the intersection of the plotted data and the locus of the t_o assumed equals t_o calculated line.

OPENING SHOCK FORCE

If the maximum shock force occurs in the finite mass regime, then the time of occurrence during the inflation process is determined by:

$$\left(\frac{t}{t_o}\right)_{@\, x_{imax}} = \left(\frac{21M}{4}\right)^{1/7}$$

and the maximum shock factor

$$x_{imax} = \frac{16}{49}\left(\frac{21M}{4}\right)^{6/7} \qquad (A5\text{-}10)$$

The limiting BMR for finite mass operation, see Appendix C, is the mass ratio which causes the maximum shock to occur when $t = t_o$.

$$1 = \left(\frac{21M}{4}\right)^{1/7}$$

TABLE 4. RATIO OF THE INTEGRAL OF EQUATION (A7-13) TO THE INFLATION REFERENCE TIME FOR VARIOUS VALUES OF "BMR" AND "n"

$$\frac{B}{t_o} = \frac{1}{t_o}\int_0^{t_o} \frac{\left(\frac{t}{t_o}\right)^6 dt}{\left[1+\frac{1}{7M}\left(\frac{t}{t_o}\right)^7\right]^{2n}}$$

M	n					
	0.5000	0.6000	0.7000	0.8000	0.9000	1.0000
0.010	0.02727	0.02102	0.01660	0.01342	0.01109	0.00934
0.020	0.04195	0.03426	0.02839	0.02386	0.02033	0.01754
0.030	0.05255	0.04403	0.03778	0.03252	0.02826	0.02479
0.040	0.06081	0.05243	0.04556	0.03989	0.03518	0.03125
0.050	0.06751	0.03916	0.05216	0.04627	0.04128	0.03704
0.060	0.07311	0.06488	0.05786	0.05186	0.04670	0.04226
0.070	0.07787	0.06982	0.06285	0.05681	0.05156	0.04698
0.080	0.08198	0.07413	0.06726	0.06124	0.05595	0.05129
0.090	0.08558	0.07793	0.07119	0.06522	0.05992	0.05522
0.100	0.08876	0.08133	0.07471	0.06891	0.06355	0.05883
0.125	0.09530	0.08839	0.08214	0.07648	0.07134	0.06668
0.150	0.10039	0.09396	0.08808	0.08268	0.07773	0.07319
0.175	0.10448	0.09849	0.09294	0.08781	0.08307	0.07867
0.200	0.10784	0.10223	0.09700	0.09213	0.08759	0.08336
0.225	0.11065	0.10539	0.10045	0.09582	0.09148	0.08740
0.250	0.11304	0.10806	0.10341	0.09900	0.09485	0.09094
0.275	0.11510	0.11041	0.10598	0.10178	0.09781	0.09405
0.300	0.11689	0.11245	0.10824	0.10423	0.10042	0.09681
0.325	0.11846	0.11425	0.11023	0.10640	0.10275	0.09927
0.350	0.11985	0.11584	0.11201	0.10834	0.10484	0.10149
0.375	0.12110	0.11727	0.11360	0.11008	0.10672	0.10349
0.400	0.12221	0.11855	0.11504	0.11166	0.10842	0.10530
0.425	0.12321	0.11971	0.11634	0.11309	0.10997	0.10696
0.450	0.12413	0.12076	0.11752	0.11440	0.11138	0.10848
0.475	0.12496	0.12173	0.11861	0.11559	0.11268	0.10987
0.500	0.12572	0.12261	0.11960	0.11669	0.11388	0.11116
0.525	0.12642	0.12342	0.12052	0.11771	0.11498	0.11235
0.550	0.12706	0.12417	0.12136	0.11865	0.11601	0.11345
0.575	0.12766	0.12486	0.12215	0.11952	0.11696	0.11448
0.600	0.12821	0.12551	0.12288	0.12033	0.11785	0.11543
0.625	0.12872	0.12611	0.12356	0.12108	0.11867	0.11633
0.650	0.12920	0.12667	0.12420	0.12179	0.11945	0.11717
0.675	0.12965	0.12719	0.12479	0.12245	0.12018	0.11796
0.700	0.13007	0.12768	0.12535	0.12308	0.12086	0.11870
0.725	0.13046	0.12814	0.12588	0.12366	0.12150	0.11939
0.750	0.13083	0.12857	0.12637	0.12422	0.12211	0.12005
0.775	0.13118	0.12898	0.12684	0.12474	0.12268	0.12068
0.800	0.13151	0.12937	0.12728	0.12523	0.12323	0.12127
0.825	0.13182	0.12974	0.12770	0.12570	0.12374	0.12183
0.850	0.13212	0.13008	0.12809	0.12614	0.12423	0.12236
0.875	0.13239	0.13041	0.12847	0.12656	0.12469	0.12286
0.900	0.13266	0.13072	0.12882	0.12696	0.12514	0.12334
0.925	0.13291	0.13102	0.12916	0.12734	0.12556	0.12380
0.950	0.13315	0.13130	0.12949	0.12771	0.12596	0.12424
0.975	0.13338	0.13157	0.12980	0.12805	0.12634	0.12466
1.000	0.13360	0.13183	0.13009	0.12839	0.12671	0.12506
1.500	0.13553	0.13529	0.13407	0.13287	0.13168	0.13050
2.000	0.13806	0.13711	0.13617	0.13524	0.13432	0.13340
2.500	0.13900	0.13823	0.13747	0.13671	0.13595	0.13521
3.000	0.13964	0.13899	0.13834	0.13770	0.13707	0.13644
3.500	0.14010	0.13954	0.13898	0.13843	0.13788	0.13733
4.000	0.14044	0.13995	0.13946	0.13897	0.13849	0.13800
4.500	0.14071	0.14027	0.13984	0.13940	0.13897	0.13854
5.000	0.14093	0.14054	0.14014	0.13975	0.13935	0.13896
5.500	0.14111	0.14075	0.14039	0.14003	0.13967	0.13932
6.000	0.14126	0.14093	0.14060	0.14027	0.13994	0.13961
6.500	0.14139	0.14108	0.14077	0.14047	0.14016	0.13986
7.000	0.14150	0.14121	0.14093	0.14064	0.14036	0.14008
7.500	0.14159	0.14133	0.14106	0.14079	0.14053	0.14026
8.000	0.14168	0.14142	0.14117	0.14092	0.14068	0.14043
8.500	0.14175	0.14151	0.14128	0.14104	0.14081	0.14057
9.000	0.14181	0.14159	0.14137	0.14115	0.14092	0.14070
9.500	0.14187	0.14166	0.14145	0.14124	0.14103	0.14082
10.000	0.14193	0.14172	0.14152	0.14132	0.14112	0.14092
10.500	0.14197	0.14178	0.14159	0.14140	0.14121	0.14102
11.000	0.14202	0.14183	0.14165	0.14147	0.14129	0.14110
11.500	0.14206	0.14188	0.14171	0.14153	0.14136	0.14118
12.000	0.14209	0.14192	0.14176	0.14159	0.14142	0.14125
12.500	0.14213	0.14196	0.14180	0.14164	0.14148	0.14132
13.000	0.14216	0.14200	0.14185	0.14169	0.14154	0.14138
13.500	0.14219	0.14204	0.14189	0.14174	0.14159	0.14144
14.000	0.14221	0.14207	0.14192	0.14178	0.14164	0.14149
14.500	0.14224	0.14210	0.14196	0.14182	0.14168	0.14154
15.000	0.14226	0.14213	0.14199	0.14186	0.14172	0.14159

LISTED VALUES ARE VALID FOR ALL ALTITUDES

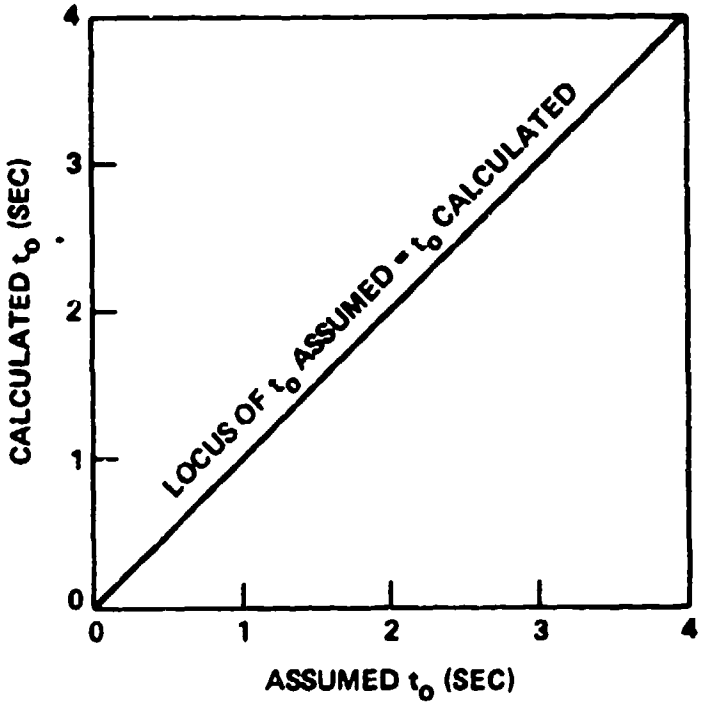

FIGURE 8. METHOD FOR LIMITING THE ITERATIONS IN CALCULATING "t_o" BY EQUATION 13

$$M_L = \frac{4}{21} = 0.1905 \qquad \text{(for } \eta = o\text{)}$$

BMR's greater than M_L require that the canopy's elasticity and structural strength be taken into account. The opening shock is defined again as

$$x_i = \frac{C_D S}{C_D S_o}\left(\frac{V}{V_s}\right)^2$$

$$\frac{C_D S}{C_D S_o} = \left(\frac{t}{t_o}\right)^6$$

$$\frac{V}{V_s} = \frac{1}{\frac{V_s}{V_o} + \frac{1}{7M}\left[\left(\frac{t}{t_o}\right)^7 - 1\right]} \qquad \text{(A9-17)}$$

$$\frac{V_o}{V_s} = \frac{1}{1 + \frac{1}{7M}} \qquad \text{(A9-18)}$$

$$x_i = \frac{\left(\frac{t}{t_o}\right)^6}{\left[\frac{V_s}{V_o} + \frac{1}{7M}\left[\left(\frac{t}{t_o}\right)^7 - 1\right]\right]^2} \qquad \text{(A9-19)}$$

Where the BMR is the same as before and the subscript "o" refers to conditions at the time t_o. The point here is that the shock factor is still a function of the BMR and, that for a constant BMR, the shock factors and velocity ratios are the same at all density altitudes throughout the inflation process.

The maximum shock factor in the elastic range of operation is determined by the canopy constructed strength, F_c, and the ultimate material elongation, ϵ_{max}. When these properties remain constant, the maximum opening shock is constant with altitude.

$$x_{imax} = \frac{\left(\frac{t_f}{t_o}\right)^6}{\left[\frac{V_s}{V_o} + \frac{1}{7M}\left[\left(\frac{t_f}{t_o}\right)^7 - 1\right]\right]^2}$$

and the maximum shock force is

$$F_{max} = F_s \, x_{imax}$$

The BMR of 2.950 exceeds the finite mass limiting mass ratio, M_L=0.1905. Therefore the maximum opening shock force will occur after time t_o, and the constructed radial strength of the canopy and the ultimate material elongation must be included.

Calculate velocity ratio and shock factor at $t=t_o$.

$$\frac{V_o}{V_s} = \frac{1}{1 + \frac{1}{7M}} = 0.9538 \qquad \text{(A9-18)}$$

$$X_o = \left(\frac{V_o}{V_s}\right)^2 = 0.9098 \qquad \text{(A10-22)}$$

The steady-state drag force of the system at 80,000 feet

$$F_s = \frac{1}{2} \rho V_s^2 C_D S_o$$

$$F_s = \frac{1}{2} \times 8.575 \times 10^{-5} \times 300^2 \times 721$$

$$F_s = 2782 \text{ lb.}$$

Initial elongation of radials

$$\varepsilon_o = \frac{X_o F_s}{F_c} \varepsilon_{max} \qquad \text{where } F_c = 30 \text{ gores} \times \frac{550 \text{ lb}}{\text{gore}}$$

$$\varepsilon_o = \frac{0.9098 \times 2782}{30 \times 550} \times 0.22$$

$$\varepsilon_o = 0.0337$$

From Figure 15 on page (A10)

$$\frac{C_D S_{max}}{C_D S_o} = 1.07$$

The ratio of inflation time, t_f, to t_o is

$$\frac{t_f}{t_o} = \left(\frac{C_D S_{max}}{C_D S_o}\right)^{1/6} \qquad \text{(A10-24)}$$

$$\frac{t_f}{t_o} = (1.07)^{1/6}$$

$$\frac{t_f}{t_o} = 1.01134$$

The maximum shock factor at t_f

$$x_{imax} = \frac{\left(\frac{t_f}{t_o}\right)^6}{\left[\frac{V_s}{V_o} + \frac{1}{7M}\left[\left(\frac{t_f}{t_o}\right)^7 - 1\right]\right]^2} \qquad \text{(A9-19)}$$

$$x_{imax} = \frac{1.07}{\left[\frac{1}{.9538} + \frac{1}{7 \times 2.950}\left[(1.07)^{7/6} - 1\right]\right]^2}$$

$$x_{imax} = 0.9661$$

The maximum shock force is

$$F_{max} = F_s \, x_{imax}$$

$$F_{max} = 2782 \times 0.9661$$

$$F_{max} = 2688 \text{ lb}$$

COMPARISON OF OPENING SHOCK FORCES AT 80,000 FEET AND AT SEA LEVEL

It has been shown that the velocity ratios and shock factors are a function of the BMR, canopy constructed strength, and ultimate material elongation. If these quantities remain constant for all alternate altitudes and the tests are conducted at constant dynamic pressure, the sea level opening shock force is exactly equal to the shock force at 80,000 feet. The inflation times over which the forces are generated vary widely, but the maxima are the same. This effect is illustrated in Figure 9. When the drag area, velocity and dynamic pressure ratios, shock factor, and force are considered as a function of the time ratio, t/t_o, the performance during inflation is identical for all altitudes as shown in Figure 10.

EFFECT OF TEST METHOD ON CANOPY STRESS DISTRIBUTION

A truly effective alternate altitude test technique should provide a stress distribution during inflation which is the same as the stresses at the original altitude. The drag-area signature is associated with a definite inflated geometry at each t/t_o during inflation. Since the drag-area signature is independent of altitude, the associated geometry and pressure distribution are likewise independent. Use of a constant BMR at alternate altitudes means that the instantaneous dynamic pressure ratio is the same at all altitudes. At a given t/t_o, C_DS/C_DS_o is constant and therefore the geometry, r/r_o, is constant, and q/q_s is constant.

$$\sigma = \Delta P r$$

$$\sigma = C_{p_{av}} \, qr$$

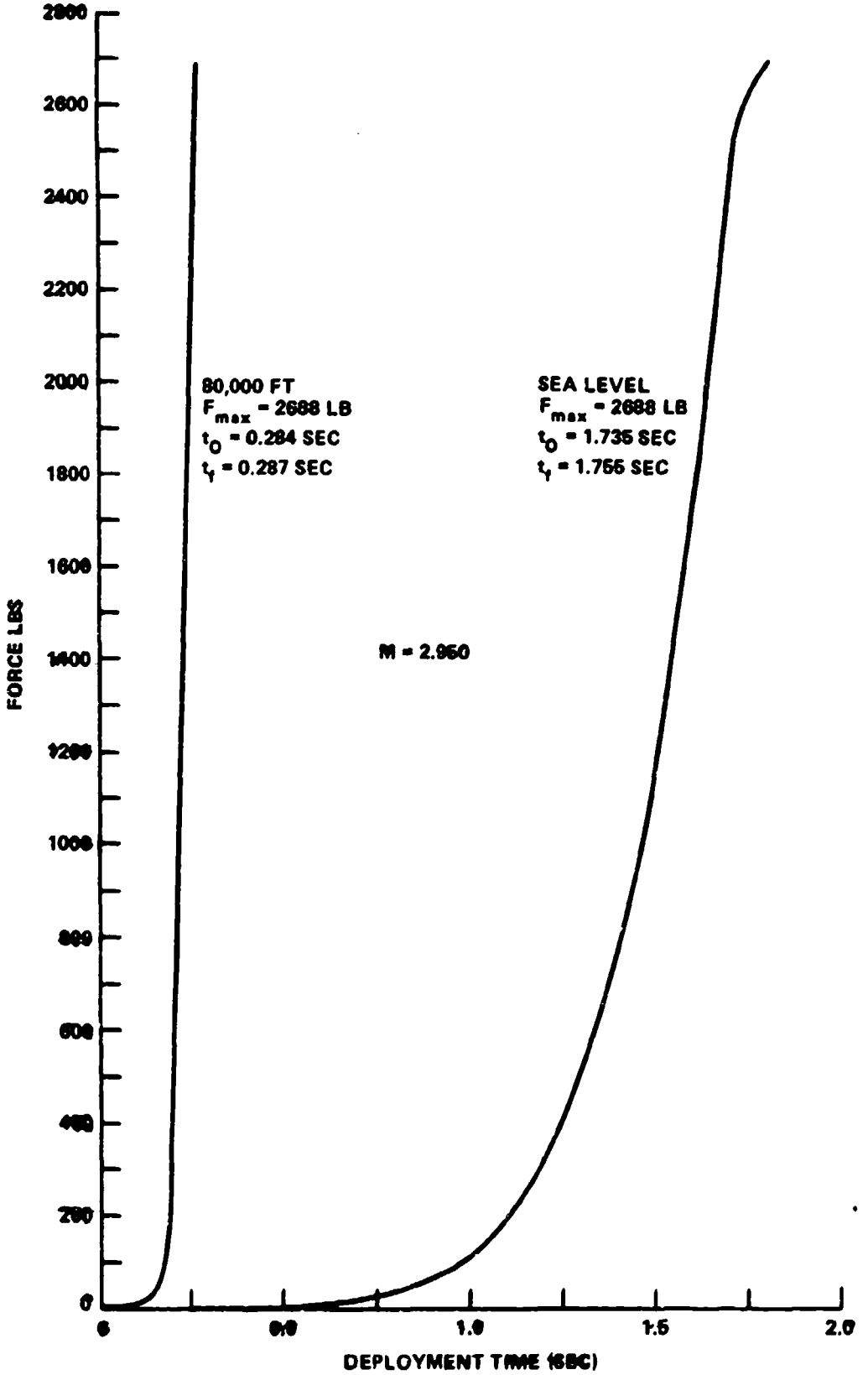

FIGURE 9. COMPARISON OF OPENING SHOCK FORCE VERSUS INFLATION REFERENCE TIME AT 80,000 FEET AND SEA LEVEL

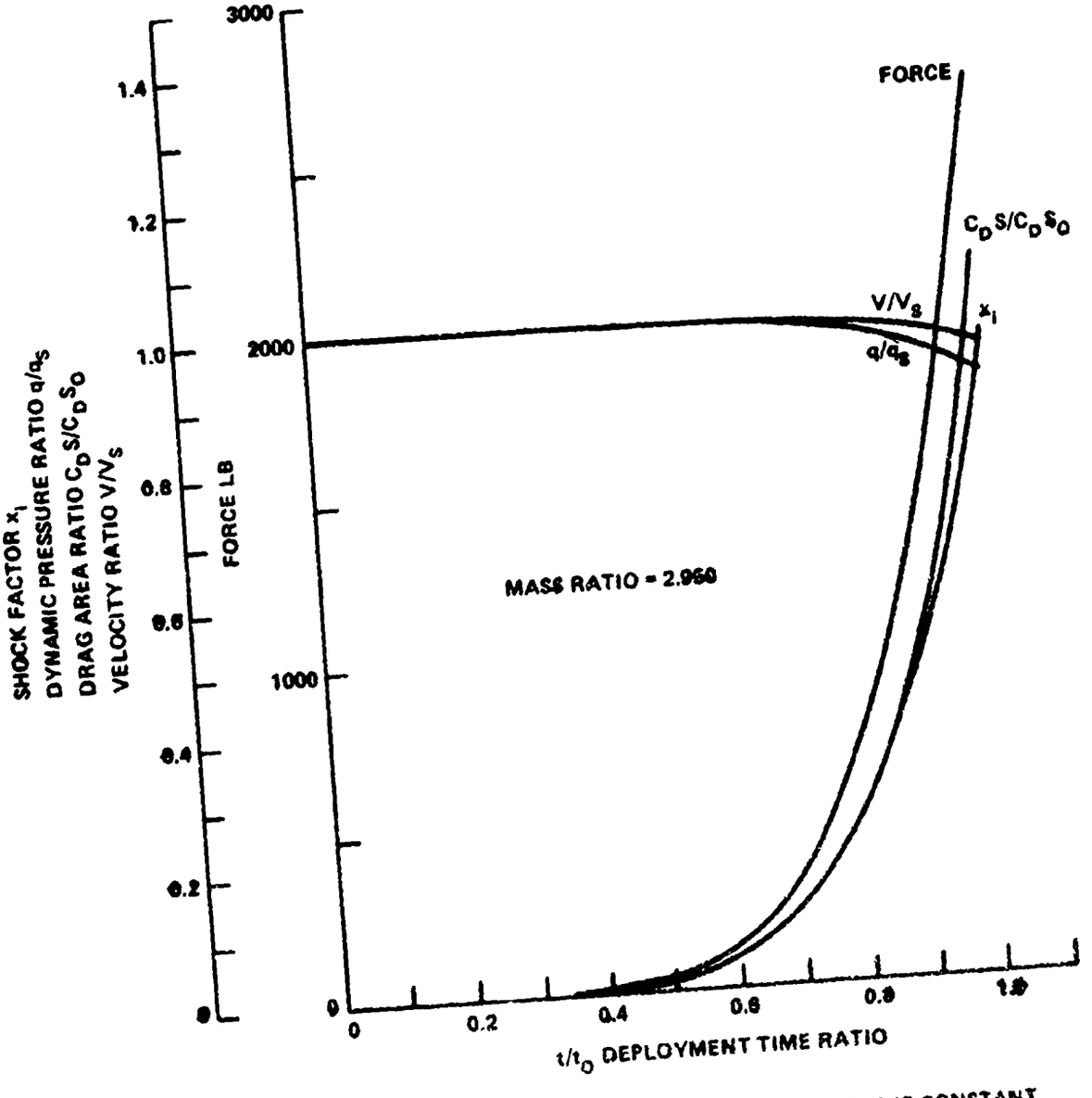

FIGURE 10. DEPLOYMENT PERFORMANCE AT ALL ALTITUDES FOR THE CONSTANT MASS RATIO FOR EXAMPLE 2

The $C_{P_{av}}$ is constant with altitude, then at a given t/t_o,

$$\sigma_{80} = f\left(C_{P_{av}}\right)\left(\frac{q}{q_s}\right)\left(\frac{r}{r_o}\right)$$

$$\sigma_{alt} = f\left(C_{P_{av}}\right)\left(\frac{q}{q_{st}}\right)\left(\frac{r}{r_o}\right)$$

$$\frac{\sigma_{80}}{\sigma_{alt}} = 1$$

The stress distributions are identical for all altitudes.

ALTERNATIVE ALTITUDE TEST METHOD

Reduction of the required test altitude is accomplished by an increase in the system mass and lowering the test velocity to maintain constant dynamic pressure. In example 2 the test goals may be achieved near sea level conditions if a test weight of 8048.6 pounds and a test velocity of 57 fps (38.9 mph) were used. The problem is to find a test vehicle which can lift that much weight at such a low velocity. Helicopters are one possibility; however, the effects of the rotors may affect test performance. Another possibility is the use of a truck with a tower mounted on it from which the test mass could be pulled during parachute deployment. For a parachute test altitude of one D_o from the lower hem of the parachute to the ground, a tower with a parachute centerline height of $D_o + \bar{a} = 46.4$ feet above the ground is required. A test rig like this may not be the most desirable system from the standpoint of personnel safety and tower wake effects. A third possibility is the use of a sled track where the test assembly can be launched from the edge of a cliff into undisturbed air. Barometric and temperature sensors permanently placed in the test area can provide a continuous monitoring of the test density altitude for correct vehicle weight and test velocity. The test vehicle can be built slightly under the programmed test weight and ballasted prior to the test for the proper mass for the test density altitude. The test mass is accelerated to a planned velocity by a truck type of reusable pusher. Upon braking the pusher disengages from the test mass which slides off the track muzzle at test velocity. A possible scenario is shown in Figure 11.

At sea level the equilibrium velocity of the system is:

$$V_e = \sqrt{\frac{2}{\rho}\frac{W}{C_D S_o}}$$

$$V_e = \sqrt{\frac{2}{0.002378} \times \frac{8048.6}{721}}$$

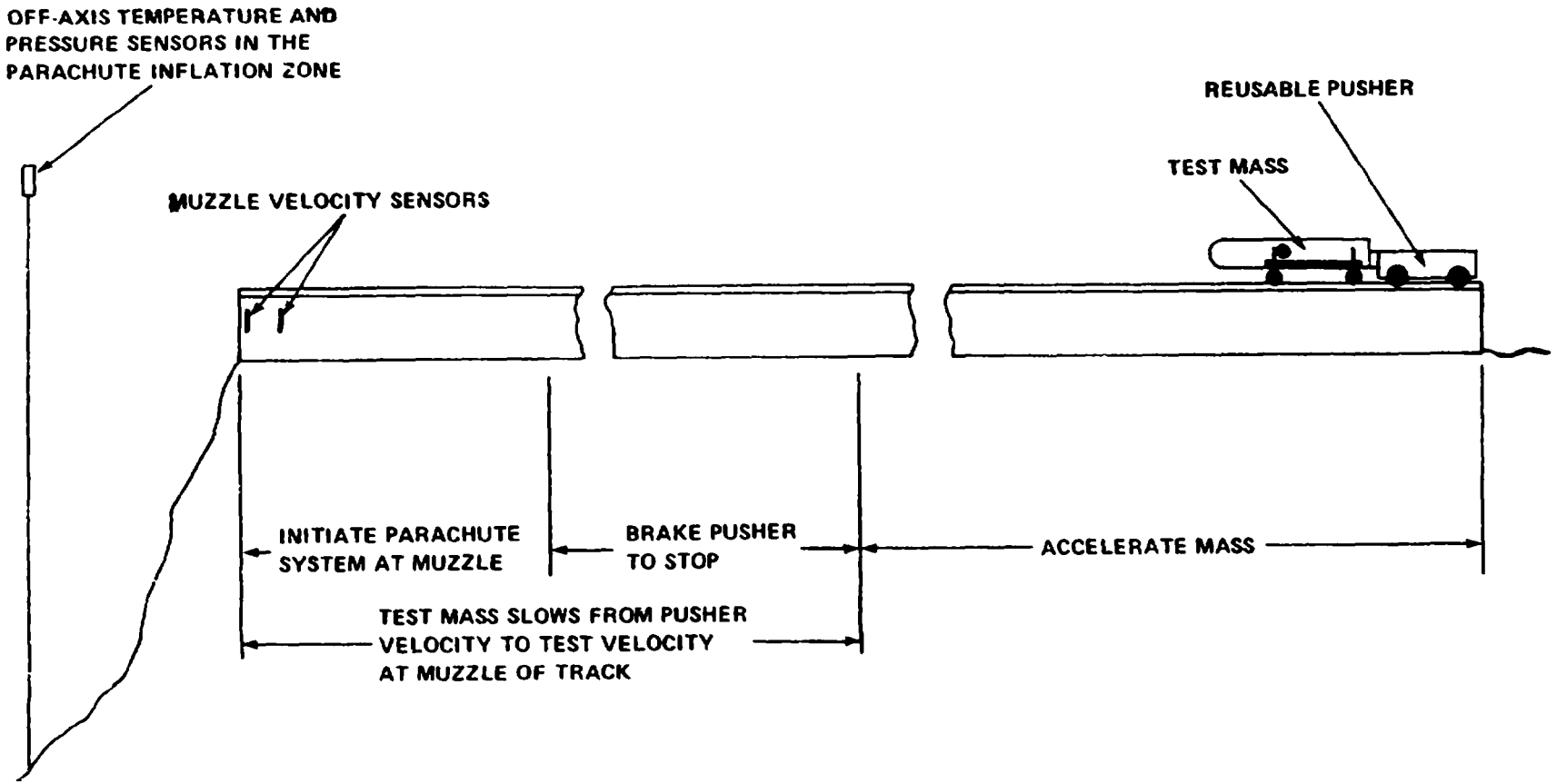

FIGURE 11. OFF THE CLIFF METHOD OF TESTING

V_e = 96.9 fps

and the on-board instrumentation must be shock mounted for impact velocities between 57 fps and 96.9 fps with consideration for the type of terrain to be encountered.

CARGO APPLICATION

Example 2 illustrated a method for performing high altitude parachute tests at lower altitudes. The alternate altitude testing proposition may also be extended to heavy cargo weights tested at low altitude and velocity. The possible advantage is that cargo weights, which require C-130 or similar aircraft as launch platforms, can be reduced to sizes which can be flown on aircraft that have multiple parent station wing racks utilizing existing test vehicles. The approach to testing parachute systems at higher altitude and velocity with lower system mass is similar to example 2, but in reverse. The method of analysis is similar to example 2 where for each altitude a particular system mass and test velocity are determined which maintain a constant BMR and hence maintain a constant opening shock force and canopy stress distributions. Some of the questions to be addressed are:

1. Does the increase in test altitude introduce unacceptable complexity in the data-acquisition process?

2. How is the required test altitude affected by system mass?

3. Is the required test dynamic pressure compatible with the available test aircraft?

Example 3 illustrates a typical analysis.

Example 3 - Various cargo weights of 4,000, 6,000, 8,000, and 10,000 pounds are to be delivered at 100 knots near sea level density altitude. The retardation system contains a solid cloth type parachute of Do = 135 feet diameter. Determine the alternate altitudes for aircraft with parent rack load capability of 2,400 and 3,000 pounds. The parachute geometry is taken as:

$$\frac{2\bar{a}}{D_o} = 0.668;\ \frac{b}{\bar{a}} = 0.6214;\ \frac{b'}{\bar{a}} = 0.7806;\ \frac{N}{\bar{a}} = 0.827$$

Therefore:

$\bar{a}$ = 45.090 ft; b = 28.019 ft; b' = 35.197 ft; N = 37.289 ft

$$S_o = A_{so} = \frac{\pi}{4} D_o^2 = 14{,}314 \text{ ft}^2$$

$$C_D S_o = 0.75 \times S_o = 10{,}735 \text{ ft}^2$$

$$A_{Mo} = \pi \bar{a}^2 \left[1 - \left(\frac{N/\bar{a} - b/\bar{a}}{b'/\bar{a}}\right)^2\right] = 5{,}944 \text{ ft}^2 \qquad (12)$$

$$\underline{V}_o = \frac{2}{3}\pi \bar{a}^3 \left[\frac{b}{a} + \frac{b'}{a}\right] = 269{,}183 \text{ ft}^3 \qquad (A14\text{-}31)$$

$k = 1.46$

$C_{P_{av}} = 1.7$

a. Use Equation (A7-14) to determine the sea level inflation distance.

$$V_s t_o = \frac{14W}{\rho g C_D S_o} \left[\varepsilon^{\frac{g\rho \underline{V}_o}{2W}\left[\frac{C_D S_o}{A_{MO} - A_{SO} k \left(\frac{C_p \rho}{2}\right)^{1/2}} - 1\right]}\right]$$

b. Calculate BMR from Equations (A4-6)

$$M = \frac{2W}{\rho g V_s t_o C_D S_o}$$

c. Calculate the required weight and inflation distance at other density altitudes.

$$W = \frac{g\rho \underline{V}_o}{2 \ln\left[1 + \frac{1}{7M}\right]} \left[\frac{C_D S_o}{A_{Mo} - A_{So} k \left(\frac{C_p \rho}{2}\right)^{1/2}}\right] \qquad (8)$$

$$V_{ST} t_o = \frac{14W}{\rho g C_D S_o} \left[\varepsilon^{\ln\left[1 + \frac{1}{7M}\right] - 1}\right] \qquad (9)$$

d. Calculate the required test velocity at other density altitudes

$$V_{ST} = V_{SL} \sqrt{\frac{\rho_o}{\rho}}$$

e. Calculate the reference inflation time at the particular density altitude.

$$t_o = \frac{V_{ST} t_o}{V_{ST}}$$

f. Calculate the time of occurrence of the maximum shock force during the inflation process

$$\frac{t}{t_{o@x_{imax}}} = \left(\frac{21M}{4}\right)^{\frac{1}{7}}$$

g. Calculate the maximum shock factor during the inflation process

$$x_{imax} = \frac{16}{49}\left(\frac{21M}{4}\right)^{\frac{6}{7}}$$

h. Calculate the maximum shock force

$$F_{max} = X_{imax} F_s = X_{imax} \frac{\rho_o}{2} V_{SL}^2 C_D S_o$$

The sea level characteristics of the various weights are tabulated in Table 5 and the effects of density altitudes up to 60,000 feet are plotted in Figures 12, 13, and 14.

TABLE 5. SEA LEVEL PARACHUTE SYSTEM CHARACTERISTICS FOR THE VARIOUS SYSTEM WEIGHTS OF EXAMPLE 3

WEIGHT lb.	INFLATION DISTANCE ft.	BMR	$t/t_o @ X_{i\,max}$	$X_{i\,max}$	MAXIMUM FORCE lb.
4000	16,962	5.748×10^{-4}	.43647	2.258×10^{-3}	833
6000	3,953	3.698×10^{-3}	.56943	1.113×10^{-3}	4106
8000	2,018	9.655×10^{-3}	.65311	2.534×10^{-2}	9348
10000	1,381	1.764×10^{-2}	.71187	4.249×10^{-2}	15670

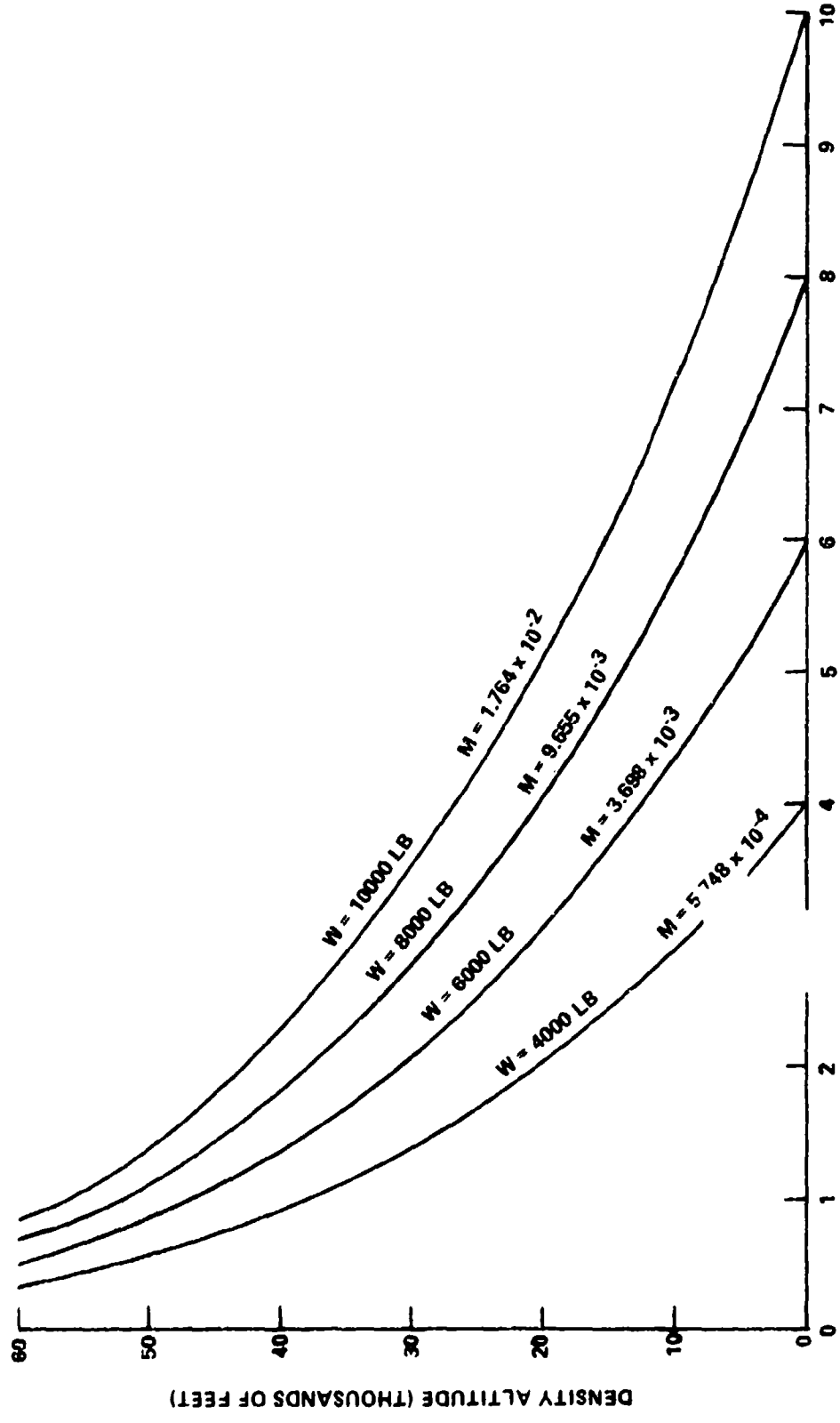

FIGURE 12. EFFECT OF DENSITY ALTITUDE ON THE REQUIRED SYSTEM WEIGHT FOR A CONSTANT BALLISTIC MASS RATIO FOR EXAMPLE 3

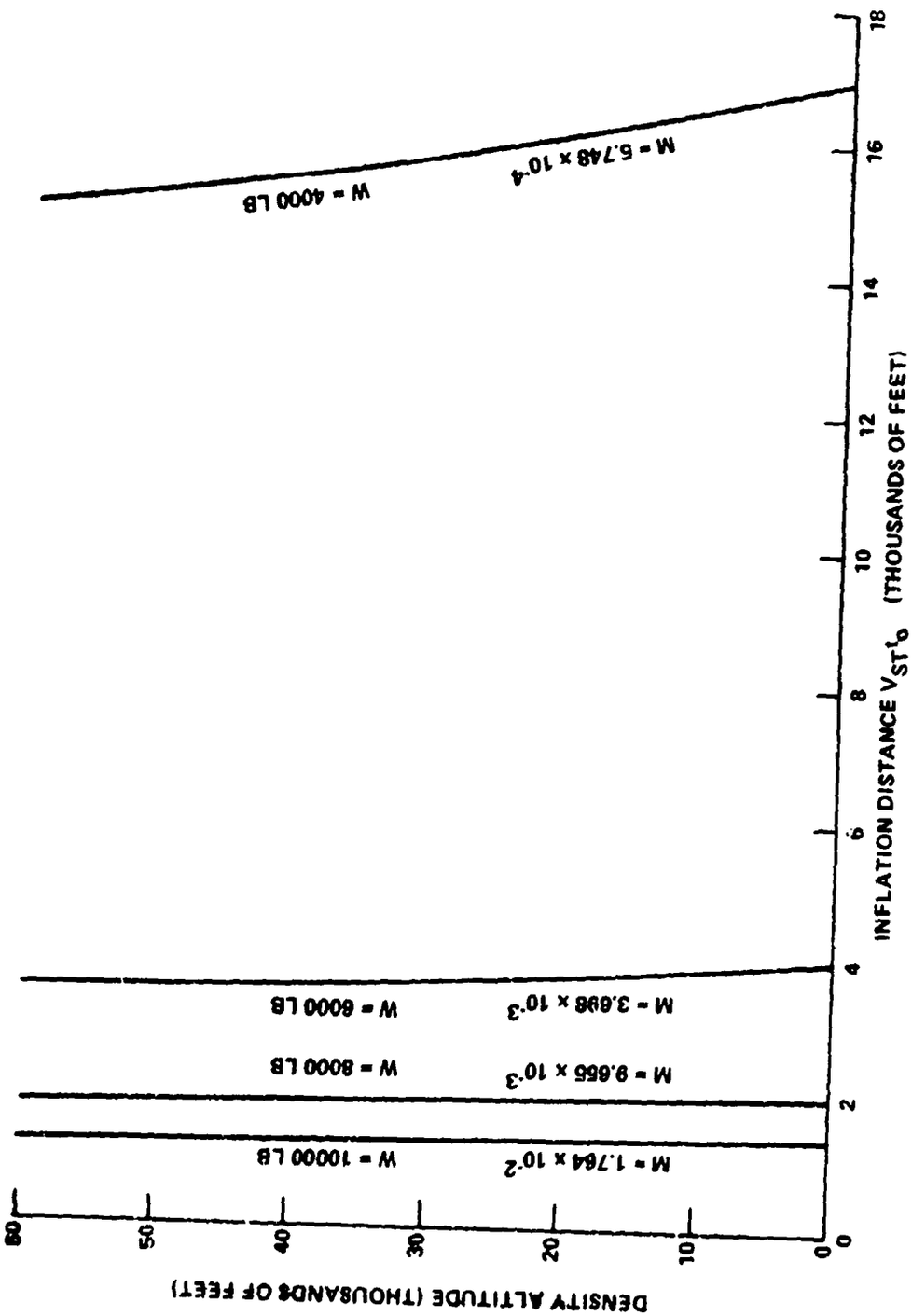

FIGURE 13. EFFECT OF DENSITY ALTITUDE ON THE INFLATION DISTANCE FOR A CONSTANT BALLISTIC MASS RATIO FOR EXAMPLE 3

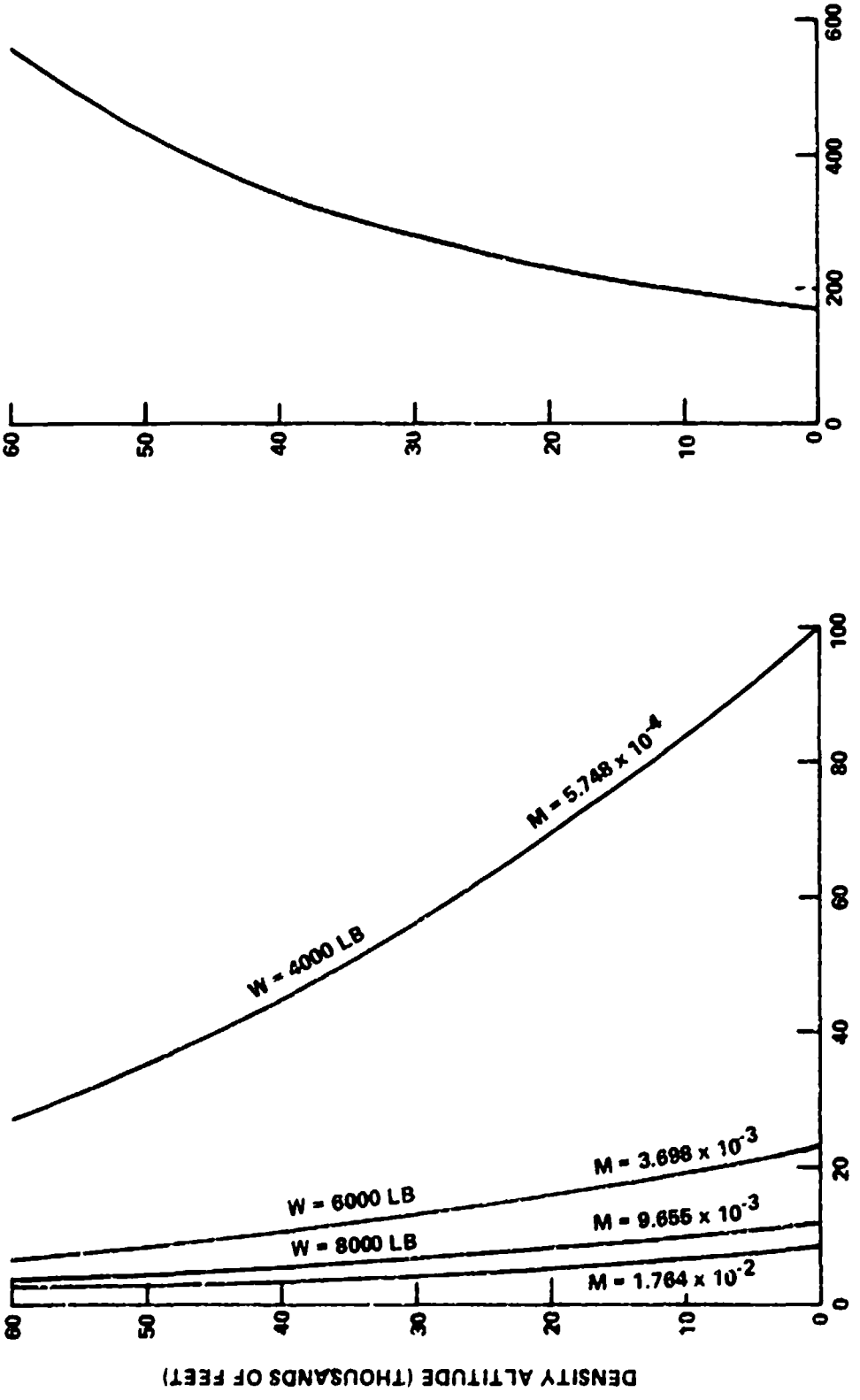

FIGURE 14. EFFECT OF DENSITY ALTITUDE ON THE REQUIRED SYSTEM TEST VELOCITY AND INFLATION REFERENCE TIME FOR A CONSTANT BALLISTIC MASS RATIO FOR EXAMPLE 3

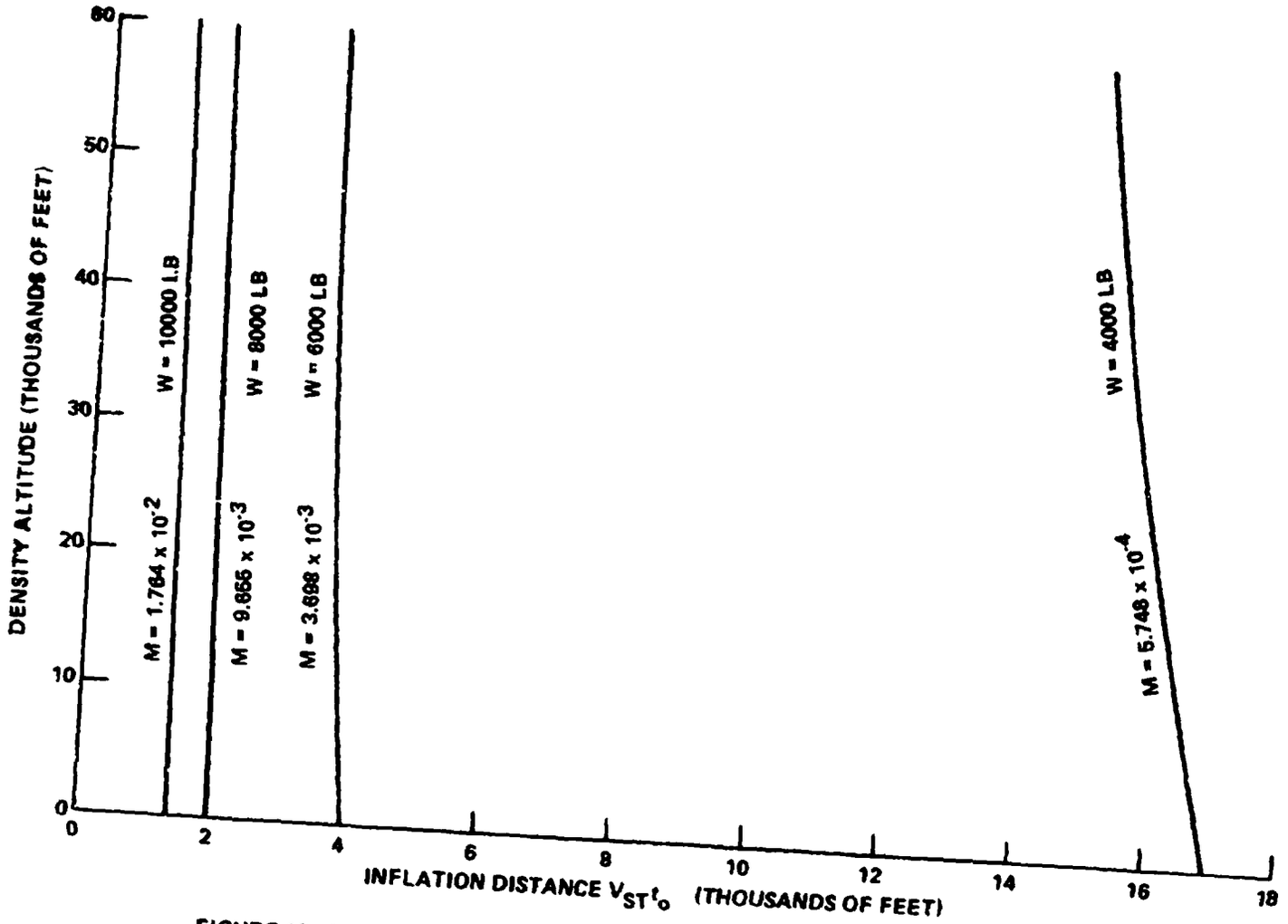

FIGURE 13. EFFECT OF DENSITY ALTITUDE ON THE INFLATION DISTANCE FOR A CONSTANT BALLISTIC MASS RATIO FOR EXAMPLE 3

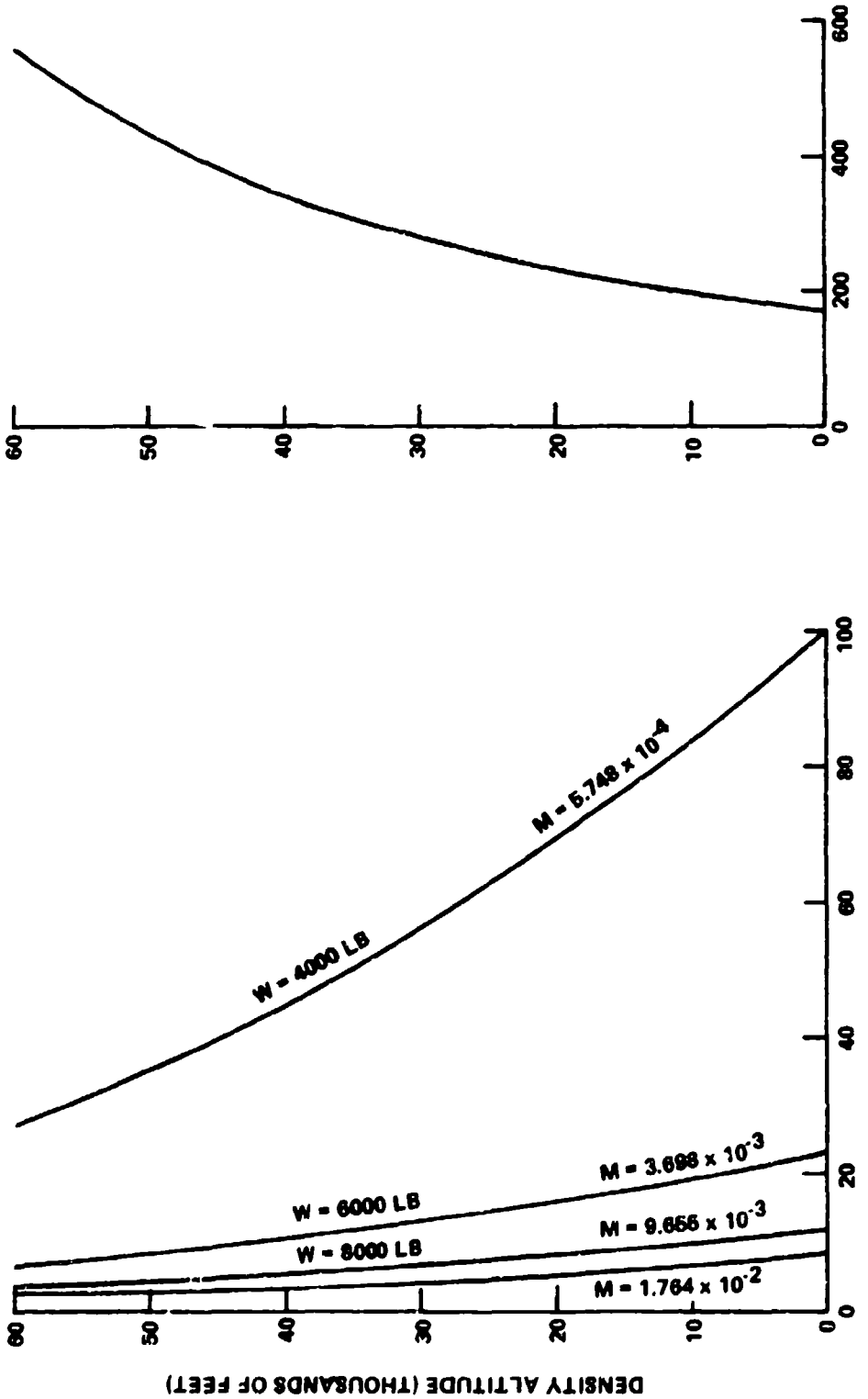

FIGURE 14. EFFECT OF DENSTIY ALTITUDE ON THE REQUIRED SYSTEM TEST VELOCITY AND INFLATION REFERENCE TIME FOR A CONSTANT BALLISTIC MASS RATIO FOR EXAMPLE 3

The weights required to maintain a constant BMR for altitudes from sea level to sixty thousand feet are presented in Figure 12. Aircraft with parent station racks of 2,400 pounds can test equivalent sea level weights of 4,000 and 6,000 pounds at approximately 15,500 feet and 26,500 feet, respectively. The sea level 8,000- and 10,000-pound equivalents require altitudes which are most likely unacceptable. An increase in parent rack capability to 3,000 pounds reduces the test altitudes for the sea level 4,000- and 6,000-pound equivalent weights to approximately 9,000 and 21,000 feet, respectively, and includes the 8,000-pound weight at approximately 28,500 feet test altitude. For these altitudes, long focal length ground-to-air photographic coverage and one or more chase aircraft for close up photographic coverage are required. The question of additional cost hinges on whether the photographic equipment and chase aircraft would or would not have been used in the C-130 low altitude tests.

The effects of density altitude on the inflation distance are presented in Figure 13, while the inflation reference time and test velocity are presented in Figure 14.

The problem in this example is the availability of an aircraft that can fly at a sea level dynamic pressure for 100 knots.

IMPULSE AND MOMENTUM DURING PARACHUTE INFLATION

Another approach to parachute opening dynamics is the use of the impulse imparted to the system by the varying forces during the time of canopy inflation. In this section a method has been developed for determining the average shock factor during the unfolding and elastic stages of inflation. The average shock factors are constant with altitude for constant BMR and η. The author is not fully satisfied with this analysis but presents the method as a different approach to the use of canopy inflation impulse.

For deployments where the BMR is less than M_L, the inflation time, t_f, is equal to the reference time, t_o. When the BMR exceeds the M_L, an additional impulse is imparted during the time from t_o to t_f as shown in Figure 15. In the general case where η is not zero, the impulse in the interval $0 \leq t \leq t_o$ is:

$$\int_o^t -Fdt = \frac{W}{g} \int_{V_s}^{V} dV$$

$$F = F_s x_i$$

$$x_i = \frac{C_D S}{C_D S_o} \left(\frac{V}{V_s}\right)^2$$

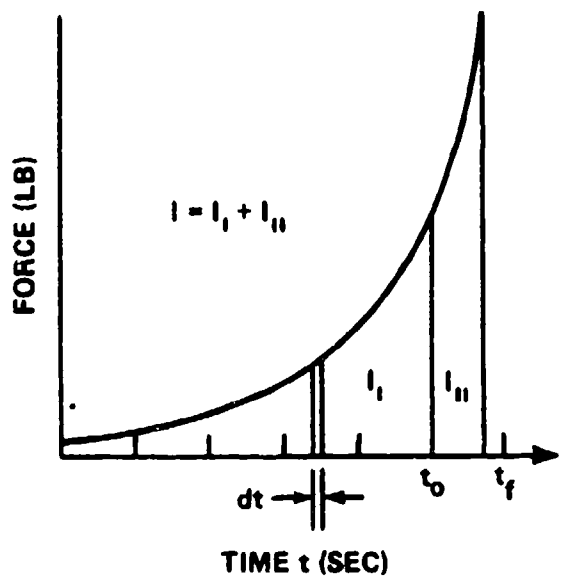

FIGURE 15. IMPULSE OF THE INFLATING CANOPY OF EXAMPLE 2

The drag-area and velocity ratios may be expressed as functions of time ratio and initial drag-area ratio. Therefore the impulse at any time $t \leq t_o$ is as follows:

Using x_i for the general case in the unfolding phase of inflation.

$$-F_s \int_o^t \frac{\left[(1-\eta)^2 \left(\frac{t}{t_o}\right)^6 + 2\eta(1-\eta)\left(\frac{t}{t_o}\right)^3 + \eta^2\right] dt}{\left[1 + \frac{1}{M}\left[\frac{(1-\eta)^2}{7}\left(\frac{t}{t_o}\right)^7 + \frac{\eta(1-\eta)}{2}\left(\frac{t}{t_o}\right)^4 + \eta^2\left(\frac{t}{t_o}\right)\right]\right]^2} = \frac{W}{g}\int_{V_s}^{V} dV$$

$$\frac{WV_s}{F_s g} = Mt_o$$

$$\int_o^t \frac{\left[(1-\eta)^2 \left(\frac{t}{t_o}\right)^6 + 2\eta(1-\eta)\left(\frac{t}{t_o}\right)^3 + \eta^2\right] dt}{\left[1 + \frac{1}{M}\left[\frac{(1-\eta)^2}{7}\left(\frac{t}{t_o}\right)^7 + \frac{\eta(1-\eta)}{2}\left(\frac{t}{t_o}\right)^4 + \eta^2\left(\frac{t}{t_o}\right)\right]\right]^2} = Mt_o\left(1 - \frac{V}{V_s}\right) \quad (14)$$

At any time ratio the average, x_{iav}, may be considered as the area under the x_i - t curve divided by t_o

$$x_{iav} = \frac{1}{t_o} \int_o^t \frac{\left[(1-\eta)^2 \left(\frac{t}{t_o}\right)^6 + 2\eta(1-\eta)\left(\frac{t}{t_o}\right)^3 + \eta^2\right] dt}{\left[1 + \frac{1}{M}\left[\frac{(1-\eta)^2}{7}\left(\frac{t}{t_o}\right)^7 + \frac{\eta(1-\eta)}{2}\left(\frac{t}{t_o}\right)^4 + \eta^2\left(\frac{t}{t_o}\right)\right]\right]^2} = M\left(1 - \frac{V}{V_s}\right) \quad (15)$$

where

$$\frac{V}{V_s} = \frac{1}{1 + \frac{1}{M}\left[\frac{(1-\eta)^2}{7}\left(\frac{t}{t_o}\right)^7 + \frac{\eta(1-\eta)}{2}\left(\frac{t}{t_o}\right)^4 + \eta^2\left(\frac{t}{t_o}\right)\right]} \quad (16)$$

The average shock factor in the unfoiding phase of inflation when $t=t_o$ is

$$x_{iav} = \frac{1}{t_o} \int_o^{t_o} \frac{\left[(1-\eta)^2 \left(\frac{t}{t_o}\right)^6 + 2\eta(1-\eta)\left(\frac{t}{t_o}\right)^3 + \eta^2\right] dt}{\left[1 + \frac{1}{M}\left[\frac{(1-\eta)^2}{7}\left(\frac{t}{t_o}\right)^7 + \frac{\eta(1-\eta)}{2}\left(\frac{t}{t_o}\right)^4 + \eta^2\left(\frac{t}{t_o}\right)\right]\right]^2} = M\left(1 - \frac{V_o}{V_s}\right) \quad (17)$$

where

$$\frac{V_o}{V_s} = \frac{1}{1 + \frac{1}{M}\left[\frac{(1-\eta)^2}{7} + \frac{\eta(1-\eta)}{2} + \eta^2\right]} \quad (18)$$

For the special case of $\eta=o$

$$x_{iav} = \frac{1}{t_o} \int_o^{t_o} \frac{\left(\frac{t}{t_o}\right)^6 dt}{\left[1 + \frac{1}{7M}\left(\frac{t}{t_o}\right)^7\right]^2} \quad (19)$$

$$x_{iav} = \frac{M}{7M + 1} \quad (20)$$

For a constant BMR and η with altitude, the x_{iav} is constant for all altitudes. Once the x_{iav} is evaluated at the initial altitude it may be used at any other altitude. The impulse of the deployment will vary since t_o varies with altitude.

When the BMR is larger than M_L an additional system impulse is imparted between $t_o \leq t \leq t_f$.

$$- F_s \int_{t_o}^{t} \frac{\left(\frac{t}{t_o}\right)^6 dt}{\left[\frac{V_s}{V_o} + \frac{1}{7M}\left[\left(\frac{t}{t_o}\right)^7 - 1\right]\right]^2} = \frac{WV_s}{g}\left(\frac{V}{V_s} - \frac{V_o}{V_s}\right) \tag{21}$$

where

$$\frac{V}{V_s} = \frac{1}{\frac{V_s}{V_o} + \frac{1}{7M}\left[\left(\frac{t}{t_o}\right)^7 - 1\right]} \tag{22}$$

and V_o/V_s is defined by equation (18)

At $t=t_f$

$$x_{iav} = \frac{1}{t_o} \int_{t_o}^{t_f} \frac{\left(\frac{t}{t_o}\right)^6 dt}{\left[\frac{V_s}{V_o} + \frac{1}{7M}\left[\left(\frac{t}{t_o}\right)^7 - 1\right]\right]^2} = M\left(\frac{V_o}{V_s} - \frac{V_f}{V_s}\right) \tag{23}$$

where

$$\frac{V_f}{V_s} = \frac{1}{\frac{V_s}{V_o} + \frac{1}{7M}\left[\left(\frac{t_f}{t_o}\right)^7 - 1\right]} \tag{24}$$

The time ratio t_f/t_o is also constant with altitude

$$X_{iav\ Total} = X_{iav}\Big|_{t=0}^{t=0} + X_{iav}\Big|_{t=t_o}^{t=t_f}$$

$$X_{iav\ Total} = M\left(1 - \frac{V_o}{V_s}\right) + M\left(\frac{V_o}{V_s} - \frac{V_f}{V_s}\right)$$

$$X_{iav\ Total} = M\left(1 - \frac{V_f}{V_s}\right) \tag{25}$$

The total system impulse, shown in Figure 16, may be considered to be a rectangular wave form which is more convenient to use as a basis for calculations than the usual force-time representation of the inflating parachute.

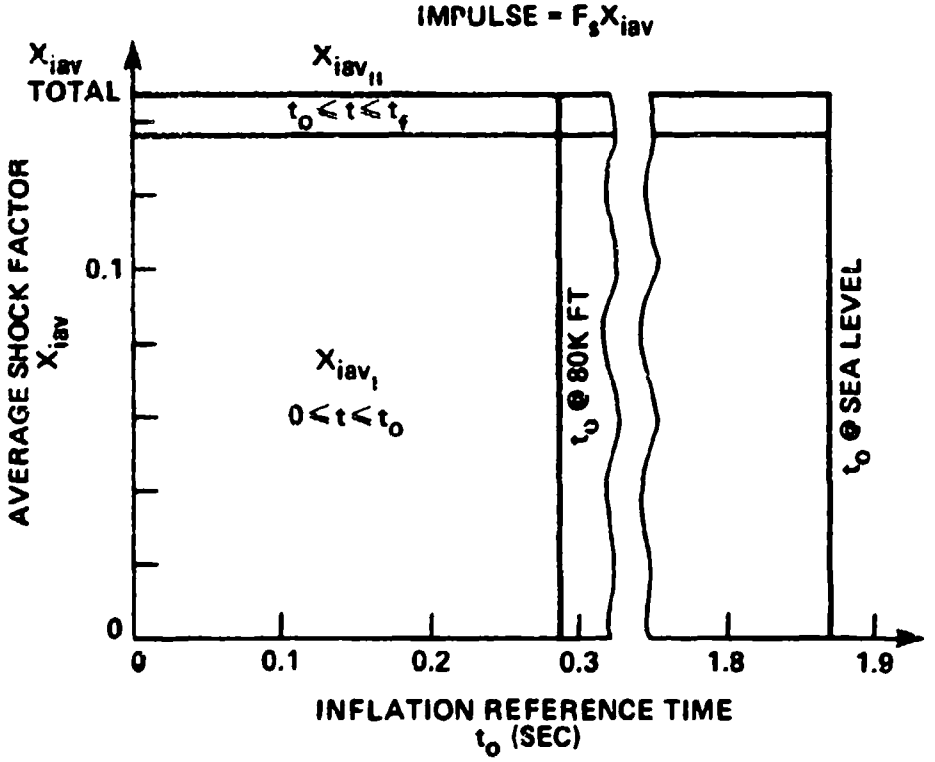

FIGURE 16. EFFECT OF ALTITUDE AND INFLATION REFERENCE TIME ON THE IMPULSE OF THE INFLATING CANOPY OF EXAMPLE 2

CONCLUSIONS

The theoretical development of the alternate altitude testing technique has demonstrated the feaseability of the idea. The Ballistic Mass Ratio meets the criteria for a genuine performance scale factor because it directly or indirectly affects all the elements which define the parachute inflation process. Although the theory was directed to solid cloth parachutes, it also applies to other decelerator types. For other decelerators the important point is to express the parachute inflation distance ($V_s t_o$) as a function of density altitude and adjust the required weight to maintain a constant BMR. Testing at a constant dynamic pressure and a constant BMR at any density altitude produces the same maximum opening shock force and stress distribution. The time ratio (t/t_o) at the time of the maximum shock force occurence during canopy inflation remains constant, although the parachute inflates more rapidly as altitude increases. When viewed from the time ratio aspect, the system geometry, instantaneous shock factor, velocity decay, dynamic pressure variation, gore pressure distribution, average pressure coefficients and stress distribution are the same for all altitudes.

Limitations to alternate altitude testing are evident in the extreme weight and low velocity required in example 2 and the low dynamic pressure required in example 3. However, there is a wide range of applications between these examples where alternate altitude testing should be a viable approach.

A method of addressing the impulse and momentum of an inflating parachute canopy was also derived. The average shock factor during canopy inflation was shown to be a function of the ballistic mass ratio.

Appendix A

AIAA Paper No. 73-477

A TECHNIQUE FOR THE CALCULATION OF THE OPENING-SHOCK FORCES FOR SEVERAL TYPES OF SOLID CLOTH PARACHUTES

by
W. F. LUDTKE
Naval Ordnance Laboratory
Silver Spring, Maryland

AIAA 4th Aerodynamic Deceleration Systems Conference

PALM SPRINGS, CALIFORNIA / MAY 21-23, 1973

A TECHNIQUE FOR THE CALCULATION OF THE OPENING-SHOCK FORCES FOR SEVERAL TYPES OF SOLID CLOTH PARACHUTES

W. P. Ludtke
Naval Ordnance Laboratory
Silver Spring, Maryland

Abstract

An analytical method of calculating parachute opening-shock forces based upon wind-tunnel derived drag area time signatures of several solid cloth parachute types in conjunction with a scale factor and retardation system steady-state parameters has been developed. Methods of analyzing the inflation time, geometry, cloth airflow properties and materials elasticity are included. The effects of mass ratio and altitude on the magnitude and time of occurrence of the maximum opening shock are consistent with observed field test phenomena.

I. Introduction

In 1965, the Naval Ordnance Laboratory (NOL) was engaged in a project which utilized a 35-foot-diameter, 10-percent extended-skirt parachute (type T-10) as the second stage of a retardation system for a 250-pound payload. Deployment of the T-10 parachute was to be accomplished at an altitude of 100,000 feet. In this rarefied atmosphere, the problem was to determine the second stage deployment conditions for successful operation. A search of available field test information indicated a lack of data on the use of solid cloth parachutes at altitudes above 30,000 feet.

The approach to this problem was as follows: Utilizing existing wind-tunnel data, low-altitude field test data, and reasonable assumptions, a unique engineering approach to the inflation time and opening-shock problem was evolved that provided satisfactory results. Basically, the method combines a wind-tunnel derived drag area ratio signature as a function of deployment time with a scale factor and Newton's second law of motion to analyze the velocity and force profiles during deployment. The parachute deployment sequence is divided into two phases. The first phase, called "unfolding phase," where the canopy is undergoing changes in shape, is considered to be inelastic as the parachute inflates initially to its steady-state aerodynamic size for the first time. At this point, the "elastic phase" is entered where it is considered that the elasticity of the parachute materials enters the problem and resists the applied forces until the canopy has reached full inflation.

The developed equations are in agreement with the observed performance of solid cloth parachutes in the field, such as the decrease of inflation time as altitude increases, effects of altitude on opening-shock force, finite and infinite mass operation, and inflation distance.

II. Development of Velocity Ratio and Force Ratio Equations During the Unfolding Phase of Parachute Deployment

The parachute deployment would take place in a horizontal attitude in accordance with Newton's second law of motion.

$$\Sigma F = ma$$

$$-\frac{1}{2}\rho V^2 C_D S = \frac{W}{g}\frac{dV}{dt}$$

It was recognized that other factors, such as included air mass, apparent mass, and their derivatives, also contribute forces acting on the system. Since definition of these parameters was difficult, the analysis was conducted in the simplified form shown above. Comparison of calculated results and test results indicated that the omitted terms have a small effect.

$$\int_o^t C_D S dt = \frac{-2W}{\rho g}\int_{V_s}^{V}\frac{dV}{V^2} \qquad (1)$$

Multiplying the right-hand side of equation (1) by

$$1 = \frac{V_s t_o C_D S_o}{V_s t_o C_D S_o}$$

and rearranging

$$\frac{1}{t_o}\int_o^t \frac{C_D S}{C_D S_o}\, dt$$

$$= \frac{-2W}{\rho g V_s t_o C_D S_o} V_s \int_{V_s}^{V}\frac{dV}{V^2} \qquad (2)$$

In order to integrate the left-hand term of equation (2), the drag area ratio must be defined for the type of parachute under

analysis as a function of deployment reference time, t_o.

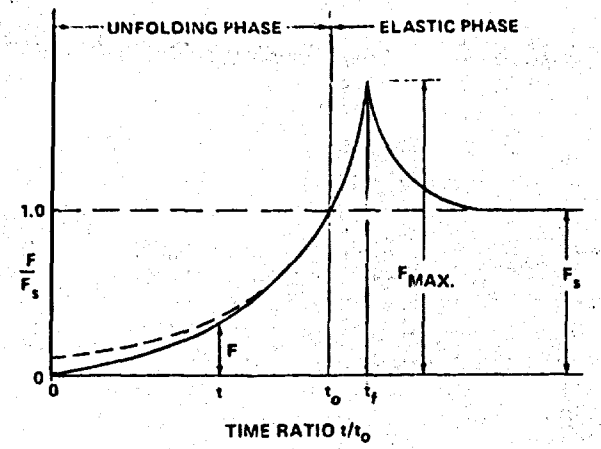

FIG. 1 TYPICAL INFINITE MASS FORCE-TIME HISTORY OF A SOLID CLOTH PARACHUTE IN A WIND TUNNEL

Figure 1 illustrates a typical solid cloth parachute wind-tunnel infinite mass force-time history after snatch. In infinite mass deployment, the maximum size and maximum shock force occur at the time of full inflation, t_f. However, t_f is inappropriate for analysis since it is dependent upon the applied load, structural strength, and materials elasticity. The reference time, t_o, where the parachute has attained its steady-state aerodynamic size for the first time, is used as the basis for performance calculations.

At any instant during the unfolding phase, the force ratio F/F_s can be determined as a function of the time ratio, t/t_o.

$$F = \frac{1}{2}\rho V^2 C_D S$$

$$F_s = \frac{1}{2}\rho V_s^2 C_D S_o$$

Since the wind-tunnel velocity and density are constant during infinite mass deployment

$$\frac{F}{F_s} = \frac{C_D S}{C_D S_o}$$

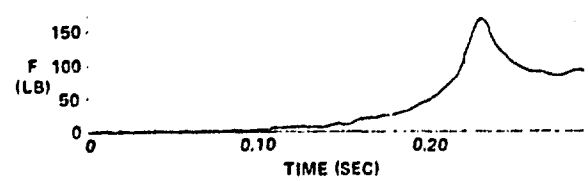

FIG. 2 TYPICAL FORCE-TIME CURVE FOR A SOLID FLAT PARACHUTE UNDER INFINITE MASS CONDITIONS.

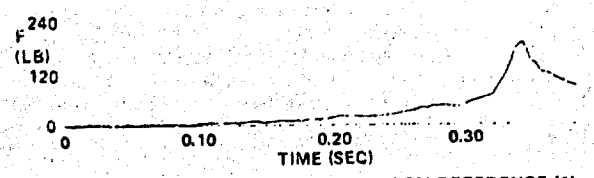

REPRODUCED FROM REFERENCE (1)

FIG. 3 TYPICAL FORCE-TIME CURVE FOR A 10% EXTENDED SKIRT PARACHUTE UNDER INFINITE MASS CONDITIONS.

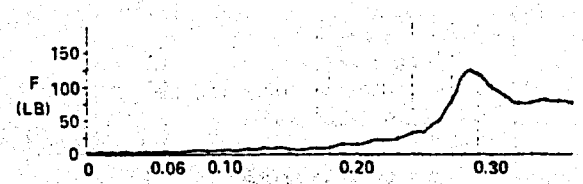

REPRODUCED FROM REFERENCE (1)

FIG. 4 TYPICAL FORCE-TIME CURVE FOR A PERSONNEL GUIDE SURFACE PARACHUTE UNDER INFINITE MASS CONDITIONS

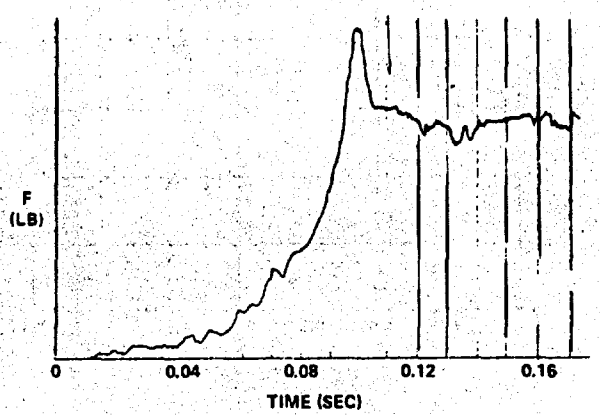

FIG. 5 TYPICAL FORCE-TIME SIGNATURE FOR THE ELLIPTICAL PARACHUTE UNDER INFINITE MASS CONDITIONS

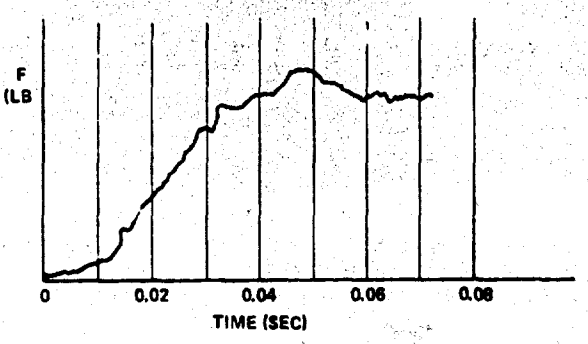

FIG. 6 TYPICAL FORCE-TIME SIGNATURE FOR THE RING SLOT PARACHUTE 20% GEOMETRIC POROSITY UNDER INFINITE MASS CONDITIONS

Infinite mass opening-shock signatures of several types of parachutes are presented in Figures 2 through 6. Analysis of these signatures using the force ratio, F/F_s, - time ratio, t/t_o, technique indicated a similarity in the performance of the various solid cloth types of

parachutes which were examined. The geometrically porous ring slot parachute displayed a completely different signature, as was expected. These data are illustrated in Figure 7. If an initial boundary

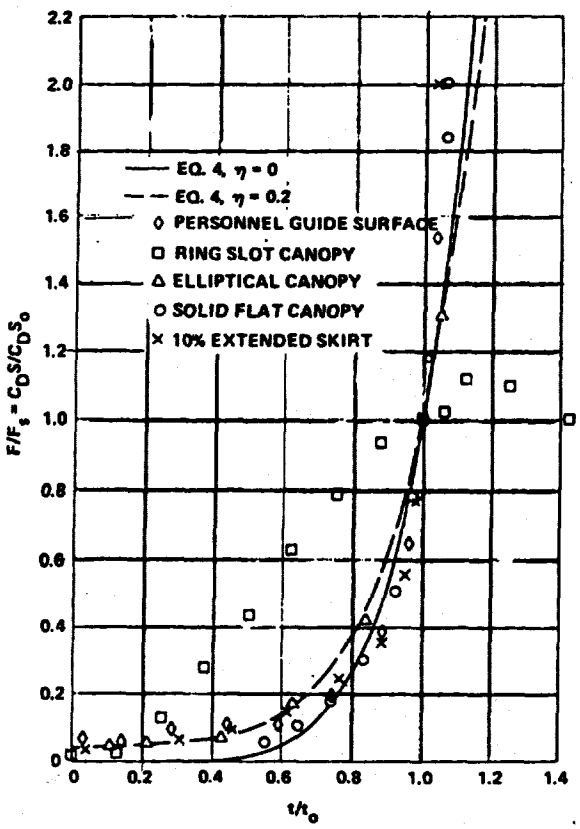

FIG. 7 DRAG AREA RATIO VS. TIME RATIO

condition of $C_DS/C_DS_o = 0$ at time $t/t_o = 0$ is assumed, then, the data can be approximated by fitting a curve of the form

$$\frac{C_DS}{C_DS_o} = \left(\frac{t}{t_o}\right)^6 \qquad (3)$$

A more realistic drag area ratio expression was determined which includes the effect of initial area at line stretch.

$$\frac{C_DS}{C_DS_o} = \left[\left(1-\eta\right)\left(\frac{t}{t_o}\right)^3 + \eta\right]^2 \qquad (4)$$

where η is the ratio of the projected mouth area at line stretch to the steady-state projected frontal area. Expanding equation (4)

$$\frac{C_DS}{C_DS_o} = \left(1-\eta\right)^2\left(\frac{t}{t_o}\right)^6 + 2\eta\left(1-\eta\right)\left(\frac{t}{t_o}\right)^3 + \eta^2 \qquad (5)$$

At the time that equation (5) was ascertained, it suggested that the geometry of the deploying parachute was independent of density and velocity. It was also postulated that although this expression had been determined for the infinite mass condition, it would also be true for the finite mass case. This phenomenon has since been independently observed and confirmed by Berndt and De Weese in reference (2).

Since the drag area ratio was determined from actual parachute deployments, it was assumed that the effects of apparent mass and included mass on the deployment force history were accommodated.

The right-hand term of equation (2) contains the expression

$$\frac{2W}{\rho g V_s t_o C_D S_o} = M \qquad (6)$$

This term can be visualized as shown in Figure 8 to be a ratio of the retarded mass (including the parachute) to an associated mass of atmosphere contained in a right circular cylinder which is generated by moving an inflated parachute of area C_DS_o for a distance equal to the product of V_st_o through an atmosphere of density, ρ.

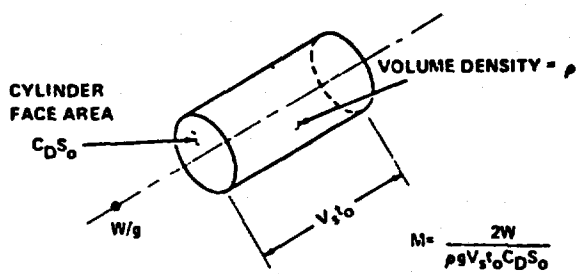

FIG. 8 VISUALIZATION OF THE MASS RATIO CONCEPT

The mass ratio, M, is the scale factor which controls the velocity and force profiles during parachute deployment. Substituting M and C_DS/C_DS_o into equation (2), integrating, and solving for V/V_s

$$\frac{V}{V_s} = \frac{1}{1+\frac{1}{M}\left[\frac{(1-\eta)^2}{7}\left(\frac{t}{t_o}\right)^7 + \frac{\eta(1-\eta)}{2}\left(\frac{t}{t_o}\right)^4 + \eta^2\frac{t}{t_o}\right]} \qquad (7)$$

The instantaneous shock factor is defined as

$$x_i = \frac{F}{F_s} = \frac{\frac{1}{2}\rho V^2 C_D S}{\frac{1}{2}\rho V_s^2 C_D S_o}$$

If the altitude variation during deployment is small, then, the density may be considered as constant

$$x_i = \frac{C_D S}{C_D S_o}\left(\frac{V}{V_s}\right)^2$$

from equations (5) and (7)

$$x_i = \frac{(1-\eta)^2\left(\frac{t}{t_o}\right)^6 + 2\eta(1-\eta)\left(\frac{t}{t_o}\right)^3 + \eta^2}{\left[1 + \frac{1}{M}\left[\frac{(1-\eta)^2}{7}\left(\frac{t}{t_o}\right)^7 + \frac{\eta(1-\eta)}{2}\left(\frac{t}{t_o}\right)^4 + \eta^2\frac{t}{t_o}\right]\right]^2} \quad (8)$$

III. Maximum Shock Force and Time of Occurrence During the Unfolding Phase

The time of occurrence of the maximum instantaneous shock factor, x_i, is difficult to determine for the general case. However, for $\eta = 0$, the maximum shock factor and time of occurrence are readily calculated. For $\eta = 0$

$$x_i = \frac{\left(\frac{t}{t_o}\right)^6}{\left[1 + \frac{1}{7M}\left(\frac{t}{t_o}\right)^7\right]^2}$$

Setting the derivative of x_i with respect to time equal to zero and solving for t/t_o at $x_{i\ max}$

$$\left(\frac{t}{t_o}\right)_{@\ x_{i\ max}} = \left(\frac{21M}{4}\right)^{\frac{1}{7}} \quad (9)$$

and the maximum shock factor is

$$x_{i\ max} = \frac{16}{49}\left(\frac{21M}{4}\right)^{\frac{6}{7}} \quad (10)$$

Equations (9) and (10) are valid for values of $M \leq \frac{4}{21}$ (0.19), since for larger values of M, the maximum shock force occurs in the elastic phase of inflation.

Figures 9 and 10 illustrate the velocity and force profiles generated from equations (7) and (8) for initial projected area ratios of $\eta = 0$, and 0.2 with various mass ratios.

IV. Methods for Calculation of the Reference Time, t_o

The ratio concept is an ideal method to analyze the effects of the various parameters on the velocity and force profiles of the opening parachutes; however, a means of calculating t_o is required before specific values can be computed. Methods for computing the varying mass flow into the inflating canopy mouth, the varying mass flow out through the varying inflated canopy surface area, and the volume of air, V_o, which must be collected during the inflation process are required.

Figure 11 represents a solid cloth-type parachute canopy at some instant during inflation. At any given instant, the parachute drag area is proportional to the maximum inflated diameter. Also, the maximum diameter in conjunction with the suspension lines determines the inflow mouth area (A-A) and the pressurized canopy area (B-B-B). This observation provided the basis for the following assumptions. The actual canopy shape is of minor importance.

a. The ratio of the instantaneous mouth inlet area to the steady-state mouth area is in the same ratio as the instantaneous drag area.

$$\frac{A_M}{A_{Mo}} = \frac{C_D S}{C_D S_o}$$

b. The ratio of the instantaneous pressurized cloth surface area to the canopy surface area is in the same ratio as the instantaneous drag area.

$$\frac{S}{S_o} = \frac{C_D S}{C_D S_o}$$

c. Since the suspension lines in the unpressurized area of the canopy are straight, a pressure differential has not developed, and, therefore, the net airflow in this zone is zero.

Based on the foregoing assumptions, the mass flow equation can be written

$$dm = m\ \text{inflow} - m\ \text{outflow}$$

$$\rho \frac{dV}{dt} = \rho V A_M - \rho A_s P$$

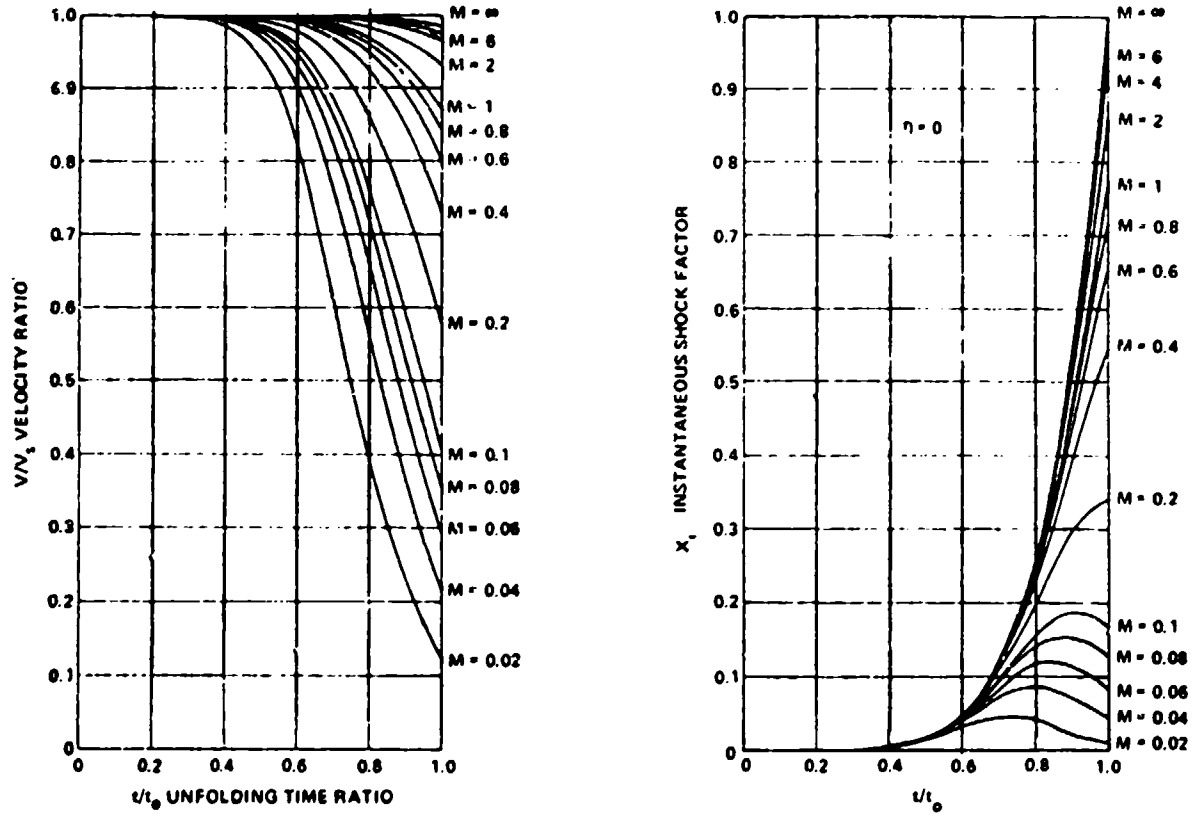

FIG. 9 EFFECT OF INITIAL AREA AND MASS RATIO ON THE SHOCK FACTOR AND VELOCITY RATIO DURING THE UNFOLDING PHASE FOR $\eta = 0$.

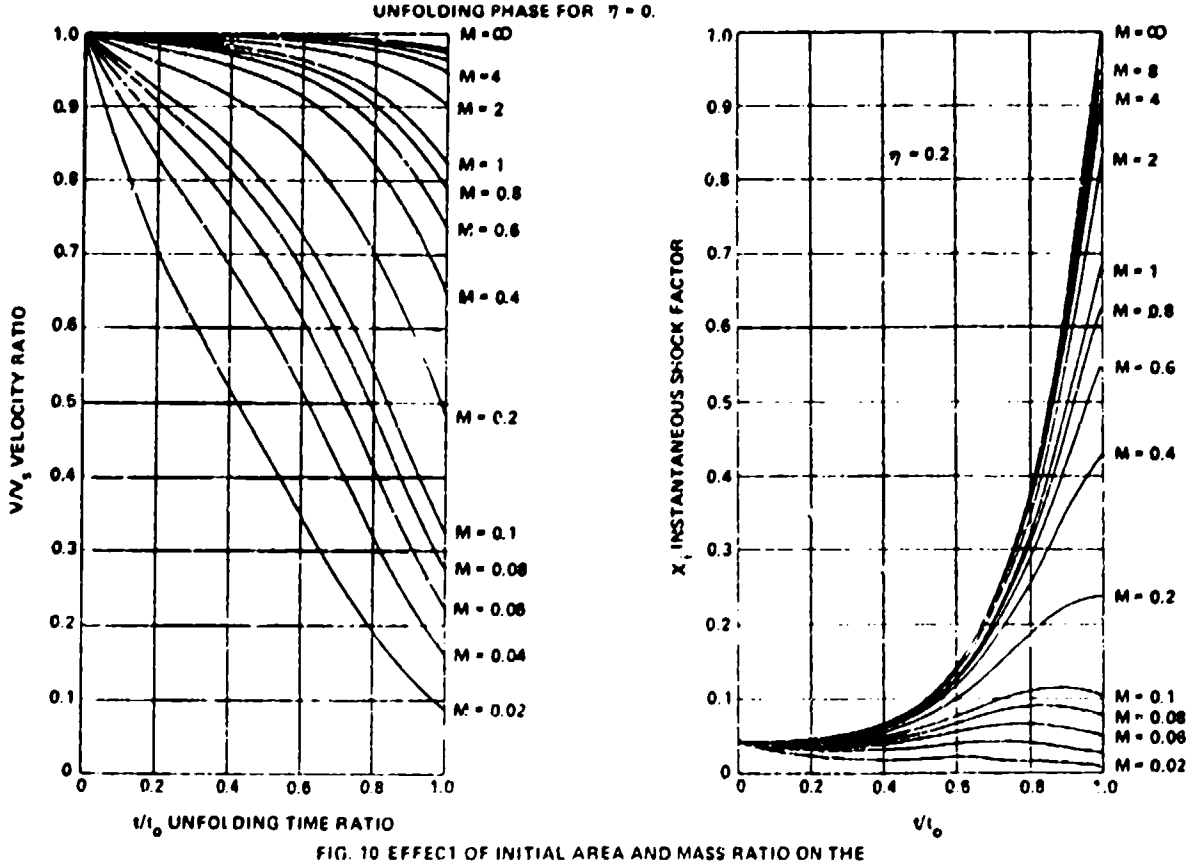

FIG. 10 EFFECT OF INITIAL AREA AND MASS RATIO ON THE SHOCK FACTOR AND VELOCITY RATIO DURING THE UNFOLDING PHASE FOR $\eta = 0.2$

$$\rho \frac{dV}{dt} = \rho V A_{Mo} \frac{C_D S}{C_D S_o} - \rho A_{So} \frac{C_D S}{C_D S_o} P \qquad (11)$$

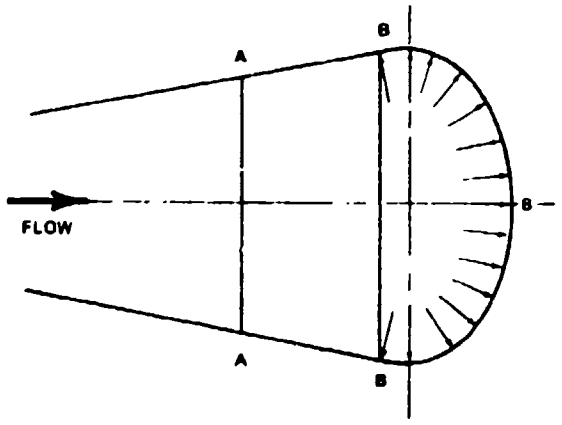

FIG. 11 PARTIALLY INFLATED PARACHUTE CANOPY

From equation (3)

$$\frac{C_D S}{C_D S_o} = \left(\frac{t}{t_o}\right)^6 \quad ; \text{ for } \eta = 0$$

From equation (7)

$$V = \frac{V_s}{1 + \frac{1}{7M}\left(\frac{t}{t_o}\right)^7} \quad ; \eta = 0$$

From equation (26)

$$P = k\left(\frac{C_P \rho}{2}\right)^n V^{2n}$$

$$\int_o^{V_o} dV = A_{Mo} V_s \int_o^{t_o} \frac{\left(\frac{t}{t_o}\right)^6}{1 + \frac{1}{7M}\left(\frac{t}{t_o}\right)^7} dt$$

$$-A_{So} k \left(\frac{C_P \rho}{2}\right)^n \int_o^{t_o} \left(\frac{t}{t_o}\right)^6 \left[\frac{V_s}{1 + \frac{1}{7M}\left(\frac{t}{t_o}\right)^7}\right]^{2n} dt \qquad (12)$$

Integrating:

$$V_o = A_{Mo} V_s t_o M \ln\left[1 + \frac{1}{7M}\right]$$

$$-A_{So} k \left(\frac{C_P \rho}{2}\right)^n \int_o^{t_o} \left(\frac{t}{t_o}\right)^6 \left[\frac{V_s}{1 + \frac{1}{7M}\left(\frac{t}{t_o}\right)^7}\right]^{2n} dt \qquad (13)$$

Measured values of n indicate a data range from 0.574 through 0.771. A convenient solution to the reference time equation evolves when n is assigned a value of 1/2. Integrating equation (13) and using

$$V_s t_o M = \frac{2W}{g\rho C_D S_o}$$

$$\text{LET } K_1 = \frac{g\rho V_o}{2W}\left[\frac{C_D S_o}{A_{Mo} - A_{So} k\left(\frac{C_P \rho}{2}\right)^{1/2}}\right]$$

$$t_o = \frac{14W}{g\rho V_s C_D S_o}\left[e^{K_1} - 1\right] \qquad (14)$$

Equation (14) expresses the unfolding reference time, t_o, in terms of mass, altitude, snatch velocity, airflow characteristics of the cloth, and the steady-state parachute geometry. Note that the term $g\rho V_o/W$ is the ratio of the included air mass to the mass of the retarded hardware. Multiplying both sides of equation (14) by V_s demonstrates that

$V_s t_o$ = a constant which is a function of altitude

Figures 12 and 13 indicate the parachute unfolding time and unfolding distance for values of n = 1/2 and n = 0.63246. Note the variation and convergence with rising altitude. The opening-shock force is strongly influenced by the inflation time. Because of this, the

value of t_o calculated by using a realistic value of n should be used in the lower atmosphere.

As an example of this method of opening-shock analysis, let us examine the effect of altitude on the opening-shock force of a T-10-type parachute retarding a 200-pound weight from a snatch velocity of V_s = 400 feet per second at sea level. Conditions of constant velocity and constant dynamic pressure are investigated. The results are presented in Figure 14. At low altitudes, the opening-shock force is less than the steady-state drag force; however, as altitude rises, the opening shock eventually exceeds the steady-state drag force at some altitude. This trend is in agreement with field test observations.

V. Correction of t_o for Initial Area Effects

The unfolding reference time, t_o, calculated by the previous methods assumes that the parachute inflates from zero drag area. In reality, a parachute has a drag area at the beginning of inflation. Once t_o has been calculated, a correction can be applied, based upon what is known about the initial conditions.

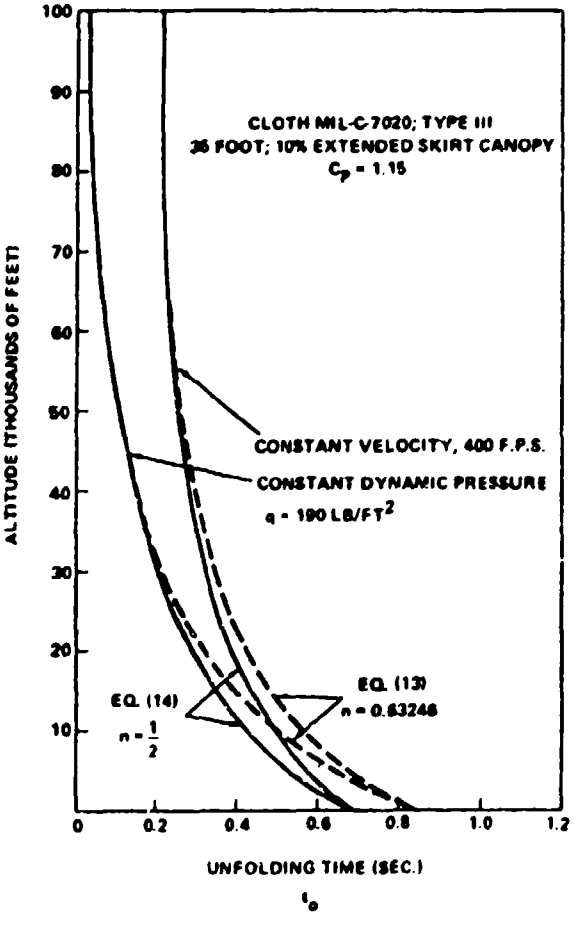

FIG. 12 EFFECT OF ALTITUDE ON THE UNFOLDING TIME "t_o" AT CONSTANT VELOCITY AND CONSTANT DYNAMIC PRESSURE FOR n = 1/2 AND n = 0.63296

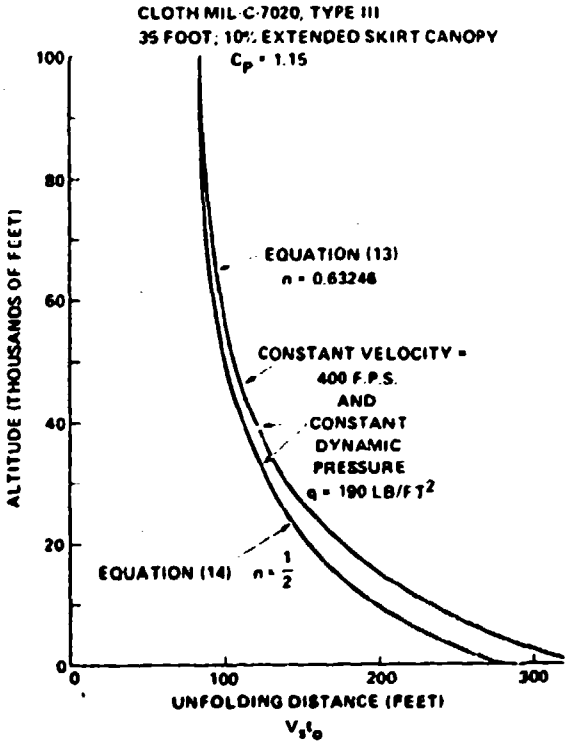

FIG. 13 EFFECT OF ALTITUDE ON THE UNFOLDING DISTANCE AT CONSTANT VELOCITY AND CONSTANT DYNAMIC PRESSURE FOR n = 1/2 AND n = 0.63246

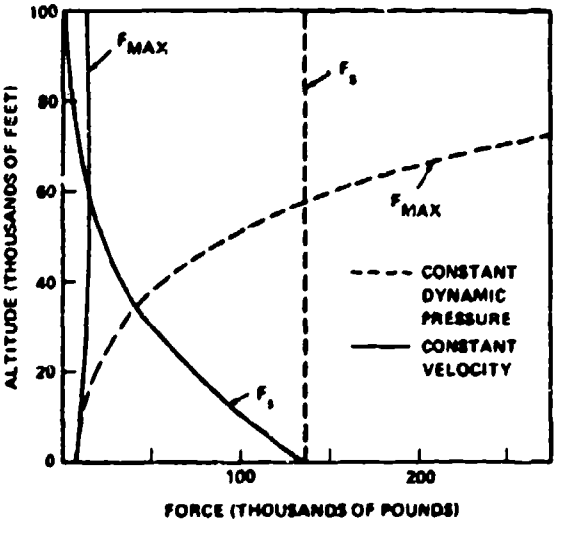

FIG. 14 VARIATION OF STEADY-STATE DRAG, F_s, AND MAXIMUM OPENING SHOCK WITH ALTITUDE FOR CONSTANT VELOCITY AND CONSTANT DYNAMIC PRESSURE

Case A - When the initial projected area is known

$$\frac{A_i}{A_c} = \left(\frac{t_i}{t_o}\right)^3$$

$$t_i = \left(\frac{A_i}{A_c}\right)^{1/3} t_{o_{calculated}}$$

$$t_{o_{corrected}} = \left[1 - \left(\frac{A_i}{A_c}\right)^{1/3}\right] t_{o_{calculated}} \qquad (15)$$

Case B - When the initial drag area is known

$$\frac{C_D S_i}{C_D S_o} = \left(\frac{t_i}{t_o}\right)^6$$

$$t_i = \left(\frac{C_D S_i}{C_D S_o}\right)^{1/6} t_{o_{calculated}}$$

$$t_{o_{corrected}} = \left[1 - \left(\frac{C_D S_i}{C_D S_o}\right)^{1/6}\right] t_{o_{calculated}} \qquad (16)$$

The mass ratio should now be adjusted for the corrected t_o before velocity and force profiles are determined.

VI. Opening-Shock Force, Velocity Ratio, and Inflation Time During the Elastic Phase of Parachute Inflation

The mass ratio, M, is an important parameter in parachute analysis. For values of $M < 4/21$, the maximum opening-shock force occurs early in the inflation process, and the elastic properties of the canopy are not significant. As the mass ratio approaches $M = 4/21$, the magnitude of the opening-shock force increases, and the time of occurrence happens later in the deployment sequence. For mass ratios $M > 4/21$, the maximum shock force will occur after the reference time, t_o. Parachutes designed for high mass ratio operation must provide a structure of sufficient constructed strength, F_c, so that the actual elongation of the canopy under load is less than the maximum extensibility, ϵ_{max}, of the materials.

Development of the analysis in the elastic phase of inflation is similar to the technique used in the unfolding phase. Newton's second law of motion is used, together with the drag area ratio signature and mass ratio

$$\frac{C_D S}{C_D S_o} = \left(\frac{t}{t_o}\right)^6$$

which is still valid, as shown in Figure 7

$$\frac{1}{Mt_o}\int_{t_o}^{t}\left(\frac{t}{t_o}\right)^6 dt = V_s\int_{V_o}^{V}\frac{-dV}{V^2}$$

Integrating and solving for $\frac{V}{V_s}$

$$\frac{V}{V_s} = \frac{1}{\frac{V_s}{V_o} + \frac{1}{7M}\left[\left(\frac{t}{t_o}\right)^7 - 1\right]} \qquad (17)$$

where $\frac{V_o}{V_s}$ is the velocity ratio of the unfolding process at time $t = t_o$.

$$\frac{V_o}{V_s} = \frac{1}{1 + \frac{1}{M}\left[\frac{(1-\eta)^2}{7} + \frac{\eta(1-\eta)}{2} + \eta^2\right]} \qquad (18)$$

The instantaneous shock factor in the elastic phase becomes

$$x_i = \frac{C_D S}{C_D S_o}\left(\frac{V}{V_s}\right)^2$$

$$x_i = \frac{\left(\frac{t}{t_o}\right)^6}{\left[\frac{V_s}{V_o} + \frac{1}{7M}\left[\left(\frac{t}{t_o}\right)^7 - 1\right]\right]^2} \qquad (19)$$

The end point of the inflation process depends upon the applied loads, elasticity of the canopy, and the constructed strength of the parachute. A linear load elongation

relationship is utilized to determine the maximum drag area.

$$\frac{\epsilon}{F} = \frac{\epsilon_{max}}{F_c}$$

$$\epsilon = \frac{F\,\epsilon_{max}}{F_c} \qquad (20)$$

The force, F, is initially the instantaneous force at the end of the unfolding process

$$F = X_o F_s \qquad (21)$$

where X_o is the shock factor of the unfolding phase at $t = t_o$

$$X_o = \frac{1}{\left[1 + \frac{1}{M}\left[\frac{(1-\eta)^2}{7} + \frac{\eta(1-\eta)}{2} + \eta^2\right]\right]^2} \qquad (22)$$

Since the inflated shape is defined, the drag coefficient is considered to be constant, and the instantaneous force is proportional to the dynamic pressure and projected area. The maximum projected area would be developed if the dynamic pressure remained constant during the elastic phase. Under very high mass ratios, this is nearly the case over this very brief time period; but as the mass ratio decreases, the velocity decay has a more significant effect. The simplest approach for all mass ratios is to determine the maximum drag area of the canopy as if elastic inflation had occurred at constant dynamic pressure. Then utilizing the time ratio determined as an end point, intermediate shock factors can be calculated from equation (19) and maximum force assessed.

The initial force, $X_o F_s$, causes the canopy to increase in projected area. The new projected area in turn increases the total force on the canopy which produces a secondary projected area increase. The resulting series of events are resisted by the parachute materials. The parachute must, therefore, be constructed of sufficient strength to prevent the elongation of the materials from exceeding the maximum elongation.

$$\epsilon_o = \frac{X_o F_s}{F_c}\,\epsilon_{max} \qquad (23)$$

The next force in the series at constant q

$$F_1 = X_o F_s \frac{A_1}{A_c}$$

where

$$\frac{A_1}{A_c} = (1 + \epsilon_o)^2$$

Subsequent elongations in the system can be shown to be

$$\epsilon_1 = \epsilon_o\,(1 + \epsilon_o)^2$$

$$\epsilon_2 = \epsilon_o\,(1 + \epsilon_o\,(1 + \epsilon_o)^2)^2$$

The required canopy constructed strength can be determined for a given set of deployment conditions. The limiting value of the series (ϵ_ℓ) determines the end point time ratio.

$$\left(\frac{t_f}{t_o}\right)^6 = \frac{C_D S_{max}}{C_D S_o} = (1 + \epsilon_\ell)^2$$

$$\left(\frac{t_f}{t_o}\right) = \left(\frac{C_D S_{max}}{C_D S_o}\right)^{1/6} = (1 + \epsilon_\ell)^{1/3} \qquad (24)$$

Figure 15 illustrates the maximum drag area ratio as a function of ϵ_o.

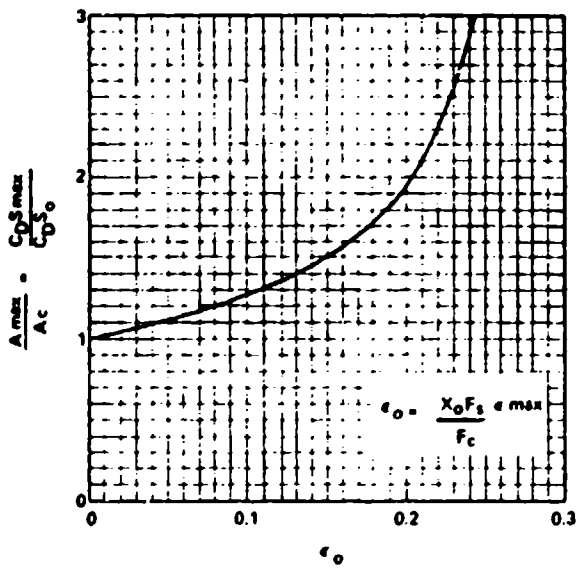

FIG. 15 MAXIMUM DRAG AREA RATIO VS. INITIAL ELONGATION

VII. Application of Cloth Permeability to the Calculation of the Inflation Time of Solid Cloth Parachutes

The mass outflow through the pressurized region of an inflating solid cloth parachute at any instant is dependent upon the canopy area which is subjected to airflow and the rate of airflow through that area. The variation of pressurized area as a function of reference time, t_o, was earlier assumed to be proportional to the instantaneous drag area ratio, leaving the rate-of-airflow problem to solve. The permeability parameter of cloth was a natural choice for determining the rate of airflow through the cloth as a function of pressure differential across the cloth. Heretofore, these data have been more of a qualitative, rather than quantitative, value. A new method of analysis was developed wherein a generalized curve of the form $P = k(\Delta P)^n$ was fitted to cloth permeability data for a number of different cloths and gives surprisingly good agreement over the pressure differential range of available data. The pressure differential was then related to the trajectory conditions to give a generalized expression which can be used in the finite mass ratio range, as well as the infinite mass case. The permeability properties were transformed into a mass flow ratio, M', which shows agreement with the effective porosity concept.

Measured and calculated permeability pressure data for several standard cloths are illustrated in Figure 16. This method has been applied to various types of cloth between the extremes of a highly permeable 3-momme silk to a relatively impervious parachute pack container cloth with reasonably good results, see Figure 17.

The canopy pressure coefficient, C_p, is defined as the ratio of the pressure differential across the cloth to the dynamic pressure of the free stream.

$$C_p = \frac{\Delta P}{q} = \frac{P(\text{internal}) - P(\text{external})}{1/2\ \rho V^2} \qquad (25)$$

where V is based on equation (7).

The permeability expression, $P = k(\Delta P)^n$ becomes

$$P = k\left(C_p \frac{\rho V^2}{2}\right)^n \qquad (26)$$

Although some progress has been made by Melzig and others on the measurement of the variation of the pressure coefficient on an actual inflating canopy, this dimension and its variation with time are still dark areas at the time of this writing. At the present time, a constant average value of pressure coefficient is used in these calculations. Figure 18 presents the effect of pressure coefficient and altitude on the unfolding time for constant deployment conditions.

It is well known that the inflation time of solid cloth parachutes decreases as the operational altitude increases. This effect can be explained by considering the ratio of the mass outflow through a unit cloth area to the mass inflow through a unit mouth area.

$$M' = \text{mass flow ratio} = \frac{\text{mass outflow}}{\text{mass inflow}}$$

where

$$\text{mass outflow} = P_\rho \frac{\text{slugs}}{\text{ft}^2\text{-sec}} \text{ (per ft}^2 \text{ cloth area)}$$

and

$$\text{mass inflow} = V_\rho \frac{\text{slugs}}{\text{ft}^2\text{-sec}} \text{ (per ft}^2 \text{ inflow area)}$$

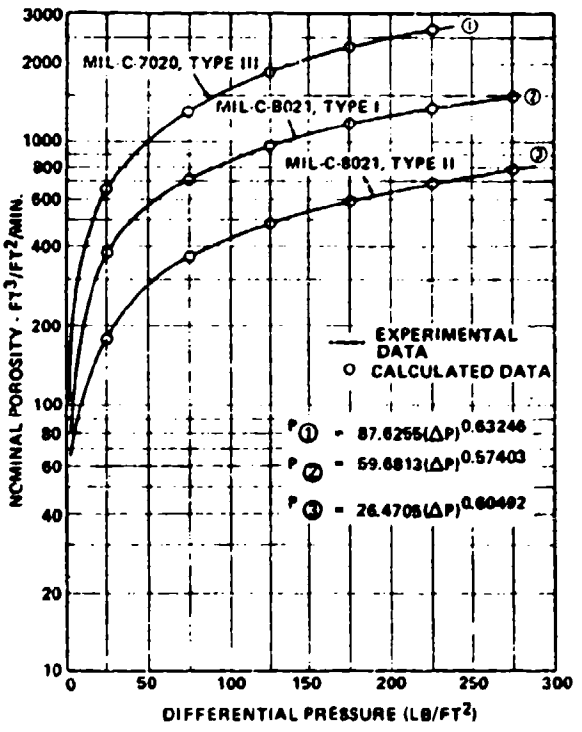

REPRODUCED FROM REFERENCE (4)

FIG. 16 NOMINAL POROSITY OF PARACHUTE MATERIAL VS DIFFERENTIAL PRESSURE.

Therefore, the mass flow ratio becomes

$$M' = \frac{P\rho}{V\rho} = \frac{P}{V}$$

$$M' = k\left(\frac{C_p\rho}{2}\right)^n V^{(2n-1)} \qquad (27)$$

Effective porosity, C, is defined as the ratio of the velocity through the cloth, u, to a fictitious theoretical velocity, v, which will produce the particular $\Delta P = 1/2\rho v^2$.

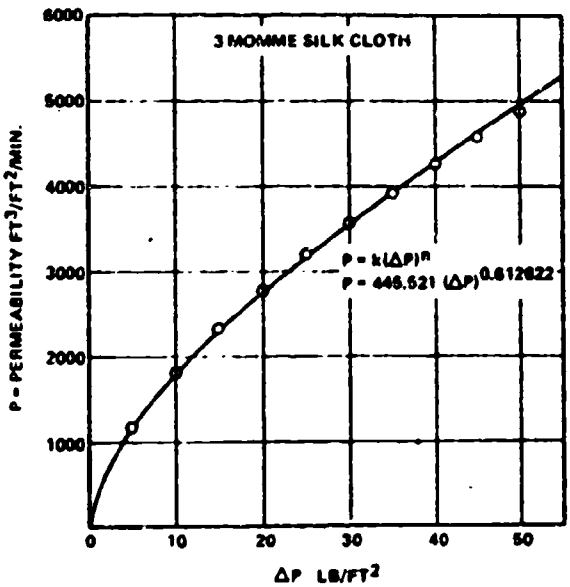

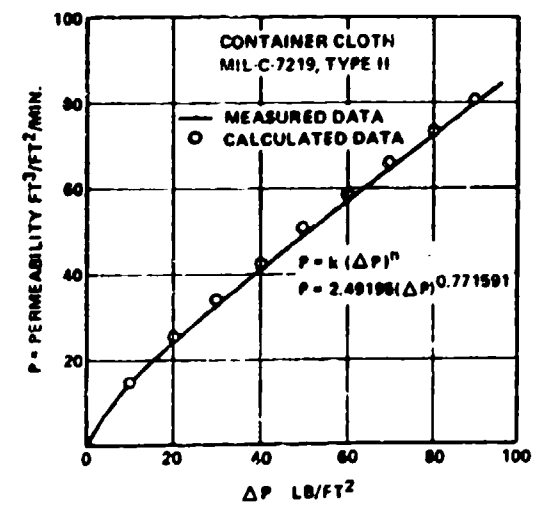

FIG. 17 COMPARISON OF MEASURED AND CALCULATED PERMEABILITY FOR RELATIVELY PERMEABLE AND IMPERMEABLE CLOTHS

AVERAGE CANOPY PRESSURE COEFFICIENT DURING INFLATION INCLUDING THE VENT

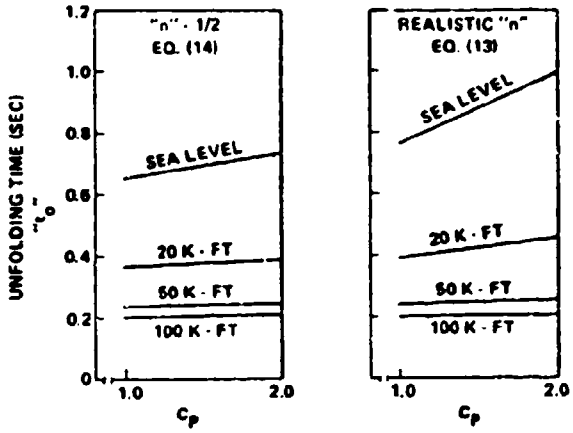

FIG. 18 EFFECT OF PRESSURE COEFFICIENT AND ALTITUDE ON THE UNFOLDING TIME.

$$\text{effective porosity, } C = \frac{u}{v} \qquad (28)$$

Comparison of the mass flow ratio and previously published effective porosity data is shown in Figure 19. The effects of altitude and velocity on the mass flow ratio are presented in Figures 20, and 21 for constant velocity and constant altitude. The decrease of cloth permeability with altitude is evident.

The permeability constants "k" and "n" can be determined from the permeability pressure differential data as obtained from an instrument such as a Frazier Permeameter. Two data points, "A" and

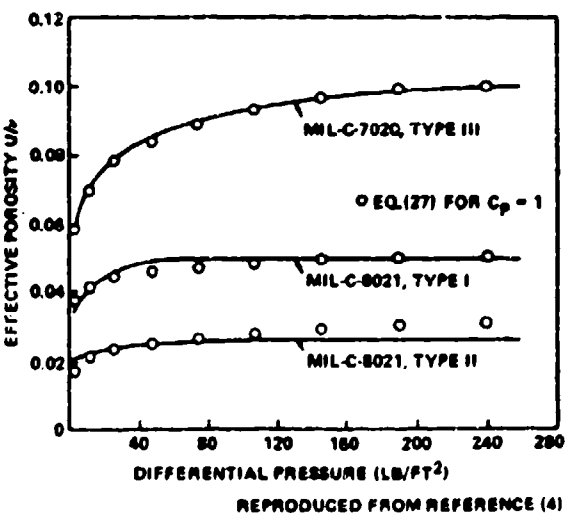

REPRODUCED FROM REFERENCE (4)

FIG. 19 THE EFFECTIVE POROSITY OF PARACHUTE MATERIALS VS. DIFFERENTIAL PRESSURE

"B," are selected in such a manner that point "A" is in a low-pressure zone below the knee of the curve, and point "B" is located in the upper end of the high-pressure zone, as shown in Figure 22.

The two standard measurements of 1/2 inch of water and 20 inches of water appear to be good data points if both are

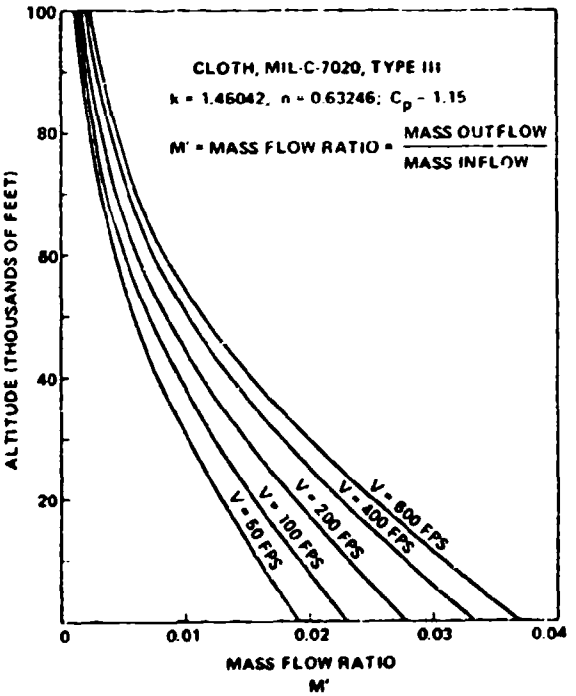

FIG. 20 EFFECT OF ALTITUDE ON MASS FLOW RATIO AT CONSTANT VELOCITY

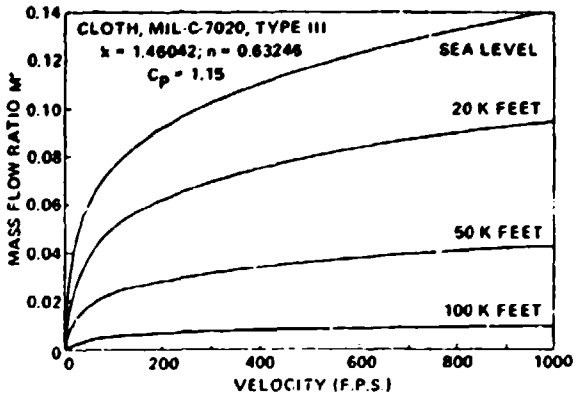

FIG. 21 EFFECT OF VELOCITY ON MASS FLOW RATIO AT CONSTANT DENSITY

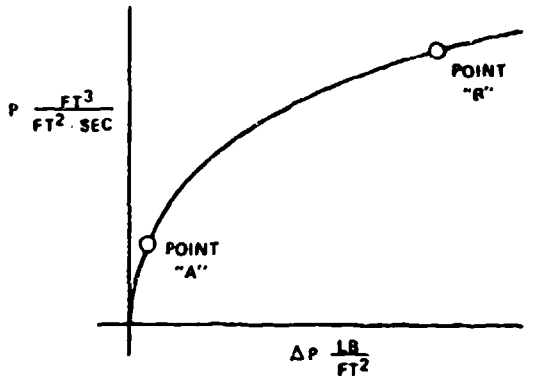

FIG. 22 LOCATION OF DATA POINTS FOR DETERMINATION OF "k" AND "n"

available on the same sample. Substituting the data from points "A" and "B" into $P = k(\Delta P)^n$:

$$n = \frac{\ln\left(\frac{P_B}{P_A}\right)}{\ln\left(\frac{\Delta P_B}{\Delta P_A}\right)} \qquad (29)$$

$$k = \frac{P_A}{(\Delta P_A)^n} = \frac{P_B}{(\Delta P_B)^n} \qquad (30)$$

VIII. Determination of the Parachute Included Volume and Associated Air Mass

Before the reference time, t_o, and inflation time, t_f, can be calculated, the volume of atmosphere, V_o, which is to be collected during the inflation process must be accurately known. This requirement dictates that a realistic inflated canopy shape and associated volume of atmosphere be determined. Figure 23 reproduced from reference (5). The technique of using lampblack coated plates to determine the airflow patterns around metal models of inflated canopy shapes was used by the investigator of reference (5) to study the stability characteristics of contemporary parachutes, i.e., 1943. A by-product of this study is that it is clearly shown that the volume of air within the canopy bulges out of the canopy mouth (indicated by arrows) and extends ahead of the canopy hem. This volume must be collected during the inflation process. Another neglected, but significant, source of canopy volume exists in the billowed portion of the gore panels.

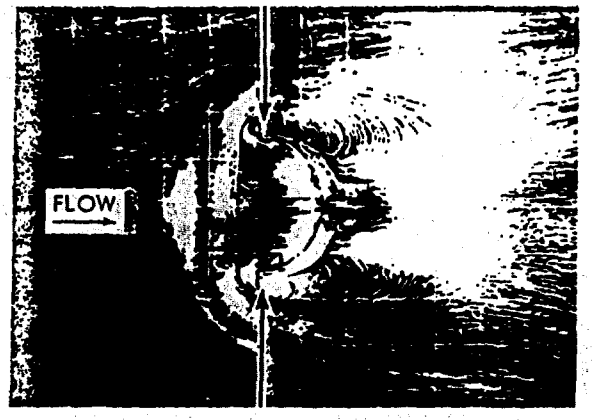

HEMISPHERE

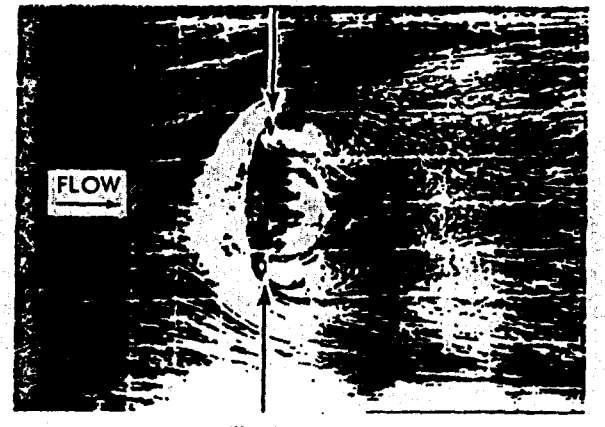

VENT PARACHUTE

REPRODUCED FROM REFERENCE (5)

FIG. 23 AIRFLOW PATTERNS SHOWING AIR VOLUME AHEAD OF CANOPY HEM

The steady-state canopy shape has been observed in wind-tunnel and field tests to be elliptical in profile. Studies of the inflated shape and included volume of several parachute types (flat circular, 10 percent extended skirt, elliptical, hemispherical, ring slot, ribbon, and cross) are documented in references (6) and (7). These studies demonstrated that the steady-state profile shape of inflated canopies of the various types can be approximated to be two ellipses of common major diameter, $2\bar{a}$, and dissimilar minor diameters, b and b', as shown in Figure 24. It was also shown that the volume of the ellipsoid of revolution formed by revolving the profile shape about the canopy axis was a good approximation of the volume of atmosphere to be collected during canopy inflation and included the air volume extended ahead of the parachute skirt hem together with the billowed gore volume.

$$\underline{V}_o = \frac{2}{3}\ \pi\bar{a}^3 \left[\frac{b}{\bar{a}} + \frac{b'}{\bar{a}}\right] \qquad (31)$$

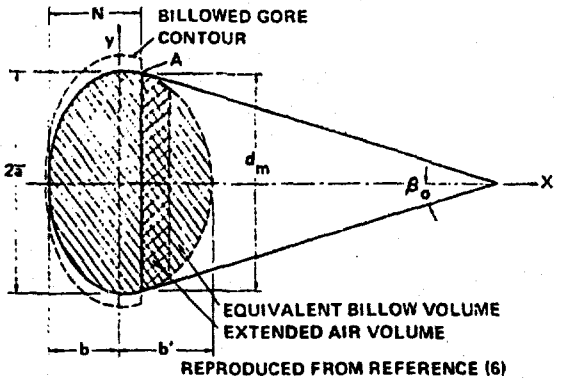

REPRODUCED FROM REFERENCE (6)

FIG. 24 PARACHUTE CROSS SECTION NOMENCLATURE

Tables I and II are summaries of test results reproduced from references (6) and (7), respectively, for the convenience of the reader.

IX. References

1. "A Method to Reduce Parachute Inflation Time with a Minor Increase in Opening Force," WADD Report TR 60-761
2. Berndt, R. J., and DeWesse, J. H., "Filling Time Prediction Approach for Solid Cloth Type Parachute Canopies," AIAA Aerodynamic Deceleration Systems Conference, Houston, Texas, 7-9 Sep 1966
3. "Theoretical Parachute Investigations," Progress Report No. 4, Project No. 5, WADC Contract AF33 (616)-3955, University of Minnesota
4. "Performance of and Design Criteria for Deployable Aerodynamic Decelerators," TR ASK-TR-61-579, AFFDL, AIRFORCESYSCOM, Dec 1963
5. "Investigation of Stability of Parachutes and Development of Stable Parachutes from Fabric of Normal Porosity," Count Zeppelin Research Institute Report No. 300, 23 Mar 1943
6. Ludtke, W. P., "A New Approach to the Determination of the Steady-State Inflated Shape and Included Volume of Several Parachute Types," NOLTR 69-159, 11 Sep 1969
7. Ludtke, W. P., "A New Approach to the Determination of the Steady-State Inflated Shape and Included Volume of Several Parachute Types in 24-Gore and 30-Gore Configurations," NOLTR 70-178, 3 Sep 1970

TABLE I SUMMARY OF PARACHUTE SHAPE TEST RESULTS FOR 12-GORE AMD 16-GORE CONFIGURATIONS

Parachute Type	No. of Gores	Suspension Line Length inches	Velocity mph	Velocity fps	Scale Factor, K $\frac{2\bar{s}}{D_o}$	$\frac{2\bar{s}}{D_F}$	$\frac{2\bar{s}}{D_R}$	$\frac{2\bar{s}}{L}$	$\frac{N}{\bar{s}}$	Axes Ratio $\frac{b}{\bar{s}}$	$\frac{b'}{\bar{s}}$	$\frac{b}{\bar{s}} + \frac{b'}{\bar{s}}$	Volume in^3 V_H	V_C	V_o	$\frac{V_o}{V_H}$
Flat Circular	12	34	50	73	.645	.650			.856	.6115	.8817	1.4932	4478	4481	6980	1.56
	16	34	50	73	.663	.668			.820	.5558	.9039	1.4597	4450	4100	7325	1.65
10% Extended Skirt	12	34	100	147	.663	.652			.881	.6424	.8860	1.5284	3928	4400	6783	1.73
	16	34	17	25	.664	.640			.785	.5590	.8502	1.4082	4051	3920	6197	1.53
Elliptical	12	34	75	110			.916		.812	.5626	.9657	1.5283		3322	5406	
	16	34	17	25			.875		.800	.6169	.8163	1.4332		2778	4405	
Hemispherical	12	34	125	183			.996		1.254	1.0005	.9080	1.9085		6224	8666	
	16	34	75	110			.994		1.185	.9129	.9380	1.8509		5521	8370	
Ringslot	12	34	25	37	.607	.654			.853	.6566	.8735	1.530	3800	3650	5903	1.55
16% Geometric	12	34	100	147	.616	.663			.922	.6566	.8735	1.530	3800	4198	6186	1.62
Porosity	12	34	200	293	.637	.686			.918	.6566	.8735	1.530	3800	4624	6826	1.90
	16	34	25	37	.611	.658			.827	.6004	.8890	1.4894	3800	3763	5685	1.50
	16	34	100	147	.617	.664			.864	.6004	.8890	1.4894	3800	3985	6030	1.59
	16	34	200	293	.645	.695			.844	.6004	.8890	1.4894	3800	4430	6807	1.82
Ribbon	12	34	25	37	.586	.632			.859	.6558	.8768	1.5326	3800	3323	5335	1.40
24% Geometric	12	34	100	147	.615	.663			.837	.6558	.8768	1.5326	3800	3714	6183	1.62
Porosity	12	34	200	293	.632	.681			.877	.6558	.8768	1.5326	3800	4280	6683	1.76
	16	34	25	37	.603	.650			.797	.5570	.8578	1.4148	3800	3432	5358	1.41
	16	34	100	147	.626	.674			.791	.5570	.8578	1.4148	3800	3804	5983	1.57
	16	34	200	293	.648	.698			.781	.5570	.8578	1.4148	3800	4164	6656	1.75
Cross Chute w/L = .264		34	25	37	.710			.543	1.242	.8867	1.2776	2.1643	1928	3768	5798	3.01
		34	100	147	.707			.540	1.270	.8867	1.2776	2.1643	1928	3810	5712	2.96
		34	200	293	.716			.547	1.286	.8867	1.2776	2.1643	1928	4212	5926	3.07
		47	25	37	.759			.580	1.113	.8494	1.2512	2.1006	1928	4062	6868	3.58
		47	100	147	.729			.557	1.205	.8494	1.2512	2.1006	1928	3973	5965	3.09
		47	200	293	.775			.592	1.110	.8494	1.2512	2.1006	1928	4292	7303	3.79

REPRODUCED FROM REFERENCE (6)

TABLE II SUMMARY OF PARACHUTE SHAPE TEST RESULTS FOR 24-GORE AND 30-GORE CONFIGURATIONS

Parachute Type	No. of Gores	Suspension Line Length inches	Velocity mph	Velocity fps	Scale Factor, K $\frac{2\bar{s}}{D_o}$	$\frac{2\bar{s}}{D_F}$	$\frac{N}{\bar{s}}$	Axes Ratio $\frac{b}{\bar{s}}$	$\frac{b'}{\bar{s}}$	$\frac{b}{\bar{s}} + \frac{b'}{\bar{s}}$	Volume in^3 V_H	V_c	V_o	$\frac{V_o}{V_H}$
Flat Circulars	24	34	50	73	.677	.679	.795	.5758	.8126	1.3894	4382	4695	7273	1.67
	30	34	17	25	.688	.689	.827	.6214	.7806	1.4020	4342	4626	7027	1.62
10% Extended*	24	34	100	147	.646	.648	.834	.5949	.8771	1.4720	4138	4446	6930	1.67
Skirt	30	34	17	25	.650	.633	.825	.6256	.7962	1.4127	4172	4076	6265	1.50
Ring Slot 16%	24	34	25	37	.663	.666	.824	.5800	.9053	1.4853	3591	3878	6031	1.68
Geometrically	24	34	100	147	.660	.662	.816	.5800	.9053	1.4853	3591	4079	6510	1.81
Porous	24	34	200	293	.694	.696	.809	.5800	.9053	1.4853	3591	4270	6924	1.93
	30	34	25	37	.677	.678	.788	.5800	.9053	1.4853	3582	3828	6404	1.79
	30	34	100	147	.684	.685	.802	.5800	.9053	1.4853	3582	4023	6588	1.84
	30	34	200	293	.698	.699	.860	.5800	.9053	1.4853	3582	4260	7012	1.96
Ribbon 24%	24	34	25	37	.671	.673	.770	.5980	.8187	1.4167	3591	3591	5968	1.66
Geometrically	24	34	100	147	.676	.678	.813	.5980	.8187	1.4167	3591	3927	6097	1.70
Porous	24	34	200	293	.687	.689	.804	.5980	.8187	1.4167	3591	4061	6389	1.78
	30	34	25	37	.655	.657	.782	.6021	.8463	1.4484	3582	3396	5666	1.58
	30	34	100	147	.669	.670	.784	.6021	.8463	1.4484	3582	3622	6022	1.68
	30	34	200	293	.677	.679	.823	.6021	.8463	1.4484	3582	4002	6256	1.75

*Since this parachute was "breathing" during the test, several photographs were taken at each speed. The data were reduced from the photograph which most reasonably appeared to represent the equilibruim state.

REPRODUCED FROM REFERENCE (7)

X. List of Symbols

A_c - Steady-state projected area of the inflated parachute, ft^2

A_M - Instantaneous canopy mouth area, ft^2

A_{Mo} - Steady-state inflated mouth area, ft^2

a - Acceleration, ft/sec^2

$2\bar{a}$ - Maximum inflated parachute diameter of gore mainseam, ft

b - Minor axis of the ellipse bounded by the major axis ($2\bar{a}$) and the vent of the canopy, ft

b' - Minor axis of the ellipse which includes the skirt hem of the canopy, ft

C - Effective porosity

C_D - Parachute coefficient of drag

C_p - Parachute pressure coefficient, relates internal and external pressure (ΔP) on canopy surface to the dynamic pressure of the free stream

D_o - Nominal diameter of the aerodynamic decelerator = $\sqrt{4S_o/\pi}$, ft

F - Instantaneous force, lbs

F_s - Steady-state drag force that would be produced by a fully open parachute at velocity V_s, lbs

F_c - Constructed strength of the parachute, lbs

F_{max} - Maximum opening-shock force, lbs

g - Gravitational acceleration, ft/sec^2

k - Permeability constant of canopy cloth

m - Mass, slugs

M - Mass ratio - ratio of the mass of the retarded hardware (including parachute) to a mass of atmosphere contained in a right circular cylinder of length ($V_s t_o$), face area ($C_D S_o$), and density (ρ)

M' - Mass flow ratio - ratio of atmosphere flowing through a unit cloth area to the atmosphere flowing through a unit inlet area at arbitrary pressure

n - Permeability constant of canopy cloth

P - Cloth permeability - rate of airflow through a cloth at an arbitrary differential pressure, $ft^3/ft^2/sec$

q - Dynamic pressure, lb/ft^2

S - Instantaneous inflated canopy surface area, ft^2

$S_o = A_{so}$ - Canopy surface area, ft^2

t - Instantaneous time, sec

t_o - Reference time when the parachute has reached the design drag area for the first time, sec

t_f - Canopy inflation time when the inflated canopy has reached its maximum physical size, sec

u - Air velocity through cloth in effective porosity, ft/sec

v - Fictitious theoretical velocity used in effective porosity, ft/sec

V - Instantaneous system velocity, ft/sec

V_o - System velocity at the time $t = t_o$, ft/sec

V_s - System velocity at the end of suspension line stretch, ft/sec

$\underline{V}_o$ - Volume of air which must be collected during the inflation process, ft^3

W - Hardware weight, lb

x_1 - Instantaneous shock factor

X_o - Shock factor at the time $t = t_o$

ρ - Air density, $slugs/ft^3$

η - Ratio of parachute projected mouth area at line stretch to the steady-state projected area

ϵ - Instantaneous elongation

ϵ_{max} - Maximum elongation

ϵ_o - Initial elongation at the beginning of the elastic phase of inflation

S.F. - Parachute safety factor = F_c/F_{max}

Appendix B

A GUIDE FOR THE USE OF APPENDIX A

At first reading, Appendix A may appear to be a complicated system of analysis because of the many formulae presented. Actually, once understood, the technique is straightforward and uncomplicated. The author has attempted to simplify the algebra wherever possible. This appendix presents, in semi-outline form, a guide to the sequence of calculations because the analysis does require use of formulae from the text, not necessarily in the order in which they were presented. Also, the user can be referred to graphs of performance to illustrate effects.

In order to compute t_o, other parameters must be obtained from various sources.

I. Determine System Parameters

1. C_DS_o, drag area, ft^2 obtained from design requirement.

2. V_s, fps, velocity of system at suspension line stretch.

3. ρ, slugs/ft^3, air density at deployment altitude.

4. W, lb, system weight (including weight of the parachute) from design requirements.

5. $\underline{V}_o$, ft^3, this volume of air, which is to be collected during inflation, is calculated from the steady-state inflated shape geometry of the particular parachute type. The nomenclature is described in Figure 24,p.A-14. When D_o or D_P is known, $\bar{a}$ can be calculated from data in Table I and Table II, p. A-15, for various parachute types and number of gores. Then the geometric volume $\underline{V}_o$ can be calculated by Equation (31), p. A-14, with appropriate values of $b/\bar{a}$ and $b'/\bar{a}$ from the tables.

6. A_{MO}, ft^2, steady-state canopy mouth area

$$A_{MO} = \pi\bar{a}^2\left[1 - \left(\frac{N/\bar{a} - b/\bar{a}}{b'/\bar{a}}\right)^2\right] \qquad (B\text{-}1)$$

where $N/\bar{a}$, $b/\bar{a}$, and $b'/\bar{a}$ are available from Tables I and II for the particular type of parachute and number of gores.

7. A_{so}, ft^2, canopy surface area = $\frac{\pi}{4}D_o^2$

8. C_p, pressure coefficient, see Figure 18, p. A-12. A constant C_p = 1.7 for all altitudes seems to yield acceptable results.

9. Constants k and n are derived from measurements of the air flow through the cloth. Only k is needed for Equation (14), but n is also required for Equation (13). These parameters can be determined for any cloth using the technique described beginning on p. A-12. The two-point method is adequate if the ΔP across the cloth is in the range of ΔP for actual operation. Check-points of cloth permeability can be measured and compared to calculated values to verify agreement. If the data are to be extrapolated to operational ΔP's greater than measured, a better method of determining k and n from the test data would be a least squares fit through many data points. This way errors due to reading either of the two points are minimized.

II. Step 1

Calculate the reference time t_o by use of Equations (13) or (14), p. A-7. If the deployment altitude is 50,000 feet or higher, Equation (14) is preferred due to its simplicity. For altitudes from sea level to 50,000 feet, Equation (13) is preferred. Figure 12, p. A-8, shows the effect of altitude on t_o and can be taken as a guide for the user to decide whether to use Equation (13) or (14). One should keep in mind that the opening shock force can be a strong function of inflation time, so be as realistic as possible. If Equation (13) is elected, the method in use at the NSWC/WO is to program Equation (13) to compute the parachute volume, V_o, for an assumed value of t_o. Equation (14), because of its simplicity, can be used for a first estimate of t_o at all altitudes. The computed canopy volume is then compared to the canopy volume calculated from the geometry of the parachute as per Equation (31), p. A-14. If the volume computed from the mass flow is within the volume computed from the geometry within plus or minus a specified delta volume, the time t_o is printed out. If not within the specified limits, t_o is adjusted, and a new volume calculated. For a 35-foot D_o, T-10 type canopy, I use plus or minus 10 cubic feet in the volume comparison. The limit would be reduced for a parachute of smaller D_o.

If V_o calculated = V_o geometry ± 10, then print answer.

If V_o calculated ≠ V_o geometry ± 10, then correct t_o as follows:

$$t_o = t_o \frac{V_{o\ \text{geometry}}}{V_{o\ \text{calculated}}} \qquad \text{(B-2)}$$

The new value of t_o is substituted in the "do loop" and the volume recomputed. This calculation continues until the required volume is within the specified limits.

III. Calculate t_o corrected for initial area. The t_o of Section II assumes that the parachute inflated from a zero initial area. If this is a reasonable assumption for the particular system under study, then the mass ratio can be determined from Equation (6), p. A-4. For $\eta = 0$ if the value of $M \leq 0.19$, then a finite state of deployment exists, and the time ratio of occurrence and the maximum shock factor can be determined from Equations (9) and (10), respectively, on p. A-5. If $\eta \neq 0$, then the limiting mass ratio for finite operations will rise slightly as described in Appendix C. Figures C-1 and C-2 illustrate the effects of initial area on limiting mass ratios and shock factors respectively. If the mass ratio is greater than the limiting mass ratio (M_L), then the maximum shock force occurs at a time greater than t_o and the elasticity of the materials must be considered (see Section VI).

If $\eta \neq 0$, then the reference time, t_o, will be reduced, and the mass ratio will rise due to partial inflation at the line stretch. Figures 9 and 10, p. A-6, illustrate the effects of initial area on the velocities and shock factor during the "unfolding" inflation. Equation (15), p. A-9, can be used to correct t_o calculated for the cases where $\eta = Ai/Ac$. If the initial value of drag area is known, Equation (16), p. A-9, can be used to correct t_o and rechecked for limiting mass ratios versus η in Appendix C.

IV. Opening shock calculations in the elastic phase of inflation. It has been considered that from time $t = 0$ to $t = t_o$ the parachute has been inelastic. At the time $t = t_o$ the applied aerodynamic load causes the materials to stretch and the parachute canopy increases in size. The increased size results in an increase in load, which causes further growth, etc. This sequence of events continues until the applied forces have been balanced by the strength of materials. The designer must insure that the constructed strength of the materials is sufficient to resist the applied loads for the material elongation expected. Use of materials of low elongation should result in lower opening shock forces as $C_D S_{max}$ is reduced.

When the mass ratio of the system is greater than the limiting mass ratio, the elasticity of the materials and material strength determine the maximum opening shock force. The maximum elongation ε_{max} and the ultimate strength of the materials are known from tests or specifications. The technique begins on p. A-9.

At the time $t = t_o$, calculate the following quantities for the particular values of M and η.

a. V_o/V_s from Equation (18), p. A-9.

b. X_o from Equation (22), p. A-10.

c. ε_o from Equation (23), p. A-10.

d. Determine $C_D S_{max}/C_D S_o$ from Figure 15, p. A-10.

e. Calculate the inflation time ratio t_f/t_o from Equation (24), p. A-10.

f. Calculate the maximum shock factor from Equation (19), p. A-9.

g. Calculate the opening shock force $F_{max.} = X_1 F_s$ where

$$F_s = \frac{1}{2}\rho V_s^2 C_D S_o$$

h. Calculate filling time, t_f(sec)

$$t_f = t_o \left(\frac{t_f}{t_o}\right)$$

V. In order to simplify the required effort, the work sheets of Table B-1 are included on pages B-5 through B-9 to aid the engineer in systematizing the analysis. The work sheets should be reproduced to provide additional copies.

Table B-1. Opening Shock Force

CALCULATION WORK SHEETS	SYMBOL	VALUE	DIMENSION
1. Parachute type -			
2. System parameters			
a. System weight, W (lb)	W		lb.
b. Gravity, g (ft/sec^2)	g		ft/sec^2
c. Deployment altitude (ft)			ft.
d. Deployment air density, ρ ($slugs/ft^3$)	ρ		$slugs/ft^3$
e. Velocity at line stretch, V_s (fps)	V_s		fps.
f. Steady state canopy data			
(1) Diameter, D_o (ft)	D_o		ft.
(2) Inflated diameter, $2\bar{a}$ (ft); $\frac{2\bar{a}}{D_o} = *$	$2\bar{a}$		ft.
(3) Surface area, S_o (ft^2); $\frac{\pi}{4} D_o^2$	$A_{so} = S_o$		$ft.^2$
(4) Drag area, $C_D S_o$ (ft^2); $C_D \times S_o$	$C_D S_o$		$ft.^2$
(5) Mouth area, A_{MO}^* (ft^2) $A_{MO} = \pi \bar{a}^2 \left[1 - \left(\frac{N/\bar{a} - b/\bar{a}}{b'/\bar{a}}\right)^2\right]$	A_{MO}		$ft.^2$
(6) Volume, V_o^* (ft^3) $V_o = \frac{2}{3} \pi \bar{a}^3 \left[\frac{b}{\bar{a}} + \frac{b'}{\bar{a}}\right]$	V_o		$ft.^3$
g. Cloth data			
(1) k } Calculate using technique beginning on p. A-12.	k		—
(2) n }	n		—

Note: Permeability is usually measured as $ft^3/ft^2/min$. For these calculations permeability must be expressed as $ft^3/ft^2/sec$

* Data for these calculations are listed in Tables 1 and 2, p. A-15.

Table B-1. Opening Shock Force (cont'd)

	SYMBOL	VALUE	DIMENSION
(3) ε_{max}; determine maximum elongations from pull test data of joints, seams, lines, etc. Use minimum ε_{max} determined from tests.			
(4) Cp; pressure coefficient	C_p		–
h. Steady state drag, F_s (lb), $F_s = \frac{1}{2}\rho V_s^2 C_D S_o$	F_s		lb.
i. Parachute constructed strength, F_c (lb); determined from data on efficiency of seams, joints, lines. Constructed strength is the minimum load required to fail a member times the number of members.	F_c		lb.
3. Force calculations			
a. Calculate t_o for $\eta = 0$; eq. 14, p. A-7. $t_o = \frac{14W}{\rho g V_s C_D S_o}\left[e^{\frac{\rho g V_o}{2W}\left[\frac{C_D S_o}{A_{MO} - A_{SO}\, k\left(\frac{C_p \rho}{2}\right)^{\frac{1}{2}}}\right]} - 1\right]$	t_o		sec.
Check Figure 13, p. A-8, for advisability of using eq. 13, p. A-7.			
b. If $\eta = 0$, proceed with steps c through e. If $\eta \neq 0$, go to step f.			
c. Mass ratio, M; eq. 6, p. A-4 $M = \frac{2W}{\rho g V_s t_o C_D S_o}$	M		–
d. If $M \leq 4/21$ for $\eta = 0$, then finite mass deployment is indicated.			
(1) Time ratio at $x_{i\,max}$; eq. 9, p. A-5 $\frac{t}{t_o @ x_{i_{max}}} = \left(\frac{21M}{4}\right)^{\frac{1}{7}}$	$\frac{t}{t_o @ x_{i_{max}}}$		–
(2) Max shock factor, x_i; eq., 10, p. A-5 $x_{i_{max}} = \frac{16}{49}\left(\frac{21M}{4}\right)^{\frac{6}{7}}$	$x_{i_{max}}$		–

Table B-1. Opening Shock Force (Cont'd)

	SYMBOL	VALUE	DIMENSION
(3) Max shock force, F_{max} (lb)			
$F_{max.} = X_{1_{max.}} F_s$	F_{max}		lb.
e. If M > 4/21; then intermediate mass or infinite mass deployment is indicated and the elasticity of materials is involved. Calculate the trajectory conditions at time $t = t_o$.			
(1) Velocity ratio @ $t = t_o$ for $\eta = 0$			
$\frac{V_o}{V_s} = \frac{1}{1 + \frac{1}{7M}}$	$\frac{V}{V_o}$		–
(2) Shock factor X_o @ $t = t_o$ for $\eta = 0$			
$X_o = \frac{1}{\left[1 + \frac{1}{7M}\right]^2} = \left(\frac{V_o}{V_s}\right)^2$	X_o		–
(3) Initial elongation, ϵ_o; eq. 23, p. A-10			
$\epsilon_o = \frac{X_o F_s}{F_c} \epsilon_{max}$	ϵ_o		–
(4) Determine $\frac{C_D S_{max}}{C_D S_o}$ from Figure 15, p. A-10	$\frac{C_D S_{max}}{C_D S_o}$		–
(5) Calculate inflation time ratio, $\frac{t_f}{t_o}$; eq. 24, p. A-10			
$\frac{t_f}{t_o} = \left(\frac{C_D S_{max}}{C_D S_o}\right)^{\frac{1}{6}}$	$\frac{t_f}{t_o}$		–
(6) Calculate maximum shock factor, $x_{i\ max}$; eq. 19, p. A-9			
$x_{i_{max}} = \frac{\left(\frac{t_f}{t_o}\right)^6}{\left[\frac{V_s}{V_o} + \frac{1}{7M}\left[\left(\frac{t_f}{t_o}\right)^7 - 1\right]\right]^2}$	$x_{i_{max}}$		–
(7) Calculate maximum shock force, F_{max} (lb),			
$F_{max} = x_{i_{max}} F_s$	F_{max}		lb.

Table B-1. Opening Shock Force (cont'd)

	SYMBOL	VALUE	DIMENSION
(8) Inflation time, sec = $t_f = t_o \left(\frac{t_f}{t_o}\right)$	t_f		Sec.
f. If $\eta \neq 0$, correct t_o for initial area effects; eq. 16, p. A-9 $t_o = \left[1-\left(\frac{C_D S_i}{C_D S_o}\right)^{1/6}\right] t_o$ calculated	t_o		Sec.
g. Mass Ratio, M, eq. 6, p. A-4 $M = \frac{2W}{\rho g V_s t_o C_D S_o}$	M		–
h. Calculate limiting mass ratio, M_L $M_L = \frac{1}{3(1-\eta)} - \left[\frac{9}{14}\eta^2 + \frac{3}{14}\eta + \frac{1}{7}\right]$	M_L		–
If $M \leq M_L$, finite mass deployment is indicated and $x_{i\ max}$ can be determined by eq. 8, p. A-5 by assuming values of t/t_o and plotting the data using the methods of Appendix C.			
i. If $M > M_L$, then intermediate mass or infinite mass deployment is indicated and the elasticity of materials is involved. Calculate the trajectory conditions at time $t = t_o$.			
(1) Velocity ratio @ $t = t_o$ for $\eta \neq 0$; eq. 18, p. A-9 $\frac{V_o}{V_s} = \frac{}{\left[1+\frac{1}{M}\left[\frac{(1-\eta)^2}{7} + \frac{\eta(1-\eta)}{2} + \eta^2\right]\right.}$	$\frac{V_o}{V_s}$		–
(2) Shock factor X_o @ $t = t_o$ for $\eta \neq 0$; eq. 22, p. A-10 $X_o = \frac{1}{\left[1+\frac{1}{M}\left[\frac{(1-\eta)^2}{7} + \frac{\eta(1-\eta)}{2} + \eta^2\right]\right]^2} = \left(\frac{V_o}{V_s}\right)^2$	X_o		–
(3) Initial elongation, ε_o; eq. 23, p. A-10 $\varepsilon_o = \frac{X_o F_s}{F_c}\ \varepsilon_{max}$	ε_o		–
(4) Determine $\frac{C_D S_{max}}{C_D S_o}$ from Figure 15, p. A-10	$\frac{C_D S_{max}}{C_D S_o}$		–

Table B-1. Opening Shock Force (Cont'd)

	SYMBOL	VALUE	DIMENSION
(5) Calculate inflation time ratio, $\frac{t_f}{t_o}$; eq. 24, p. A-10 $\frac{t_f}{t_o} = \left(\frac{C_D S_{max}}{C_D S_o}\right)^{\frac{1}{6}}$	$\frac{t_f}{t_o}$		–
(6) Calculate maximum shock factor, $x_{i\ max}$; eq. 19, p. A-9 $x_{i_{max}} = \frac{\left(\frac{t_f}{t_o}\right)^6}{\left[\frac{V_s}{V_o} + \frac{1}{7M}\left[\left(\frac{t_f}{t_o}\right)^7 - 1\right]\right]^2}$	$x_{i_{max}}$		–
(7) Calculate maximum shock force, F_{max}(lb) $F_{max} = x_{i_{max}} F_s$	F_{max}		lb.
(8) Calculate inflation time, t_f(sec) $t_f = t_o \left(\frac{t_f}{t_o}\right)$	t_f		Sec.

Appendix C

EFFECT OF INITIAL AREA RATIO ON THE LIMITING MASS RATIO AND SHOCK FACTOR FOR THE FINITE STATE OF SOLID CLOTH PARACHUTE DEPLOYMENT

Very low mass ratios are indicative of finite mass parachute deployment, wherein the maximum shock force occurs before the parachute is fully inflated during the unfolding phase of deployment. As the mass ratio is increased, the maximum shock force occurs later in the inflation process. At some value of mass ratio, the maximum shock force will occur at the time t_o. This particular mass ratio is defined as the limiting mass ratio (M_L) for finite mass deployment. A further increase in mass ratio will result in the maximum shock force occurring after the parachute has achieved the design drag area ($C_D S_o$) for the first time.

Equation (8), from p. A-5, Appendix A, defines the instantaneous shock factor during the unfolding phase of parachute deployment.

$$X_i = \frac{(1-\eta)^2\left(\frac{t}{t_o}\right)^6 + 2\eta(1-\eta)\left(\frac{t}{t_o}\right)^3 + \eta^2}{\left[1 + \frac{1}{M}\left[\frac{(1-\eta)^2}{7}\left(\frac{t}{t_o}\right)^7 + \frac{\eta(1-\eta)}{2}\left(\frac{t}{t_o}\right)^4 + \eta\frac{t}{t_o}\right]\right]^2}$$

This expression is to be analyzed for the following purposes:

a. Determine the effect of the initial area ratio (η) on the limiting mass ratio (M_L).

b. Determine the variations of the instantaneous shock factor during the unfolding phase of deployment as a function of limiting mass ratio and η.

c. Determine the expression for the time of occurrence of the maximum shock force for finite mass ratios less than the limiting mass ratio.

The maximum shock force occurs at the point in finite mass deployment where $dx_i/dt = 0$. Setting the derivative $dx_i/dt = 0$ and solving for mass ratio as a function of η and t/t_o results in the following equality:

$$M = \frac{\left[(1-\eta)^2\left(\frac{t}{t_o}\right)^6 + 2\eta(1-\eta)\left(\frac{t}{t_o}\right)^3 + \eta^2\right]^2}{3\left[(1-\eta)^2\left(\frac{t}{t_o}\right)^6 + \eta(1-\eta)\left(\frac{t}{t_o}\right)^2\right]} - \left[\frac{(1-\eta)^2}{7}\left(\frac{t}{t_o}\right)^7 + \frac{\eta(1-\eta)}{2}\left(\frac{t}{t_o}\right)^4 + \eta^2\frac{t}{t_o}\right] \quad \text{(C-1)}$$

Since the limiting mass ratio occurs at $t/t_o = 1$, Equation (C-1) can be reduced to:

$$M_L = \frac{1}{3(1-\eta)} - \left[\frac{9}{14}\eta^2 + \frac{3}{14}\eta + \frac{1}{7}\right] \quad \text{(C-2)}$$

The effects of initial area ratio on the limiting mass ratio are described in Equation (C-2) and Figure C-1. Note that the time of occurrence of the maximum shock force for $\eta = 0$ in Equation (C-1) is:

$$\frac{t}{t_o}\bullet x_{i_{max}} = \left(\frac{21M}{4}\right)^{\frac{1}{7}} \quad \text{(C-3)}$$

which is the same as Equation (9), p. A-5, Appendix A.

The variation of the instantaneous shock factor during the unfolding phase of deployment for limiting mass ratios is presented in Figure C-2. Initial area at the beginning of inflation causes the initial force to increase, but this is compensated for by reduced maximum shock forces. As η increases, the initial loads can be greater than the maximum shock force. However, values of η are usually small and depend on the deployment systems for magnitude and repeatability. Values of $\eta = 0.4$ are more representative of a parachute being disreefed rather than initially deployed. This does demonstrate, however, that the analysis presented in Appendix A can be adapted to the disreefing of solid cloth parachutes by considering the next stage to be a deployment with a large value of η. Variation in initial area is one of the causes of variation in opening shock forces. The variation of opening shock forces for finite mass, intermediate mass, and infinite mass states of deployment can be evaluated by successive calculations with various expected values of η.

For known mass ratios less than the limiting mass ratio, the time of occurrence of the maximum shock force can be ascertained from Equation C-1. If η approaches zero, then the time ratio of

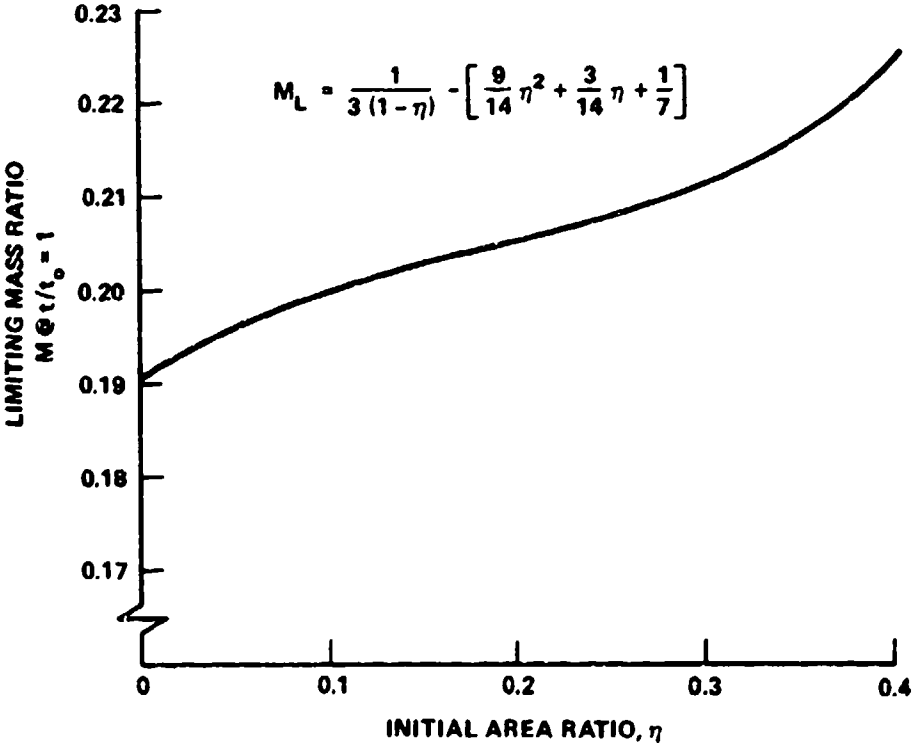

FIGURE C-1. EFFECT OF INITIAL AREA RATIO ON THE LIMITING MASS RATIO FOR THE FINITE STATE OF PARACHUTE DEPLOYMENT FOR SOLID CLOTH PARACHUTES

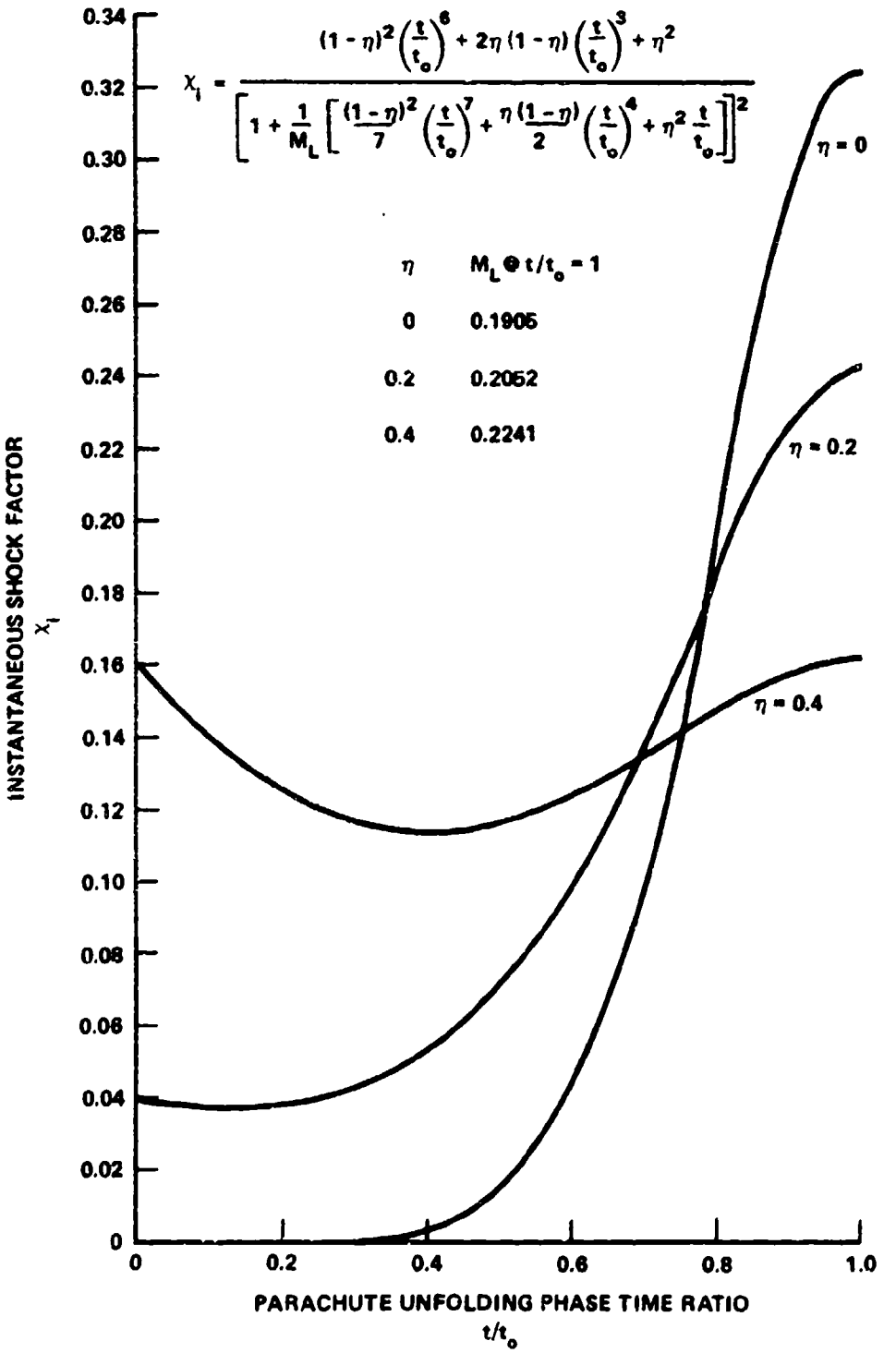

FIGURE C-2. VARIATION OF THE FINITE MASS SHOCK FACTOR DURING THE UNFOLDING PHASE OF SOLID CLOTH PARACHUTES FOR LIMITING MASS RATIOS AND INITIAL AREA EFFECTS

occurrence of the maximum shock force can be initially estimated from Equation (C-3), or determined by plotting

$$x_i = f\left(M,\ \eta,\ \frac{t}{t_o}\right)$$

as in Figure C-2.

DISTRIBUTION

	Copies
Commander Naval Air Systems Command Attn: Library Washington, DC 20361	5
Commander Naval Sea Systems Command Attn: Library Washington, DC 20362	5
Commanding Officer Naval Ship Research and Development Center Attn: Library Washington, DC 20007	2
Office of Naval Research Attn: Library Washington, DC 20360	4
U. S. Naval Academy Attn: Library Annapolis, MD 21402	2
Commanding Officer U. S. Naval Air Development Center Attn: Library Thomas J. Popp Maria C. Hura Johnsville, PA 18974	2 1 1
Commanding Officer U. S. Army Mobility Equipment Research and Development Center Attn: Technical Document Center Fort Belvoir, VA 22660	2
Commander U. S. Army Aviation Systems Command Attn: Library St. Louis, MO 63166	2
Commander U. S. Army Munitions Command Attn: Technical Library Dover, NJ 07801	2
Commander U. S. Army Weapons Command Attn: Technical Library Research and Development Directorate Rock Island, IL 61201	2
Commander U. S. Army ARRADCOM Attn: Library Thomas D. Hoffman DRDAR-LCA-F Ray W. Kline DRDAR-LCA-F Dover, NJ 07801	1 1 1
Commander U. S. Army Natick R&D Labs Attn: Library Calvin K. Lee M. P. Gionfriddo Joseph Gardella Timothy E. Dowling DRDNA-UAS Kansis Street Natick, MA	2 1 1 1 1

DISTRIBUTION (Cont.)

	Copies
Commanding Officer Wright-Patterson AFB Attn: William Casey ASD/ENECA William Pinnell AFWAL/FIER Robert L. Hesters Jr. ASD/YYEE E. Schultz AFWAL/FIER Daniel J. Kolega Bldg. 25 Area B Patrick J. O'Brian Bldg. 25 Area B H. Engel ASD/ENEC OH 45433	1 1 1 1 1 1
Commanding Officer Air Force Flight Test Center Attn: Airframe Systems Division Aerodynamic Decelerator Branch Edwards AFB CA 93523	2
Commanding Officer Air Force Space Division Attn: Library P. O. Box 92960 Worldway Postal Center Los Angeles, CA 90009	2
Commanding Officer Air Force Aerophysics Laboratory Attn: Library Hanscom Field, MA	2
Commanding Officer Kelly AFB Attn: SA-ALC/MMIR Library TX 78241	2 2
Commanding Officer McClellan AFB Attn: Library SA-ALC/MMIR CA 95652	2 2
Defense Technical Information Center Cameron Station Alexandria, VA 22314	12
Library of Congress Attn: Gift and Exchange Division Washington, DC 20540	10
NASA Langley Research Center Langley Station Attn: Research Program Recording Unit, Mail Stop 122 Raymond L. Zavasky, Mail Stop 177 Andrew S. Wright, Jr., Mail Stop 401 Hampton, VA 23365	1 1 8
NASA Ames Research Center Attn: Library, Stop 202-3 Moffett Field, CA 94035	1
NASA Flight Research Center Attn: Library P. O. Box 273 Edwards, CA 93523	1
NASA Goddard Space Flight Center Attn: Library Greenbelt, MD 20771	1
Jet Propulsion Laboratory 4800 Oak Grove Drive Attn: Library, Mail 111-113 Pasadena, CA 91103	1
NASA Manned Spacecraft Center Attn: Library, Code BM6 2101 Webster Seabrook Road Houston, TX 77058	1
NASA Marshall Space Flight Center Attn: Library Huntsville, AL 25812	1
NASA Goddard Space Flight Center/ Wallops Flight Facility Attn: Library Mr. Mendle Silbert Mr. Anel Flores Wallops Island, VA 23337	1 1 1

DISTRIBUTION (Cont.)

	Copies
NASA Lewis Research Center Attn: Library, Mail Stop 60-3 21000 Brookpark Road Cleveland, OH 44135	1
NASA John F. Kennedy Space Center Attn: Library, Code IS-CAS-42B Kennedy Space Center, FL 32899	1
NASA Headquarters Attn: Library Washington, DC 20546	2
Sandia National Laboratories Attn: Code 1632	1
Library	1
Dr. Dean Wolf	1
Dr. Carl Peterson	10
R. Kurt Baca	1
Albuquerque, NM 87185	
University of Minnesota Dept. of Aerospace Engineering Attn: Dr. W. L. Garrard Minneapolis, MN 55455	2
Internal Distribution:	
U13 (W. P. Ludtke)	75
U13 (J. F. McNelia)	1
U13 (D. W. Fiske)	1
U13 (J. Murphy)	1
U13 (J. G. Velez)	1
U13 (M. L. Fender)	1
U13 (A. G. Fritz)	1
U13 (R. L. Pense)	1
U13 (C. J. Diehlman)	1
U131 (E. Noel)	1
U43 (J. Rosenberg)	1
U43 (B. Deire)	1
E231	9
E232	3